GENETIC STUDIES OF EMOTIONAL BEHAVIOUR IN RATS

TESI DOCTORAL DE

Carme Mont i Cardona

Departament de Psiquiatria i Medicina Legal.
Facultat de Medicina. Institut de Neurociències.
Universitat Autònoma de Barcelona

Aquest treball ha estat realitzat sota la supervisió del
Dr. Alberto Fernández Teruel i Prof. Jonathan Flint

Departament de Psiquiatria i Medicina Legal - Unitat de Psicologia Mèdica –
Institut de Neurociències de la Universitat Autònoma de Barcelona.

Universitat Autònoma de Barcelona

Bellaterra, 2014

ACKNOWLEDGEMENTS

We would never accomplish much if working alone. I am genuinely indebted to all those who helped and encouraged me during the four years of this project.

My biggest thank you goes to my supervisors. Alberto, thank you for your support, your advice and your long skype calls whenever they were needed. Thank you for all your scientific imput in this thesis, despite being "más dura que el desierto de Tabernas". Jonathan, thank you so much for your help, your supervision and your support during these four years. Joining the Flint lab has made my PhD an exciting and inspiring challenge, and that I have to thank to you. You have been an excellent mentor, and you have been always available and encouraging whenever things got difficult.

Besides my supervisors, I am very grateful to other scientists whom have devoted time to support my work. A very special thank you goes to Richard Mott and his invaluable help, supervision and good advice in the chapter 6 of this thesis. I also want to thank David Bannerman for all the interesting discussions and support, as well as Peter Oliver for his advice and help. And a very special thank you goes to James Groves, who took lots of his time to teach me the most elemental concepts of molecular genetics, who generously shared his work and his knowledge, and always replied to all my calls for help.

In the Flint group I need to thank everyone for all those little things that made everything better: Martina, GJ, Mona, James C., Amelie, Jerome, Andrew, Rosie, Cai Na, Jon Khron, Martin, Binnaz, Jessie, Leo, Rebekah, Amarjit and very specially Polinka for all her help. No me imagino cómo habrían sido todas las perfusiones e inyecciones sin ti. Y que hubiera hecho sin los cafés, y tus buenos consejos! I also want to mention Kirandeep Ghataorhe, Agnès perquè quan tu hi eres tot era MOLT més guai i no m'he refet mai!, and Regina per els "tu, tranquila", els bons consells, i les tardes de Patisserie Valerie.

A big shout out goes to "the house". Robbie (maw), Kiran (coolio), Na (and how to kill a cow with a butter knife) and Maria (la Suciu!). You guys have been a big source of fun and good times, interesting scientific discussions, and life-saving cups of rooibos.

Vull també agraïr al departament de Medicina Legal i Psiquiatria de la UAB el seu suport i la seva ajuda en tot moment, i mencionar especialment la Glòria, la Regina, el Toni, la Marta, i l'Esther. Tot i que definitivament hem rigut més junts que treballat junts, és molt especial trobar un grup de gent tan espectacular. Des dels "No me cuentes tus penas", als berenars de la tarda, Amsterdam, Milà, i els moments d'estabulari dels inicis... sou el millor!

And at risk of getting way too sentimental, a big thank you goes to those friends and family whom make my life better just by being in it: Adriana, Jared, Maria, Mitus i els meus pares (Anna i Guillem).

This work has received generous suport from the FPI scholarship (BES-2010-032398), the Wellcome Trust Centre for Human Genetics and University of Oxford, as well as the European projects/consortiums “EURATRANS” (grant agreement HEALTH-F4- 2010-241504) and “EURATools (grant LSHG-CT-2005-019015), and from the MICINN (projects PSI2009-10532 and PSI2013-41872-P), the “Fundació La Maratò TV3” (ref. 092630/31) and the “Direcció General de la Recerca” (ref. 2009SGR-0051).

Abbreviations

BAC: bacterial artificial chromosome

BBB: blood brain barrier

CA, CA1-CA3, CA2: Cornus Ammonis, subfields 1, 2 and 3

CY5: cyanine

DAPI: 4',6-diamidino-2-phenylindole

DNA: deoxyribonucleic acid

DPX: Dibutyl phthalate in xylene

DT: diphtheria toxin

ES: embryonic stem cells

FLP, Flpo: flippase, flipase O

fMRI: functional magnetic resonance image

FRT: flippase recognition target

GABA: γ-Aminobutyric acid

GFP: green fluorescent protein

HB-EGF, EGF: heparin-binding epidermal-growth-factor-like growth factor

hDTR: human diphtheria toxin receptor

HPA: hypothalamus-pituitary-adrenal

HS: heterogeneous stock

IP: intraperitoneal

LTP: long term potentiation

MLS: membrane localisation signal

NIH-HS: National Institute of Health- Heterogeneous Stock

NLS: nuclear localisation signal

NMDA: N-methyl-D-aspartic acid

pA: synthetic simian virus-40-polyadenilation signal

PBS: phosphate buffered saline

PCR: polymerase chain reaction

POE: parent-of-origin effect

QTL: quantitative trait locid

RNA: ribonucleic acid

SEM: standard error median

SSR: site-specific recombination

TRECK: toxin receptor mediated cell knockout

TRITC: Tetramethyl Rhodamine Iso-Thiocyanate

TUNEL: Terminal deoxynucleotidyl transferase dUTP nick end labeling

UV: ultraviolet

WT: wild type

INDEX

1. ABSTRACT/RESUM

1. ABSTRACT/RESUM

The present work explores two approaches to the study of behaviour through genetics. The first approach is an interventional transgenic model that aims to study the behavioral function of the Cornus Ammonis (CA) sub region in the hippocampus. I describe the steps to validate an interventional model using a diphtheria-induced cell knockout rat, and our results confirm the insertion of the transgenic construct and a partial expression. We report the results and discuss the feasibility of the model.

The second approach is an observational study of the heritability of complex traits such as anxious behaviour analysing phenotypic and genotypic data. Using a large sample of outbred heterogeneous stock rats, I describe how the heritability of complex traits has a parent-of-origin effect in rats, and focus the analysis on coping style behaviour.

Aquest treball doctoral explora dues aproximacions a l'estudi de la conducta a través de la genètica. La primera és una aproximació de caire intervencionista l'objectiu de la qual és estudiar la funció conductual de la regió del Cornus Ammonis (CA) a l'hipocamp utilitzant un model transgènic. La tesi descriu els processos per a validar aquesta aproximació mitjançant un model d'ablació cel.lular induïda per la toxina diftèrica, i els nostres resultats demostren la inserció del constructe i una expressió parcial. Describim els resultats tot analitzant la viabilitat d'aquest model per a l'estudi de la conducta.

La segona aproximació és un estudi observacional de l'heretabilitat dels trets complexos com el comportament ansiós mitjançant l'anàlisi de dades genotípiques i fenotípiques. Analitzant una llarga mostra de rates heterogènies describim com l'heretabilitat dels trets complexos té un efecte lligat al parent d'origen (*parent-of-origin effect*) en rates, i centrem l'anàlisi en les conductes i estratègies d'enfrontament davant d'estímuls estressants (*coping style*).

2. GENERAL INTRODUCTION

2. GENERAL INTRODUCTION

The relationship between behaviour and the brain has been widely explored through observational and interventional models. Observation has been key in the origin of science, when examining naturally occurring events and their relationships was fundamental to inferring their connection. To understand the structure of a causal system, there are two basic approaches that will provide knowledge. The observational approach makes inferences based on sampling the system's autonomous behaviour, and the interventional approach will collect samples conditioned on the particular values of one or more variables that have been manipulated (Steyvers et al. 2003). Neuroscience has been and is still largely an observational discipline. Most theories of brain function arise from interpreting observations of the structure of the brain, and the characteristics associated with brain injuries.

The scope of modern neuroscience includes among others the study of molecular, physiological, genetic, developmental, functional, medical and evolutionary aspects of the nervous system. Each of these fields contributes a wide array of observational but also interventional techniques to study brain function. In this context, molecular and statistical genetics have developed several methodologies to tackle the relationship between genes and physiological function. Not only understanding the relationship between genome and phenome provides information on the function and structure of the brain

and its afflictions, but manipulating the genome also provides a valuable interventionist approach. The consequences of genetic manipulation help understand the relationship between brain, function and malfunction.

This thesis explores two approaches to the study of behaviour through genetics. The first approach is an interventional transgenic model that aims to study the behavioral function of the Cornus Ammonis (CA) sub region in the hippocampus. The second approach is an observational study of the heritability of complex traits such as conditioned and unconditioned anxious behaviour (which is known to be hippocampus dependent) analysing phenotypic and genotypic data.

This chapter will introduce the rationale for both approaches. It describes what is known about the function of the hippocampus and its connections to anxiety and why a rat cellular ablation model was thought to be useful. It also provides an overview of the strategies available for selectively inactivating neurons and introduces the model that forms the basis of the interventional approach of this thesis. The chapter also presents the heterogeneous rat stock and why this particular model is advantageous when studying Quantitative Trait Loci (QTL). It will also describe how genotypic and phenotypic data provide insight about the heritability of behavioural traits and their genetic basis.

2.1. INTERVENTIONAL STUDY: GENETIC MANIPULATION OF THE BRAIN

Only recently have tools become available that make possible the type of interventionist science that other disciplines have enjoyed. One of the reasons for the relatively late appearance of these tools is the difficulty when attempting to dissociate individual components of brain function. In 1664, the anatomist Thomas Willis published the first description of the anatomy of the brain and suggested that different brain areas could control different functions; but it was not until physician Paul Broca's work in the middle of the 19th century with aphasic patients that there was evidence that a highly specific disorder was connected to a specific cortical area (Gross, 1987). He observed that patients with similar symptoms had lesions in the left frontal cortex, in the exact same region.

The study of memory and learning from a strict psychological point of view started arousing interest, and in 1901 Willard Small initiated systematic studies on animal learning using mazes. He was the first to use a rat and a maze for behavioral testing. By 1913, John Watson had accumulated enough evidence from rats learning experiments on mazes to conclude that learning could be understood in terms of stimuli and response associations.

Studies with animals not only provide the chance to manipulate the environment but also to manipulate the brain, and the consequences of said manipulation can be observed. In the study of the hippocampus, animal models have been widely used in a great variety of interventions.

2.1.1 The hippocampus and the hippocampal formation: anatomy and morphology

The hippocampus is a brain structure located in the medial temporal lobe, on the floor of the lateral ventricle. While there is no universal agreement of which structures should be included in the hippocampal formation (David G. Amaral, Ishizuka, and Claiborne 1990; Witter and Amaral 2004; Andersen et al.), in this thesis I will refer to the hippocampal formation as the group of structures including the hippocampus proper (which is divided into CA1, CA2 and CA3 and the dentate gyrus), the subiculum, the parasubiculum, the presubiculum and the entorhinal cortex.

The rat hippocampus is located in the temporal lobe under the corpus callosum at its most frontal point (the septal pole, sometimes referred as dorsal hippocampus) and it extends caudally resembling a C or a banana, the inferior part (the temporal pole) being referred as the ventral hippocampus (fig. 1A).

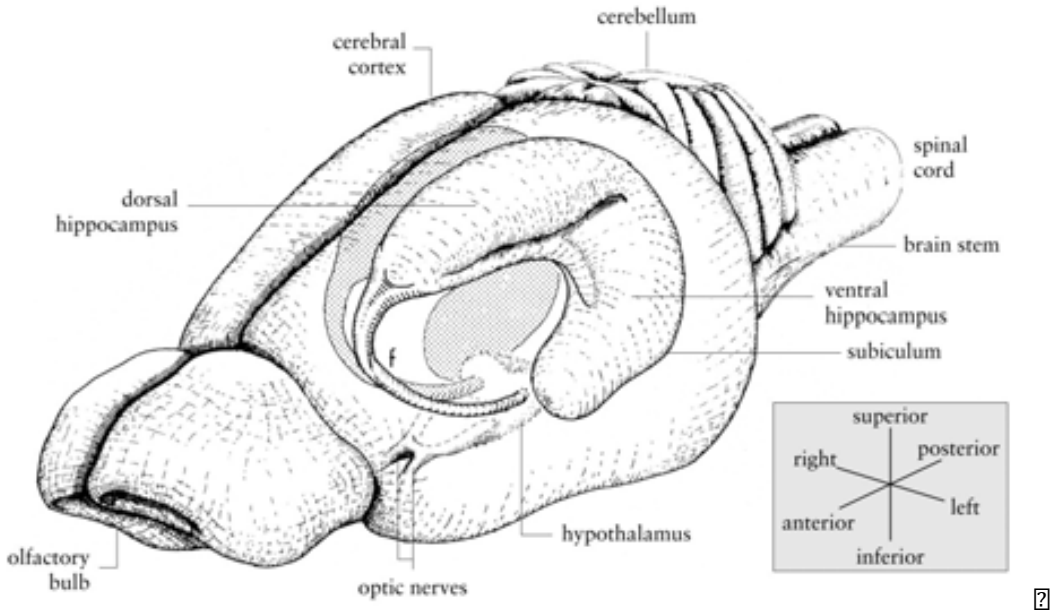
cerebellum
cerebral cortex
spinal cord
dorsal hippocampus
brain stem
ventral hippocampus
subiculum
hypothalamus
olfactory bulb
optic nerves
superior
right
posterior
left
anterior
inferior

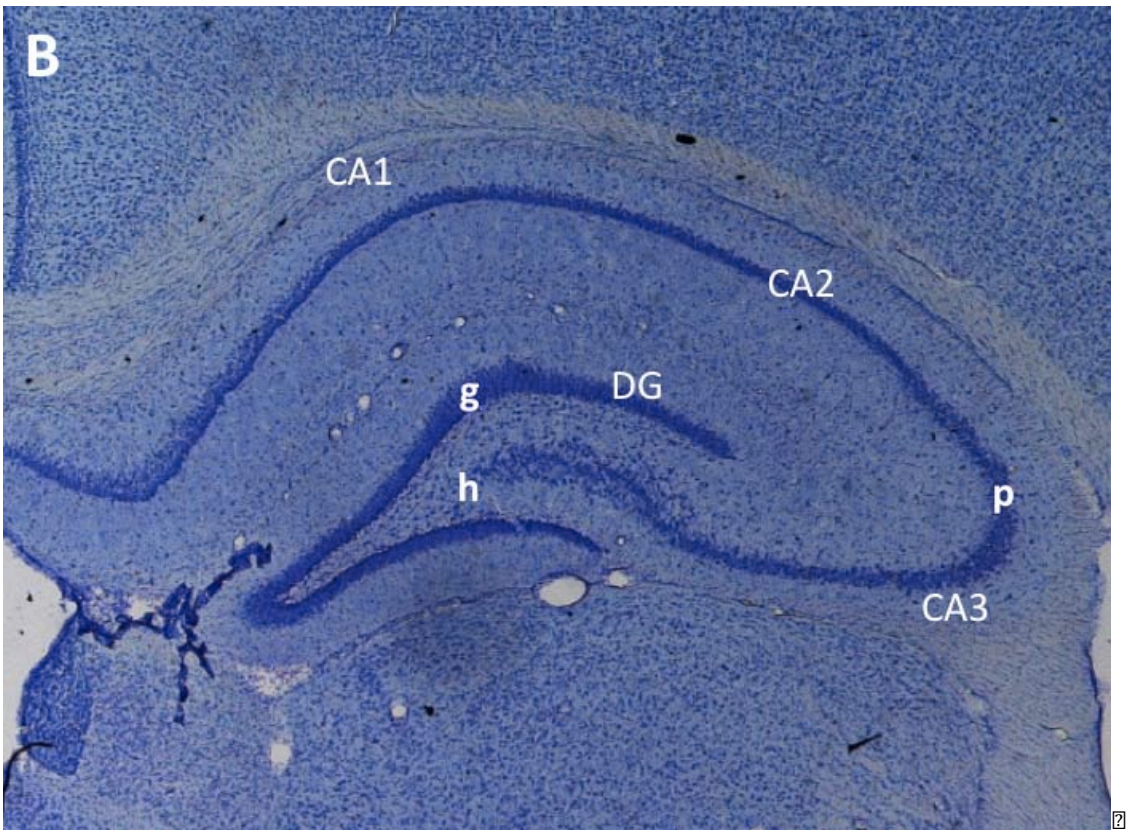
B
CA1
CA2
g
DG
h
p
CA3

The focus of this thesis will be on the hippocampus proper, specifically the CA1-CA3 subfields. A comprehensive review of all the findings related to the hippocampus anatomy, physiology, morphology and connectivity can be found in The Hippocampus Book, (Andersen et al. (2007).

2.1.1.1. The Hippocampus proper

The hippocampus proper is a sub structure of the hippocampal formation that contains the dentate gyrus and the CA1-CA3 subfields (fig. 1B). While describing briefly the dentate gyrus morphology, this section mostly focuses in the CA morphology and cytoarchitecture.

2.1.1.1.1. The dentate gyrus

Three different cell layers compose the dentate gyrus. The molecular layer is sparse in cells and the granular cell layer is a dense, four to eight cell thick layer. Together they form the fascia dentata, which resembles a flat V shape. They enclose the polymorphic cell layer, also called the hilus, which is the third layer of the dentate gyrus. The hilus contains the mossy cells, which are covered by very large and complex spines, named thorny eferescences, but much denser that the ones in the CA3 pyramidal cells (David G. Amaral, Scharfman, and Lavenex 2007). The granular cell layer is one of the few places in the brain where new cells are continuously generated (fig. 1B).

2.1.1.1.2. The CA sub fields

The CA constitutes the pyramidal layer, which is the biggest cellular layer of the hippocampal formation and it is formed almost entirely of pyramidal neurons. The presence of pyramidal neurons in the forebrain areas (as cortex, hippocampus, and amygdala) but not in other structures such as the olfactory bulb, the midbrain or the spinal cord suggests they are related to higher cognitive functions (Spruston 2008). Pyramidal neurons have a basal dendritic tree that extends to the substratum oriens, and an apical dendritic tree that extends into the hippocampal fissure (Witter and Amaral 2004). They are covered with thousands of dendritic spines, some of them which can contain multiple synapses (Spruston 2008) and they are the most abundant cell type in the hippocampus.

Lorente de Nó (1934), one of Ramón y Cajal students, appreciated anatomical differences through the layer and suggested three divisions: CA1, CA2 and CA3 (fig. 1B). These divisions have proved not only to relate to anatomical differences but also to different connectivity within the layer. He also noted sub divisions within the CA3 into three parts (CA3 a, b and c) and within the CA1 (also in three parts). However more recent literature suggest there is no reason for these further subdivisions despite some subtle morphological differences (Ishizuka, Cowan, and Amaral 1995).

Pyramidal cells in the CA3 are large, with extensive dendrites, but the whole sub region is very heterogeneous. The CA3 pyramidal neurons close to the dentate gyrus have a dendritic length of approximately 9300 μm (the smallest of all the layer) and this length seems to increase up to the largest dendritic length of all the CA, 15800 μm next to the CA2 (Ishizuka, Cowan, and Amaral 1995; Witter and Amaral 2004; Andersen et al. 2007). The CA2 pyramidal neurons have similar body cells to CA3 (Witter and Amaral 2004), but they lack thorny excrescences on their proximal dendrites (Ishizuka, Cowan, and Amaral 1995). The CA2 section differs from CA3 more in connectivity than in morphology, but this will be further explained in section 2.1.2.1 of this chapter. The pyramidal cell bodies of CA1 are smaller than the ones in CA2 or CA3, but they are very homogeneous through the whole CA1 sub region both in cellular body size and dendritic length (Pyapali et al. 1998; Ishizuka, Cowan, and Amaral 1995).

These differences between the neuronal morphology of the very same layer suggest some sort of functional differentiation within this hippocampal structure, suggestion that is emphasized by its connectivity pattern.

2.1.2 Hippocampal connectivity

The hippocampal formation connectivity has certain characteristics that are rare in the rest of the brain. It receives multiple external inputs, but also has a rich and multiple internal circuitry. Most of its connections are internal, such as

contralateral and ipsilateral connections, as well as collateral (for instance in CA2 and CA3).

Another main distinction is the lack of reciprocal connections between some areas, creating a unidirectional pathway that describes a loop through all the hippocampal formation. This loop is known as the trisynaptic pathway as it involves three synapses. The major external input enters the hippocampal formation at the entorhinal cortex, and connects to synapse at the granular cells of the molecular layer of the dentate gyrus. The mossy fibers project from the molecular layer to synapse in the pyramidal cells of CA3. CA3 projects to CA1 via the Schaffer collateral connections and synapses in the pyramidal cells. From the pyramidal cells of CA1, the pathway continues to the subiculum, which has the major output in the entorhinal cortex, closing the trisynaptic loop.

However, it is important to take into account that there are parallel connections to the trisynaptic pathway that terminate in different areas of the hippocampal formation (Witter and Amaral 2004). One example is the connections from the entorhinal cortex to the CA3, where the pyramidal cells in the CA3 receive connections from the entorhinal cortex monosynaptically and disynaptically via the dentate gyrus (the trisynaptic pathway) at the same time. This monosynaptic connection is known as the temporo-ammonic pathway. It is unknown if these connections happen in the same cell at the same time.

Another important input comes also from the entorhinal cortex to connect with the dentate gyrus, with a topographical structured connectivity. The perforant

pathway connects the lateral sections of the entorhinal cortex with the septal pole of the dentate gyrus, whereas the medial sections have more connections with the temporal pole. This differentiation between the poles connectivity has been linked with differences in function (Bannerman et al. 2004; Kjelstrup et al. 2002).

2.1.2.1 The CA1-CA3 connectivity

The CA1-CA3 subfields of the hippocampus receive inputs from multiple sources, but its most important connections are within the hippocampus.

The CA3 subfield receives inputs from outside of the hippocampal formation such as the amygdala and the septum, and within the hippocampus from the dentate gyrus via the mossy fibers and the entorhinal cortex. However the most characteristic display of the CA3 is the associational and commissural connections with CA2, CA1 and CA3 itself. All CA3 pyramidal cells send projections to all the sections of the CA within the ipsilateral hippocampus by collateral axons, called the associational connections between CA3 and CA2-CA3, and the Schaffer collaterals between CA3 and CA1. All of these connections demonstrate a systematic gradient-like projections pattern (Andersen et al., 2007). At the same time, CA3 connects with the same fields in the contralateral hippocampus, called the commissural connections. Some fibers will also innervate the polymorphic layer of the dentate gyrus.

The CA2 subfield has a very similar connectivity pattern as CA3. It also participates in the commissural and associational connections, innervating the ipsilateral and contralateral CA3, CA2 and CA1 fields; and also in the connections with the polymorphic layer of the dentate gyrus. However CA2 is the only sub field that receives a prominent innervation from the posterior hypothalamus and the only subfield not to receive inputs from the amygdala.

The CA1 subfield receives input from the septum, the entorhinal cortex, the perirhinal cortex, and the amygdala. From within the hippocampus proper, CA1 main inputs are the innervations from CA2 and mostly CA3. The CA3 innervations, named the Schaffer collaterals are part of the trysinaptic loop. CA1 itself lacks the associational connections that are so prominent in CA3 and CA2, but raises important output pathways. The first is a topographically organized projection to the subiculum, the presubiculum, and the postsubiculum (Fanselow and Dong 2010). The second is the cortical connections, since it is the only subfield to send connections to the entorhinal, perirhinal and retrosplenial cortex and also to the medial frontal lobe. Besides the cortical projections, it also sends fibers to the lateral septal nucleus and the amygdala.

2.1.3 The Function of the Hippocampus

The hippocampus anatomy and physiology has many particularities that point at high cognitive and singular functions. The granular cell layer of the hippocampus is one of the few places in the brain where new cells are continuosly generated.

This neurogenesis creates de novo neurons that generate axons and dendrites to fully integrate in the brain circuitry. The hippocampal connectivity pattern presents unique features as the trisynaptic loop or the recurrent synapses in CA3. The presence of large pyramidal cells which are present in the forebrain areas (as cortex, hippocampus, and amygdala) but not in other more primitive brain structures such as the midbrain or the spinal cord suggests they are related to high cognitive functions (Spruston, 2008). Besides the anatomical and morphological particularities, studies with the aim to define hippocampal function have raised different theories. There is evidence that neurogenesis can be influenced by external factors such as exercise (van Praag, Kempermann, and Gage 1999) or stress (Gould et al. 1997), but there is no clear role of how this *de novo* cells contribute to hippocampal function since several studies report contradictory information (Kempermann, Wiskott, and Gage 2004; Groves et al. 2013a; Shors et al. 2001; Deng, Aimone, and Gage 2010). While they are backed up by scientific research, numerous findings challenge the accuracy of these theories at explaining sufficiently the hippocampus function.

2.1.3.1 The declarative memory theory

Following Scoville and Milner's report of the side effects of surgery to palliate epilepsy, the theory that the hippocampus subserved declarative memory gained ground. The surgery sectioned the medial temporal lobe bilaterally to an extension of 8 cm, damaging the hippocampal formation and the amygdala to some extent. The patient, H.M., showed complete anterograde amnesia and a

three year retrograde amnesia, but had intact cognitive function, language, and procedural memory. It was concluded that the hippocampus had a role in information retention (Scoville and Milner 1957).

This paper suggested for the first time that memory was not a disseminated brain function but was specific to a brain region, and that there were different types or divisions of memory functions. The declarative memory theory sets the hippocampus as the core where semantic and episodic memory processes take place (Eichenbaum 2011). This type of memory is very different from procedural memory, which is memory for learned abilities or automated behaviors such as riding a bike or playing the piano, which cannot be explained easily with words but can be demonstrated without difficulty. In comparison, declarative memory is memory of facts or episodes that can be explained with words, for instance semantic memory is the knowledge of facts such as "Italy is a country in Europe", whereas episodic memory is the knowledge of events of one individual's life such as "last summer I spend my holidays in Italy". The case of the HM patient was consistent with this separation between declarative memory, which was impaired since the surgery, and procedural memory that he had intact.

However, later studies with animal models point to a necessary cortex-hippocampus interaction for the consolidation of long term memories (Frankland et al. 2001; Eichenbaum 2011) and a necessary role of the cortex for conservation of long term memories (Wang and Morris 2010; Eichenbaum 2011; Winocur, Moscovitch, and Sekeres 2007). While it is established that the hippocampus works with other necessary brain structures to encode and

consolidate declarative memories, it is still considered a key structure (Andersen et al., 2007).

2.1.3.2. The cognitive map theory

Measuring hippocampal neuron activity in living rats led O'Keefe and Dostrovsky to discover place cells (O'Keefe, 1979). Place cells are neurons that increase their firing rate specifically when the animal is in a particular spatial location. If the animal leaves that particular spatial location, those neurons decrease their firing rate. These findings lead to the view that the hippocampus function cannot only be the association of declarative memories, but must be involved in the processing of spatial information.

The cognitive map theory proposes that hippocampus functions to construct and maintain spatial maps, encoded as a mental framework by two separate systems (O'Keefe and Nadel 1978). The first uses egocentric cues to construct a map of navigation or route, using proprioceptive information of the navigation. The second uses allocentric cues or landmarks in the environment to construct a representation of the space where the navigation takes place. The integration of these two maps allows the animal to navigate, and the hippocampus would be the place where these maps are stored.

To test this theory, numerous lesion animal studies were performed in spatial mazes such as the water maze, or the T-maze. The water maze makes use of

allocentric visual cues as well as egocentric cues to locate a platform that is below the water level and not visible to the animal. Separate testing between allocentric and egocentric navigation is possible by removing the cues or changing the platform position in the maze. In support of the cognitive map theory, hippocampal lesions in rat impaired their spatial place navigation and their spatial discrimination, but not their egocentric navigation (Morris et al. 1982; Hagan et al. 1988; O'Keefe 1979).

The discovery of two further types of cell types supported the difference between an allocentric map and an egocentric map. "Head-position" cells, found in the subiculum, fire according to the head position of the animal independently of the environment and are consistent with the existence of an egocentric map (Taube, Muller, and Ranck 1990). Grid cells, found in the entorhinal cortex represent spatial cues in a three dimensional manner and support the existence of an allocentric map (Hafting et al. 2005).

Human studies are also consistent with this theory. The introduction of fMRI studies allowed to measure brain activity allowed to measure changes in the hippocampus related to extensive spatial navigation (Maguire et al. 2000; Maguire, Nannery, and Spiers 2006) and the existence of grid cells in the human brain has also been demonstrated (Doeller, Barry, and Burgess 2010a).

Despite these findings, several other experiments challenge the cognitive map theory. There is evidence that lesions of the hippocampus do not necessarily impair spatial navigation. Lesioned rats take several more trials to learn the

platform location compared to controls but are not impaired in the water maze (Morris et al. 1990). Furthermore, several experiments report different deficits depending on the lesions location. Lesions located in the dorsal hippocampus reported deficits in spatial navigation, whereas lesions located in the ventral hippocampus had no impact in spatial navigation but resulted in altered anxious behavior (Kjelstrup et al. 2002; Bannerman et al. 2003; Bannerman et al. 2004). Although being necessary for spatial navigation, these conflicting findings suggest that the hippocampus function is not totally explained by the cognitive map theory.

2.1.3.3 The configural association theory

The configural association theory is an approach to the function of the hippocampus that has its focus on learning configuration of stimuli. The theory emerged from a set of experiments in which rats with a lesioned hippocampus could not learn the association of two stimuli with a reward, but they could learn the association of each of them separately with the reward (Rudy and Sutherland 1989).

The theory makes a distinction between associative learning and configural associative learning. In this distinction, associative learning is not hippocampus dependent, and it is the association between a simple stimulus and the experiences of the organism with that stimulus. The configural associative learning would be hippocampal dependent, and it is the representation of simple

stimulus events to construct a unique representation that can be associated or distinguished from other representations. Therefore, associations between two stimuli would not be discriminated versus a single one of those stimuli presented alone, and contextual memory would be impaired (Sutherland and Rudy 1989; Rudy and Sutherland 1989).

Several studies challenged these findings, demonstrating that lesioned rats could actually learn configural associations (Davidson, McKernan, and Jarrard 1993). The authors further refined the theory, suggesting a division of labor between the cortex and the hippocampus. The cortex would be responsible for a slow learning, extracting generalities of experiences and the hippocampus would be responsible for the fast learning of arbitrary contents of individual experiences. This re-formulation of the theory was based on a computational neural network model (O'Reilly and Rudy 2001). However, the theory fails to explain why animals with hippocampal lesions can solve biconditional association problems compared to the controls if they are not using contextual memory (Good, de Hoz, and Morris 1998).

2.1.3.4 The behavioral inhibition theory

The behavioral inhibition theory suggests that the hippocampus acts as a mediator in a conflict between the responses to a stimulus. When incompatible goals such as exploration versus avoiding a predator appear, the hippocampus would act as a comparator generating the necessary responses to solve the

conflict (Gray 1982; McNaughton and Gray 2000). When a situation elicits competing goals, the hippocampus reinforces the value of the affectively negative goal, and the remaining competing goal response would be inhibited. In this context, amnesic patients or animals with hippocampal lesions would have the inability to inhibit irrelevant experiences. The hippocampus would be uncapable of selecting the event that is trying to recall by failing at inhibiting all the non relevant remaining events.

According to Gray and McNaughton, this conflict processing operates as an algorithm that would be applied in the hippocampus along the septotemporal axis (Bannerman et al. 2014). It has been reported that lesioning the dorsal hippocampus affects spatial navigation, but lesions in the ventral hippocampus affect anxious behavior (Kjelstrup et al. 2002; Bannerman et al. 2003; Bannerman et al. 2004). Anxiety arises from a conflict between two competing goals and in a situation of potential danger. It differs from fear, which is a reaction to imminent danger linked to the amygdala. This hippocampal functional dissociation is hardly explained or accounted for in the cognitive map theory or the configural association theory. Since the dorsal hippocampus receives its input from the entorhinal cortex but the ventral hippocampus receives it from the amygdala, the theory would explain the functional differences between hippocampal regions. The inability of the hippocampus to inhibit one of the competing goals responses would result in altered anxious behavior.

Consequently, behavioural disinhibition (i.e. decreased anxiety) is observed in animals with hippocampic lesions when presented with an approach-avoidance conflict such as the Geller-Seifter conflict task, or to the passive-avoidance/active-avoidance conflict as in the two-way active-avoidance paradigm (Gray 1982; Gray and McNaughton 2000).

The fact that despite extensive research and efforts there is no common agreement about the hippocampal function points out several factors. First, that the hippocampal function has to be more sophisticated than has been anticipated. Its connectivity and morphology are unusual anywhere else in the brain and such complexity has to be necessary to sustain the function of the hippocampus. Second, experiments with more refined techniques will have to take place in order to further understand the complexity of its function. Genetically engineered models have the capacity to control the expression of a protein, offering the ability to manipulate cell receptors or populations selectively. Such a level of control will be required in order to be able to tackle the complexity of the behavioral function.

2.1.4 Brain interventions

2.1.4.1 Physical and chemical lesions

A classic intervention when studying function is to damage a small part of the brain and observe what has been altered or impaired. In several studies of

spatial navigation, the physical destruction of the hippocampus has been achieved by mechanic means, such as aspiration (Morris et al. 1982; Sutherland and Rudy 1989). This method however is less common now since it has very little control over the extent of the lesion. The use of chemical lesions proves more successful at impairing hippocampus function, with the added advantage that it does not damage passing fibers. Excitotoxins such as ibotenic acid have been used widely to hyperexcite glutamatergic neurons causing their death (Hagan et al. 1988; Morris et al. 1990; Good, de Hoz, and Morris 1998) when injected. However it is also possible to target cell populations that have a shared neurotransmitter and affect their function. This type of pharmacological impairment can be achieved by blocking the receptor of the neurotransmitter (Saucier and Cain 1995).

While all of these methods have proved helpful, they require a great degree of intervention on the animal. Surgeries rely on stereotaxic coordenates, and brain morphology is complex. It can be difficult if not impossible to target very small populations of cells or tissue subsets with those methods. The use of genetically engineered models has overcomed some of these problems.

2.1.4.2. Genetically modified models

2.1.4.2.1. Mice models

Advances in molecular biology have made it possible to genetically modify animals. In 1992, mutant mice lacking the synaptic protein alpha-calcium-calmodulin dependent kinase II (alpha-CamKII), showed impaired long term potentiation (LTP), a form of neuronal synaptic plasticity (Silva et al. 1992), (Grant et al 1992), and became the first mice model used for the study of hippocampal function.

Genetically modified mice have proved very successful in dissecting the hippocampus. The use of site-specific recombinant technology allows using the expression profile of a gene to target very specific subregions. Using a Cre/loxP system, it was possible to knock out the NMDA receptor of the CA1 uniquely to study its implication in spatial memory and nonspatial learning (Tsien, Huerta, and Tonegawa 1996) and later on to do so with the CA3 (Nakazawa et al. 2002; Nakazawa et al. 2003) leaving the rest of the CA intact.

Mice that exhibit impaired AMPA receptors (lacking the Glu1A subunit) have been extremely useful at finally revealing important functional implications with long term spatial memory (Bannerman et al. 2012) or disassociations between spatial working memory versus spatial reference memory (Sanderson and Bannerman 2012). More recently, NMDA receptor hippocampus specific knock out mice have challenged the long standing understanding of LTP (Bannerman et al. 2014).

These models provide excellent spatial resolution, but they lack the temporal control of the lesion that excytotoxic or pharmacological models do have. However a combination of both models is the expression of a toxin receptor in a

tissue of interest, controlling cell death with the toxin administration, creating a "toxin receptor-mediated cell knock out", a TRECK model (Saito et al. 2001). In this case, mice are insensitive to the diphtheria toxin. By introducing a receptor in selected cells, they become sensitive to the toxin (Cha et al. 2003). Since the diphtheria toxin crosses the blood brain barrier (BBB), this method has been used successfully to ablate selected cells in the brain (Buch et al. 2005a; Arruda-Carvalho et al. 2011).

2.1.4.2.2 Rat models

The mouse might not be the best model to study hippocampal function. While mice are the choice for molecular studies, most of the cognitive and learning studies have been performed in the rat (Andersen et al. 2007; Zheng et al. 2012), emotional, cognitive and learning tests have been developed initially for rats (Porsolt, Le Pichon, and Jalfre 1977; Morris 1984; Pellow et al. 1985) and despite some of them can be used in mice, social interactions and some operant tasks appear to be far beyond the abilities of mice (Crawley 1999).

However, while several transgenic or mutant mice models have been developed allowing very interesting results, very few rat models have been developed. The use of ES cells (embryonic stem cells) has been very successful in mice since the 1980s, while a stable use of ES cells in rat models just recently started appearing (Kawamata and Ochiya 2010; Zheng et al. 2012).

The human hippocampus is 100 times bigger than the rat, but its structure, cell structure and most of its neuronal connections and pathways remain analogous, as the basic architecture of the hippocampus is akin in humans, rats and monkeys. The main morphological differences are the thickness of the CA1 field, which in humans can be up to thirty cells thick, and the entorhinal cortex, which has more complexity in the human brain, accounting for at least eight sub divisions versus the two subdivisions of the rat entorhinal cortex. Regarding connectivity, the main difference are the commissural connections, which in humans are practically inexistent as an input at the dentate gyrus (Andersen et al., 2007). But the overall connectivity networks remains comparable. Anatomy and electrophysiology studies in the hippocampus begun using the rat (which are much easier than with mice), and have made most of its discoveries using it as a model.

The use of transposon-mediated mutagenesis or zinc finger nucleases have improved the generation of transgenic rats by decreasing the time of production and increasing the ratios of germline transmission but they still present with high off-target effects. One alternative is the use of BACs (bacterial artificial chromosomes), which can carry big sequences allowing full mammalian genes and most of their regulatory sequences, as well as having an accurate spatial and physiological expression pattern. (Zheng et al. 2012; Giraldo and Montoliu 2001) With the use of recombineering technology, a construct containing the regulatory sequences to express a toxin receptor can be introduced into the rat genome, creating an analogous model to the TRECK mice in the rat. BACs have been used to generate transgenic rats expressing fluorescent proteins (Uematsu

et al. 2008) and more recently to successfully ablate neurogenesis in the hippocampus (Groves et al. 2013).

2.2. OBSERVATIONAL STUDY: GENETIC ANALYSIS OF BEHAVIOUR IN RODENTS

Genetic analysis of behavioural phenotypes and psychiatric disorders has proved more difficult than initially expected. The highly polygenic nature of behavioural traits and complicated gene-environment interactions make the dissection of the molecular basis of behavioural traits an ambitious challenge. However, genetic mapping of behavioural phenotypes in laboratory animal models has provided robust evidence of an association between chromosomal regions and behavioural phenotypes or psychiatric disorders (Flint 2003; Flint and Mott 2001). When a genetic region contributes to quantitative trait, this Quantitative Trait Loci (QTL) can be mapped to find candidate regions and genes that have an effect on the phenotype (Mott et al. 2000).

2.2.1. QTL mapping

Behavioural phenotypes measuring anxiety or fearful behaviour are analysed with a quantitative measure: how many seconds does a rodent spend freezing in front of a novel situation? When mapping behavioural quantitative traits, QTL

mapping is useful to find candidate regions by testing which regions in the genome are associated with a phenotypic quantitative trait. Each locus mapped may contain one or more genes that have some effect on the phenotype.

One approach is to use an F2 intercross of animals that have been selectively bred for a trait. Several QTLs have been reported associated with behavioural phenotypes using this strategy for emotionality (Flint et al. 1995; Talbot et al. 1999), fear-like behaviour (Gershenfeld and Paul 1997), locomotor activity (Koyner et al. 2000), and anxiety (Fernández-Teruel et al. 2002a). These mapping experiments allowed the association between chromosomal regions and phenotypes of interest. However, and because of their poor resolution, to identify genes using this approach the number of animals to be used in these experiments would have to reach the tens of thousands (Flint and Mott 2001).

One of the problems that we face when using animal models is that the number of QTLs mapped to rats and mice are now in the order of the thousands but a much smaller number of candidate genes has been identified (Flint et al. 2005). This limitation is due to the available mapping techniques, which have a poor mapping resolution that made it impossible to identify candidate genes. Another reason is that when trying to fine-map a single QTL with a large effect it was often found that the single QTL was not a single QTL at all. Rather it was caused by numerous smaller effect loci positioned within the same chromosomal region (Legare, Bartlett, and Frankel 2000). The difficulty is to achieve sufficiently high resolution mapping to enable gene identification (Valdar, Solberg, Gauguier, Burnett, et al. 2006).

2.2.2 The rat heterogeneous stock

The highest resolution in terms of fine mapping has been achieved by using outbred mice or rats of known ancestry that have been crossed for many generations, ensuring a high ratio of recombination events and small sized QTLs. One advance in fine mapping of QTLs in rodents came from using outbred mice stock to perform fine mapping (Mott et al. 2000). Heterogeneous Stock (HS) mice are derived from crossing eight progenitor founder strains that had been subjected to a rotational breeding scheme for several generations in order to produce a high number of recombinations. The use of the HS mice allowed the fine mapping of QTLs for complex traits and the identification of candidate genes (Mott et al. 2000; Yalcin et al. 2004; Valdar, Solberg, Gauguier, Burnett, et al. 2006). In their paper, Valdar and colleagues used an hetereogeneous mice stock that had been crossed for over 50 generations to map 843 QTLs within an interval of 2.4 Mb (Valdar, Solberg, Gauguier, Burnett, et al. 2006). The QTLs reported contributed to the variation of 97 traits and measured related to asthma, diabetes, obesity and anxiety among others (Valdar, Solberg, Gauguier, Burnett, et al. 2006).

It was assumed that the use of a rat HS would attain the same level of mapping resolution. Compared to mice, rats have some advantages for genetic studies. Since the rat is a larger animal it is better suited for some physiological measures. For instance higher blood volume allows for a better characterisation

of hematology tests. Rats are more similar to humans in some of their behavioural measures (Lindblad-Toh 2004).

The heterogeneous rat stock (NIH-HS) was established as a colony in the 1980 in the US National Institutes of Health. This rat stock descends from eight inbred rat strains (BN/SsN, MR/N, BUF/N, M520/N, WN/N, ACI/N, WKY/N and F344/N) which have been set up in a rotational breeding scheme designed to reduce inbreeding (Hansen and Spuhler 1984; Boucher and Cotterman 1990). After more than 50 generations, each animal has a unique random mosaic of the founding strains chromosomes and it is estimated that the average distance between recombinations allows QTL mapping intervals to a resolution of less than a centimorgan (Mott et al. 2000). The accumulated recombination events reduce the size of the QTLs, allowing the identification of candidate genes.

Following this work, and as part of a large collaborative project, the Rat Genome Sequencing and Mapping Consortium has genotyped and phenotyped 1407 heterogeneous stock outbred rats in our laboratory and performed genetic mapping over 160 phenotypes. The experimental design included phenotyping multiple measures related to disease models (anxiety, multiple sclerosis, osteoporosis, hypertension, diabetes and aortic lamina raptures) as well as physiological measures known to be risk factors for disease (such as cholesterol levels, body weight and hematology). The results report a combined genetic and sequencing mapping analysis that identified more than 350 QTLS for 122 phenotypes, and which identified 35 causal genes for 31 of the phenotypes (Baud et al., 2013).

2.2.3 Coping styles

The capacity to cope with the demands of challenges of different environmental conditions is essential for the survival of all organisms. When an organism faces an aversive situation, the ability to react successfully determines its ability to survive. Coping style is the pattern of responses that an individual consistently displays when facing a stressful stimulus or conflicting situation (Koolhaas 2008).

The concept of coping style is mostly based in the work of Henry and Stephens, who distinguished two widely observable patterns of responses in the presence of a stressful stimulus (Henry and Stephens 1977). The first pattern of response was first described in the works of Henry Cannon who defined a fight-flight active response to a threat (Cannon 1915). The second pattern is the conservation-withdrawal response, a passive response towards the stressful stimulus (Engel and Schmale 1972). The two response patterns are diametrically opposed one each other and have been described as defense versus defeat (von Holst 1998). Individuals display one of these two patterns when confronted with a stressful stimulus across situations and over time (Koolhaas 2008).

Reactive and pro-active coping styles have been observed in multiple organisms such as humans (von Holst 1998; Busjahn et al. 1999; Jang et al. 2007), mice (Koolhaas 2008), great tits (Dingemanse et al. 2004; van Oers et al. 2004), carps

and trouts (MacKenzie et al. 2009), pigs (Schouten and Wiegant 1997) and rats (Driscoll et al. 1998; Díaz-Morán et al. 2012; Coppens et al. 2013). Being common to several organisms, coping styles are also highly heritable (Busjahn et al. 1999; Dingemanse et al. 2002; van Oers et al. 2004; Jang et al. 2007), with an estimated heritability of up to 50% (Drent, van Oers, and van Noordwijk 2003).

The pro-active coping style is characterised by active responses directed to address the aversive situation, either to confront stressful stimuli or to increase the distance between the stressful stimuli and the individual (Benus et al. 1991). The pro-active coping style has been associated with increased exploratory behaviour (Wechsler 1995; Steimer and Driscoll 2003; MacKenzie et al. 2009; Coppens et al. 2013), aggressive behaviour (Dingemanse et al. 2004; Koolhaas 2008), and struggling (Schouten and Wiegant 1997; Steimer and Driscoll 2003; Koolhaas et al. 2007). By contrast, the reactive coping style is defined by inactivity and disengagement when in an aversive situation, and only reacting if absolutely necessary. The reactive coping style has been associated with non-aggressive behaviour (Dingemanse et al. 2002; Koolhaas et al. 2007), absence of responses (Engel and Schmale 1972; Steimer and Driscoll 2003; Koolhaas 2008), immobility and extended latency (Schouten and Wiegant 1997; von Holst 1998; Steimer and Driscoll 2003; MacKenzie et al. 2009).

Neuroendocrine responses under stress for reactive and pro-active coping style animals also have a distinct profile. It has been observed that the reactive coping style correlates with an increased activation of the HPA (hypothalamus-pituitary-adrenal) axis with increased levels of corticosterone and prolactin

compared to the pro-active coping style animals (Steimer, Fleur, and Schulz 1997; MacKenzie et al. 2009; Koolhaas et al. 2010: Díaz-Morán et al. 2012). Higher activation of the HPA axis is consistent with behavioural measures such as higher levels of freezing in the shuttle box, less number of entries in the open arms on the elevated zero maze, and less struggling in the forced-swim test (Koolhaas et al. 2007; MacKenzie et al. 2009; Díaz-Morán et al. 2012).

Using the behavioural measures and the genotypic information available from the Rat Genome Sequencing and Mapping Consortium, we can analyse behavioural measures that are consistent with the emotional profile of the coping style. It has been previously established that the HS rats exhibit a reactive coping style in tests such as the forced-swimming test and an elevated HPA axis response to stress (Díaz-Morán et al. 2012). Since coping styles are highly heritable, it is also plausible to analyse these phenotypic measures separately and estimate whether their heritability has a parent-of-origin component.

In summary, this thesis aims to study the biological bases of behaviour from two approaches. With an interventional model, I target one of the anatomical structures of anxious behaviour. Using a TRECK rat model expressing a diphtheria toxin receptor in the cells of CA1 to CA3, I can induce a very selective brain lesion and study the changes in behaviour. With the observational model, I describe how the heritability of most of the complex traits analysed in this thesis has a parent-of-origin component. Then I focus on the hippocampus dependent behavioural measures, specially those that are constituent of an active or passive coping style and analyse its heritability.

3. AIM AND SCOPE

3. AIM AND SCOPE

The main aim of this thesis is to use advanced genetic techniques to question brain function related to anxious/fearful behaviour. In the first approach, I describe the steps to validate an interventional model using a diphtheria-induced cell knockout rat, and discuss the feasibility of the model. The hypothesis is that the ablation of the neuronal population in CA1-CA3 will cause behavioural changes that will allow determining the function of this neuronal layer. The aims for this work are:

i) Validate the insertion of the NeuroD6 construct in the rat genome and its expression in the targeted areas.

ii) Validate the recombination of the constructs in the *NeuroD6* TRECK rat and establish which dosing regime induces ablation with the diphtheria toxin.

iii) Assess the neuronal death and feasibility of the *NeuroD6* TRECK rat as a model to study hippocampus-dependent behaviour.

iv) Characterise the behavioural changes in the *NeuroD6* TRECK rat to determine the consequences of CA1-CA3 ablation.

The second approach is an observational study of the heritability of complex traits such as anxious behaviour in the HS rats. The data generated in the Consortium allows the study of the heritability of complex traits as well as their genetic architecture. The hypothesis is that complex traits heritability in the HS

rats has a parent-of-origin effect as seen in the HS mice. The aims for this work are:

v) To analyse the heritability of complex traits in the HS rats to determine if it has a parent-of-origin effects component.

vi) To assess if behavioural phenotypes and particularly coping style heritability has a parent-of-origin effects.

As part of the interventional approach chapter four of this thesis describes the experiments to tackle aims i and ii, and chapter five describes the experiments to accomplish aims ii and iii. Due to the results of aims i, ii, and iii, the aim iv remains unaccomplished and the hypothesis for the first approach could not be demonstrated. The results are widely discussed in chapter four and chapter five, where limitations and future work are outlined.

For the observational approach, chapter six describes all the analysis done to accomplish aims v and vi. The results and hypothesis are thoroughly discussed in chapter six with the limitations of the study and the plans for future work.

Finally, main results, limitations and conclusions are briefly outlined and summarised in chapter seven for both approaches, and chapter eight includes all material and methods for this thesis work. Section nine includes the bibliography used in the writing of this thesis, and the appendix provides full results for the parental and parent of origin heritabilities.

4. THE *NEUROD6* TRECK RAT MODEL VALIDATION

4. THE *NEUROD6* TRECK RAT MODEL VALIDATION

4.1 Introduction to TRECK models

A TRECK (Toxin receptor cell knock-out) rat is a transgenic model that aims to express a human diphtheria toxin receptor (hDTR) in a tissue of interest (Saito et al. 2001). Rodents are naturally resistant to the diphtheria toxin, making cells that express the hDTR vulnerable to the toxin while sparing the rest (Cha et al. 2003). By expressing this receptor cells become vulnerable to the toxin, allowing a temporally and spatially controlled ablation of the cells when the toxin is administered. Due to the temporal and spatial control that provide, TRECK systems have been successfully used in mice to study a wide variety of tissues (Buch et al. 2005a; Arruda-Carvalho et al. 2011; Chen, Kohno, and Gong 2005; Sonntag et al. 2012; Golub et al. 2012). In rats, a TRECK model accomplished to model the human glomerulesclerosis-related renal failure by expressing the hDTR in the kidney podocytes to a much more faithful condition than mice (Wharram et al. 2005).

Because a single molecule of the diphtheria toxin in the cell cytosol is capable of induce apoptosis, expressing the hDTR in the tissue of interest and nowhere else is crucial. Using a Site Specific Recombinase (SSR) system to combine to transgenic models allows the expression of the hDTR to occur only in the tissues

where both transgenes are expressed. This extra spatial restriction allows the administration of the toxin systemically, and prevents unwanted phenotypes.

The *NeuroD6* TRECK rat is a double transgenic model that as the result of the crossing of two models uses the promoter region of the *NeuroD6* gene to express an hDTR using an SSR system. This SSR (specifically a Flpo/FRT system) contains a flippase with the power to excise anything comprised between two FRT (Flipase Recognition Target) sites. One of the models (*NeuroD6* hDTR) has the hDTR flanked by FRT and a stop cassette, which does not allow its expression. The other rat model (*CamkII*α-Flpo) contains the flipase that excises the recognition-flanking sites and the stop casette. By crossing the *NeuroD6* hDTR rat with the *CamkII*α-Flpo rat, we allow the receptor to be expressed in those tissues where the two transgenes overlap.

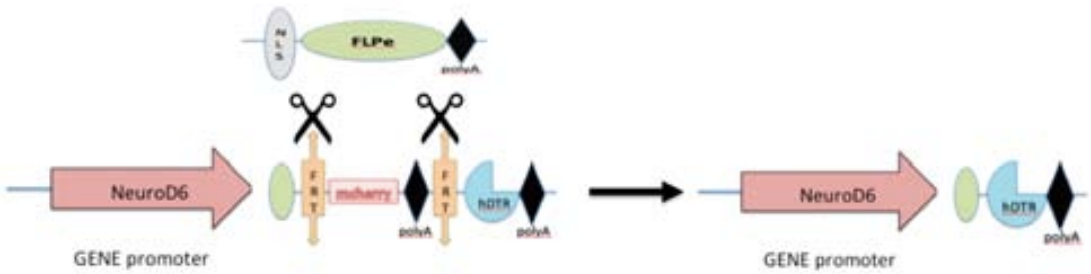

Figure2 : Figure showing the action of the flippase on the *NeuroD6* construct. The flippase present in the *CamkII*α-Flpo construct recognises the FRT sites and excises everything between them, hence removing the polyA cassette that prevents the expression of the hDTR. The *NeuroD6* TRECK rat then expresses the hDTR in the membrane of the cells were both constructs are expressed.

The aim of this chapter is to validate the *NeuroD6* hDTR rat model, and the *NeuroD6* TRECK rat model. In order to do so, a set of experiments will look at the insertion of the constructs at a genomic level, as well as to confirm the expression of them at a protein level, and the recombination between both constructs.

4.1.2 The *NeuroD6* hDTR rat

The *NeuroD6* construct uses the promoter of the *NeuroD6* gene. It also contains the hDTR and a Stop Cassette, which has an mCherry fluorescence to allow visualization of the expression in the brain. The construct was designed and engineered by Nicholas Suarez and James Groves.

4.1.2.1 The *NeuroD6* hDTR construct

The *NeuroD6* gene belongs to the NeuroD gene family, which is formed by genes necessary for the neuronal differentiation in the hippocampus and other regions in the nervous system (Miyata, Maeda, and Lee 1999). The *NeuroD6* gene is expressed in several tissues including the spinal cord, hippocampus, and the retina (Kay et al. 2011). In the hippocampus the expression is limited to the CA1-CA3 pyramidal layer (Lein et al. 2007a). By using the *NeuroD6* promoter, the expression of the construct will mimic the expression of the *NeuroD6* gene. In

order to obtain higher spatial definition, a Stop cassette precedes the hDTR, to avoid its expression.

The construct is inserted in a BAC containing the *NeuroD6* gene (CH230-502A3) and contains:

- Two sequences encoding for a membrane localization signal (MLS), to ensure the expression of the fluorescence in the membrane of the pyramidal cells.
- The coding sequence for the mCherry red fluorescent marker protein.
- A sequence encoding for the neomycin antibiotic resistance.
- Three synthetic simian virus-40-polyadenilation signals (pA)

Besides the stop cassette, the construct also contains:

- Two FRT sites flanking the stop cassette.
- The hDTR (human Diphtheria Toxin Receptor)
- A synthetic simian virus-40-polyadenilation signal (pA)

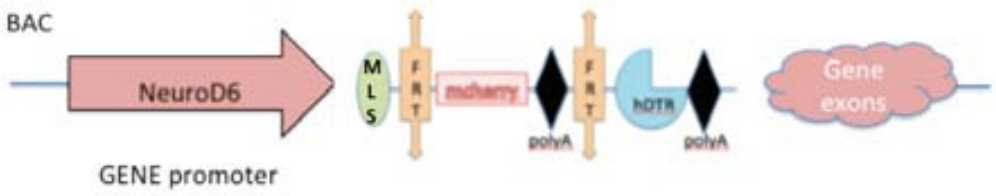

Figure 3: Image showing the structure of the *NeuroD6* construct. MLS: membrane localisation signal, FRT: flippase recognition target, mCherry fluorescence, polyA: synthetic simian virus-40-polyadenilation signal, hDTR: human diphtheria toxin receptor.

When two FRT sites exist in the same orientation its recombinase will excise the entire nucleotide sequence in between them, leaving one site intact. Therefore, if the recombinase is not present, transcription will stop when reaching the pA signals. If the recombinase is present, the excision will allow the expression of the hDTR and remove the mCherry protein. By design of the construct, the presence of the mCherry indicates the unavailability of the hDTR, and the absence of the mCherry would indicate that the hDTR is expressed.

The hDTR is a human mutated receptor that allows the diphtheria toxin to enter the cell cytosol. Rodent cells don't have a functional receptor, but when expressing the human receptor, one single molecule can kill a cell (Sapoznikov and Jung 2008). The B-subunit of the toxin binds to the hDTR and gets endocytosed. The A-subunit then gets released, terminating the protein synthesis and causing cell death (Saito et al. 2001).

4.1.3. The *CamkIIα*-Flpo Rat

The *NeuroD6* gene is expressed in the CA1-CA3 layers in the hippocampus but it is also expressed in the retinas or the spinal cord. In order to restrict the spatial expression of the hDTR to the CA1-CA3 fields to avoid unwanted effects, a FLP recombinase must be expressed in the CA1-CA3 and not in any other region where the *NeuroD6* is expressed. For this a breeding will be set up between a rat expressing a FLP recombinase in the brain with the *NeuroD6* hDTR rat model. The *CamkIIα*-Flpo construct was engineered by James Groves (Groves, 2011).

4.1.3.1 The CamkIIα-Flpo construct

The Calmodulin-dependent protein kinases (CAMK) are a group of serine/threonine-specific protein kinases that are involved in neurotransmitter release, transcriptor factor regulator and glycogen metabolism. A mouse expressing CRE was created with the promoter of the *CamKIIα* gene, the alpha subunit which is most abundantly expressed in the brain, with greater expression in CA1 pyramidal cells than in other cell populations within the hippocampus (Tsien, Huerta, and Tonegawa 1996).

The *CamkIIα*-Flpo rat uses the same gene promoter as the previously described mouse model, and aims to express a FLP recombinase to ensure SSR within the targeted cells in the hippocampus. A BAC containing the *CamkII-α* gene (BAC CH230-315A17) was selected to insert the construct expressing the FLP recombinase. The construct contains:

- An amino-terminal nuclear localisation signal (nls) to ensure targeting of the FLP recombinase to the nucleus of the cell.
- The coding sequence for a FLPo recombinase
- A synthetic simian virus-40 polyadenylation signal (pA) to stop transcription.

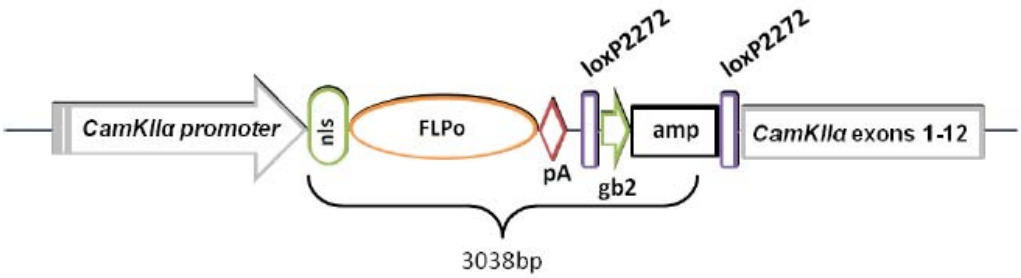

Figure 4: *The CamkIIα*-Flpo construct. NLS: nuclear localisation signal, FLPo: Flippase site specific recombinase O, pA: polyA: synthetic simian virus-40-polyadenilation signal, two loxP sites, and a gene encoding ampicillin resistance. Adapted from (Groves, 2011).

The construct also contains the ampicillin resistance gene as well as two criptic loxP sites (loxP2272), which were added to facilitate selection following insertion to the BAC. However, when attempting removal, the construct experimented unwanted recombination, with loss of additional regions of the BAC. Therefore, the ampicillin resistance gene and the criptic loxP sites remain in the construct (Groves, 2011).

4.1.4. Generation of the Models

Constructs were injected into fertilized Sprague Dawley embryos and transferred into foster mothers (whole procedures are described in Groves, 2011). Genomic DNA was extracted from the tails of pups and analysed by PCR using genotyping primers for each construct. Four male founder rats were identified positive for the insertion of the *CamkII*α-Flpo transgene and ten founder rats (five males and five females) are positive for the *NeuroD6* hDTR. All the animals were sent to the Oxford laboratory.

4.2. STUDY 1: VALIDATION OF THE *NEUROD6* HDTR RAT MODEL

In this section we include a series of experiments, which aim to validate the *NeuroD6* hDTR rat model. Results are included and discussed in section 5 of this chapter, as well as methodology is detailed in the Material and Methods chapter of this thesis.

4.2.1 Genotyping through PCR

The ten founders positive for the insertion of *NeuroD6* hDTR were ear-clipped once arrived to the Oxford laboratory, and a PCR was performed to amplify the transgene to confirm insertion. One of the females showed no positive band for the construct. The rest of the animals were set up for breeding with wild type (WT) Sprague Dawley. While one of the females never managed to have a successful pregnancy, the offspring of the remaining 8 breeding pairs was genotyped, and proved that six founders had integrated the construct in the germ line and were able to produce pups positive for the transgene.

4.2.2 Visualization of the mCherry protein

The *NeuroD6* hDTR rat expresses an mCherry protein following the expression profile of the *NeuroD6* gene. This protein is in the stop cassette of the construct

and should be expressed when the stop cassette has not been excised by the FLP recombinase. If the construct is present at a genomic level the mCherry protein proves that is being expressed at a protein level, and shows where specifically is being expressed. In order to test the tightness of the expression profile we inspected the organs where the *NeuroD6* gene is expressed according to the literature available (spinal cord, brain and retina) in the transgenic offspring but also other organs to make sure there are not unwanted side effects.

Offspring for each of the breeding pairs (positive and non positive for the transgene as controls) were selected for histological analyses. Animals were transcardially perfused in order to fix the tissue, and the following organs were extracted: brain, spinal cord, eyes (retinas), heart, cerebellum, liver, and spleen. A full description of the perfusion and preparation of the organs can be read in the methods chapter, but in brief organs were perfused with saline and fixed with a 4% paraformaldehide solution, followed by immersion in a 30% sucrose solution. Tissues were sliced with a microtome at a 30 um thickness and kept as free floating sections in an antifreeze solution at -20 C, except for the retinas, which were embedded and sliced with a cryostat. Slices were washed in PBS and mounted in slides with a mounting media containing fluorescent DAPI, and visualized at different excitations on a confocal microscope.

The mCherry protein has an excitation and emission maxima of 587nm and 610 nm respectively. Tissues were visualised through a TRITC filter (pass bandwidth of 656-605 nm) to detect the mCherry protein and under a UV light to visualise the DAPI (330-360 nm) counterstaining, which binds to all the cell nuclei.

4.2.2.1. Brain, Retina and Spinal Cord

According to the Allen Brain Atlas (Lein et al. 2007) the *NeuroD6* gene is expressed in the brain (CA1 to CA3, and with very little intensity in the entorhinal cortex), in the spinal cord and in the retinas. Therefore slides containing transgenic and control samples for these tissues were examined using a confocal microscope.

4.2.2.1.1. Expression in the brain

The expression of the construct was assessed by light excitation of the tissue in order to visualise the mCherry protein. The areas predicted by the Allen brain atlas for the *NeuroD6* gene expression are the CA1 to CA3 fields in the hippocampus and the entorhinal cortex. The fluorescence was detected in these areas under the excitation of the TRITC filter as estimated by the literature. However, upon inspection of several brain sections we found two places where the mCherry protein was expressed which were not reported by the literature to have expression of the *NeuroD6* gene. The first one is located between the dentate gyrus blades, in the hilus and the second one is in a small cortical area, located in the secondary visual cortex.

4.2.2.1.1.1. The entorhinal cortex

The *NeuroD6* expression profile in the brain includes CA1-CA3 in the hippocampus and a small neuronal population in the entorhinal cortex.

The entorhinal cortex has ben associated to spatial navigation and some of its neurons, named grid cells, fire according to coordenates in space helping to elaborate a spatial map (Jarrard 1993; Hafting et al. 2005; Doeller, Barry, and Burgess 2010b; Yartsev, Witter, and Ulanovsky 2011). Some neurons in the entorhinal cortex exhibit the mCherry protein as expected by the expression profile of the *NeuroD6* gene. This expression is quite modest as very few neurons are detectable.

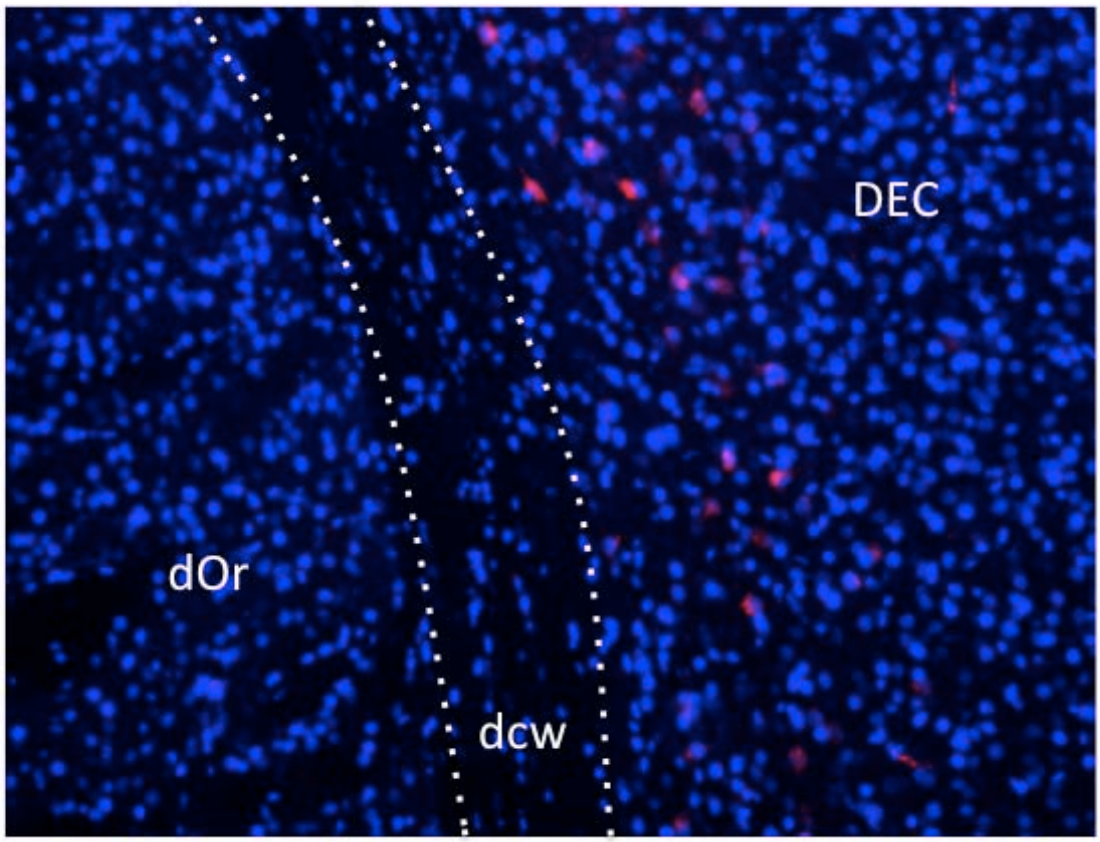

Figure 5: Picture of neurons expressing the mCherry fluorescence in the entorhinal cortex. DEC: dorsal entorhinal cortex, dOR: dorsal Oriens, dcw: deep cerebral white matter. The nuclei of the cells are stained with DAPI, and visible in blue. Overlapped images under the TRITC and uV light excitation.

4.2.2.1.1.2 The secondary visual cortex

When inspecting the whole brain, three of the lines exhibited a small population of pyramidal neurons expressing the mCherry protein in the secondary visual cortex. This finding was not expected, as the Allen Brain atlas does not list the secondary visual cortex as one of the areas where the *NeuroD6* gene is expressed. The shape of the soma as a clear triangle indicates that the neurons expressing the mCherry protein in this region are pyramidal neurons, as well as its location in the internal pyramid layer V.

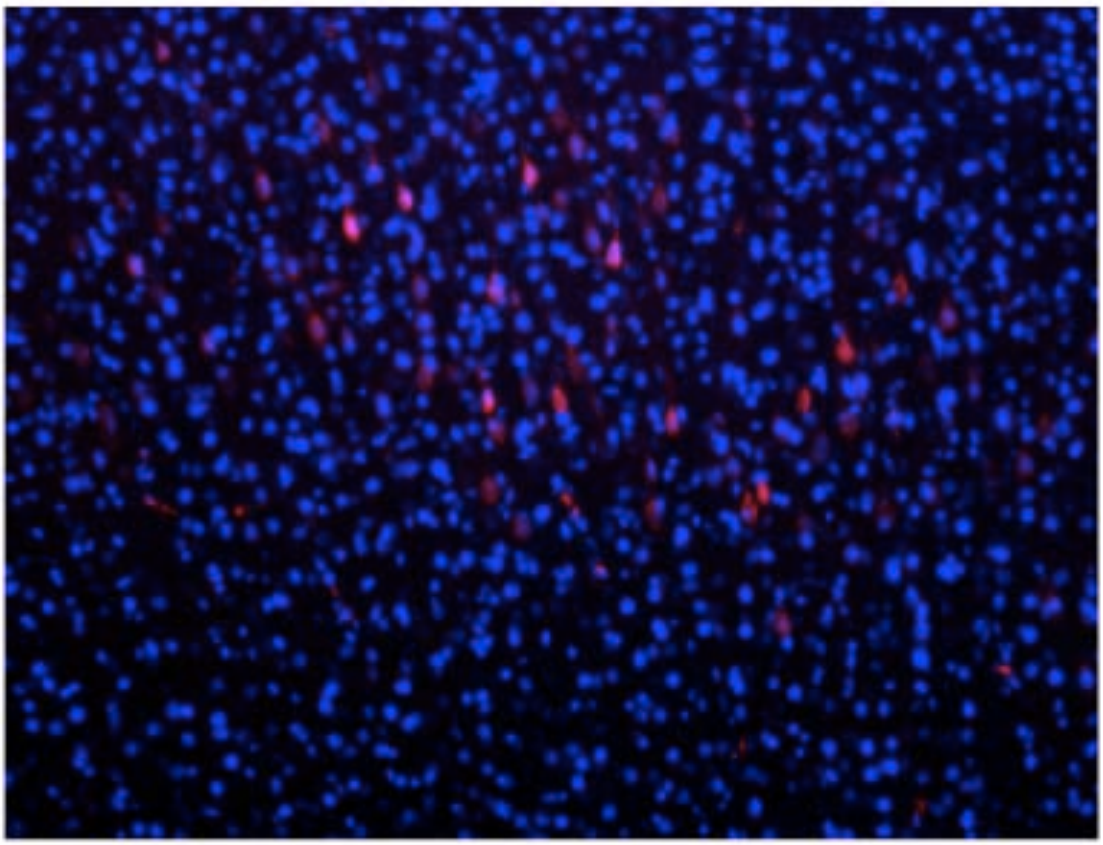

Figure 6: Picture of pyramidal neurons expressing the mCherry fluorescence in the secondary visual cortex. The nuclei of the cells are stained with DAPI, and visible in blue. Overlapped images under the TRITC and uV light excitation.

4.2.2.1.1.3 The CA1-CA3 fields

The pattern of expression through the CA1 to the CA3 subfields is consistent with the pattern of expression of the endogenous *NeuroD6* gene. The mCherry protein is expressed all over the pyramidal layer, through all the fields of the Cornus Ammonis (CA1-CA3). CA1, CA2 and CA3 have a similar pattern of expression, though the mCherry protein appears extremely bright in the beginning of the CA3 section. This could be due to the fact that pyramidal cells in the CA2 and the CA3 are bigger than pyramidal cells in the CA1 subfield (Ishizuka, Cowan, and Amaral 1995; Pyapali et al. 1998).

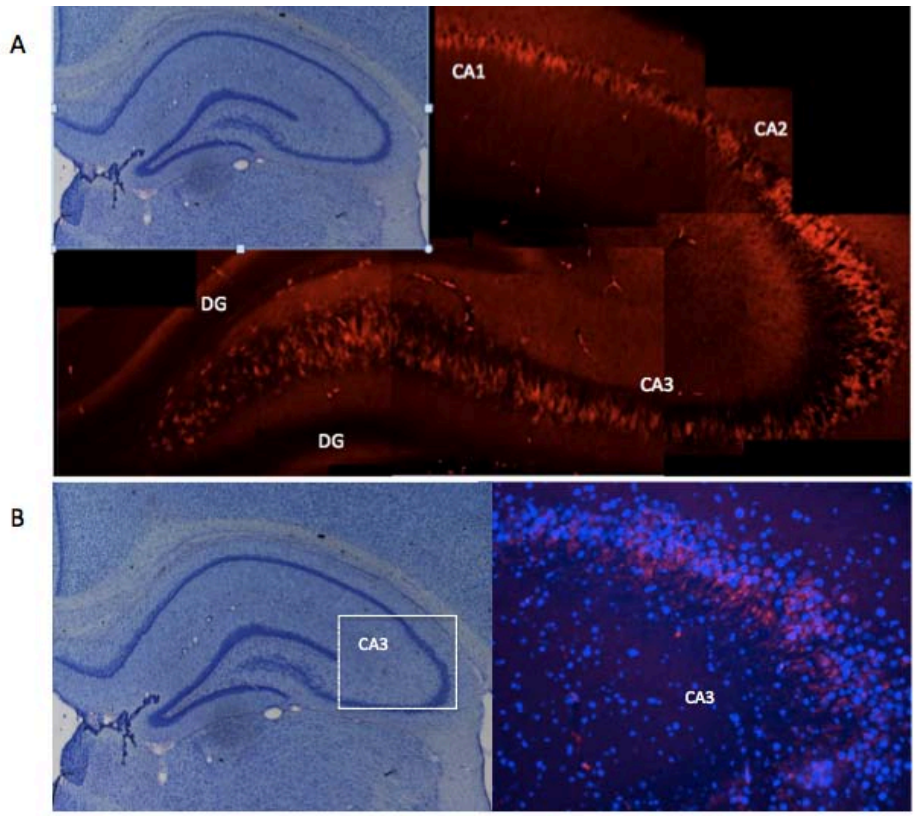

Figure 7: The mCherry expression in the *NeuroD6* rat brain. A) Pictures of a *NeuroD6* rat hippocampus, excited under a TRITC filter to visualise the extent of the mCherry expression. For comparison, a picture of a Nissl staining of a control rat brain showing the hippocampus in the left upper corner of the image. CA1, CA2, CA3: Cornus Ammonis sections 1, 2 and 3, DG: dentate gyrus. B) Left: picture of a Nissl staining of a wild type rat hippocampus with a frame on the CA3 subfield. Right: Close up picture of the CA3 subfield of a *NeuroD6* rat showing intense mCherry expression under a TRITC filter.

4.2.2.1.1.4 The hilus

The hilus is located between the blades of the fascia dentata, in a region that blends the CA3 pyramidal neuron layer once it enters the area comprised within the dentate gyrus. When examining the expression of the mCherry protein in the CA1-CA3 fields in the hippocampus, some neurons expressing the fluorescence could be observed in the hilus region. This expression was unexpected. The soma of the pyramidal neurons can be clearly observed in the polymorphic region of the hilus. Despite the location of these neurons in the polymorphic region where the CA3 blends with the hilus make it difficult to establish its separation from CA3, some of the neurons expressing the mCherry protein are outside of the CA3 subfield.

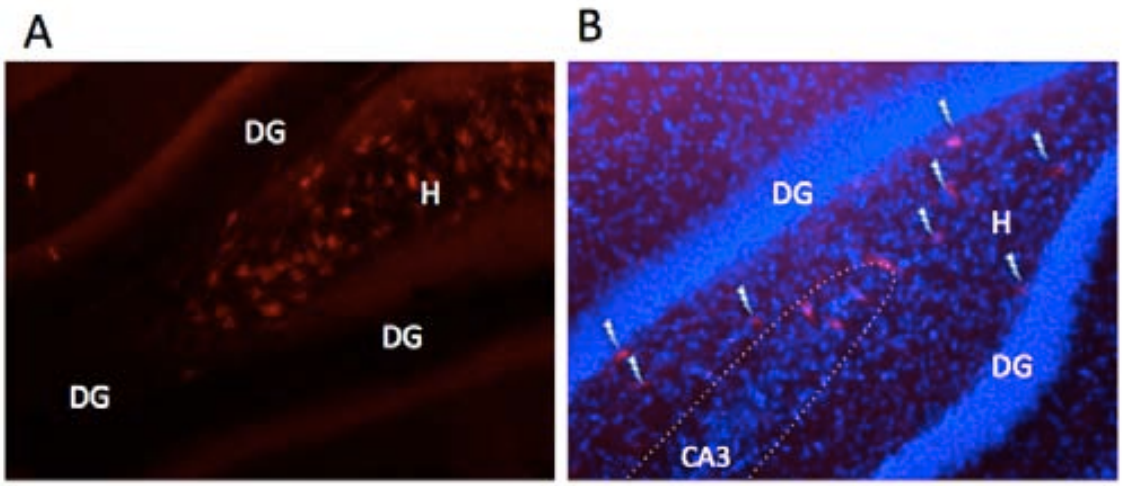

Figure8: Picture of the mCherry fluorescence expression in the hilus region. DG: dentate gyrus, H: hilus, CA3: cornus ammonis subfield 3.
A) Image of the hilus of a *NeuroD6* rat where the fascia dentata converge under TRITC excitation. The neurons of the dentate gyrus do not glow under TRITC excitation, as they do not express the mCherry fluorescence.
B) Overlapped images of the hilus of a *NeuroD6* rat under TRITC and uV light. Some neurons expressing the mCherry fluorescence can be seen outside the CA3 layer (framed in a dotted line) in the hilus region (marked with white arrow heads).

4.2.2.1.2 Expression in the retina

The *NeuroD6* gene expression in the retina is limited to the amacrine cells. Amacrine cells are inhibitory interneurons present in the ganglionar layer in the retina. With more than 30 subtypes, amacrine cells are involved in inhibitory responses and are divided into two types: wide field and narrow field. Wide field amacrine cells are GABAergic whereas narrow field amacrine cells are glycinergic. It is the *NeuroD6* expression which defines the new retinal amacrine cells subtypes and determines their fate from their progenitors (Kay et al. 2011).

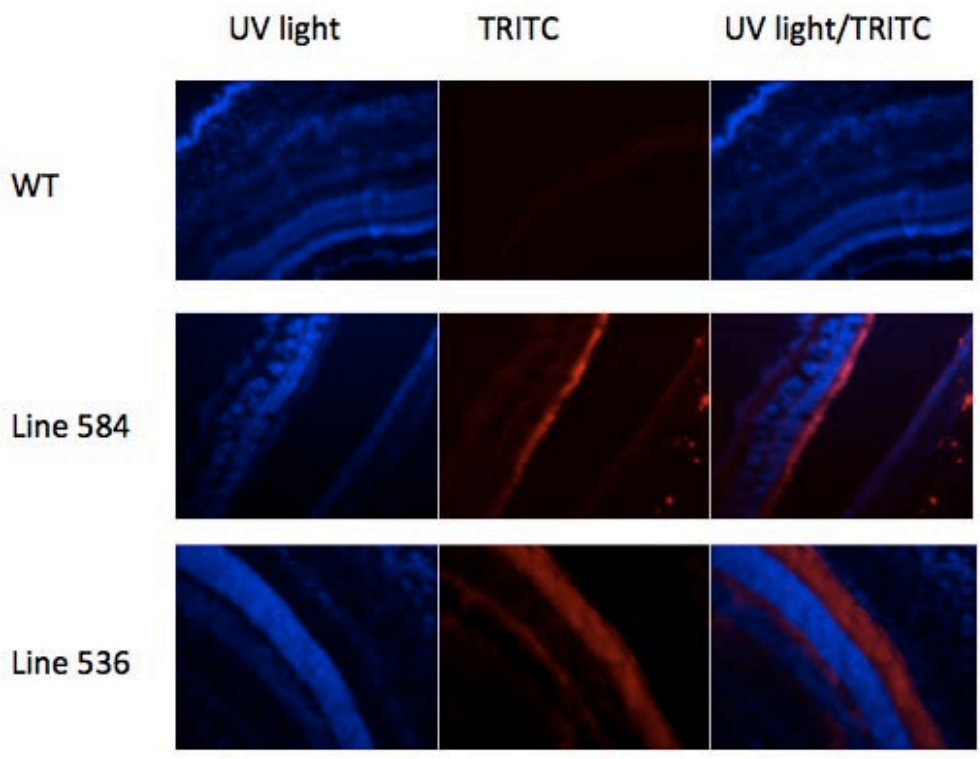

Figure 9: Picture showing the expression of the mCherry protein in the retina. Lines 536 and 584 are *NeuroD6* rats belonging to different founders, which express the mCherry protein in the amacrine cells under TRITC excitation. WT rat is a wild type littermate, which does not express the mCherry under the TRITC filter. The images on the right column are the overlapped images from the left, showing the other cells staining with DAPI and excited with a uV light.

The expression of the *NeuroD6* hDTR construct will be present in the amacrine cells and it can be assessed by exciting retinal samples to visualize the mCherry protein. All the transgenic animals expressed the mCherry protein in their retinas.

4.2.2.1.3. Expression in the Spinal Cord

Expression of the *NeuroD6* in the spinal cord is limited to the gray matter. The white matter (containing the ascending and descending neuronal tracts of the sensory and motor neurons) is located peripherally to the gray matter. The gray matter surrounds the central canal, has a higher cellular body density and exhibits a characteristic butterfly shape. The expression of the mCherry coincides with the gray matter, and it is visible in all the transgenic lines.

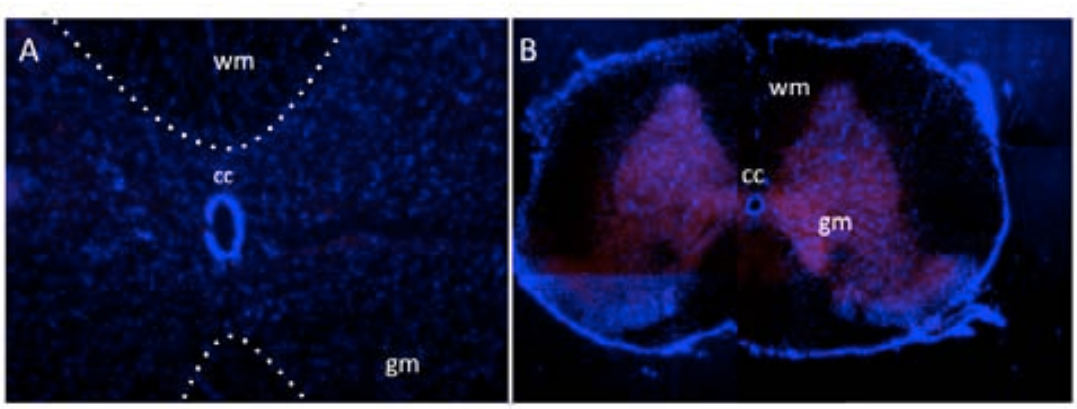

Figure 10: Picture showing the expression of the mCherry in the spinal cord. Cc: central canal, gm: gray matter, wm: white matter.
A) Overlapped pictures of a coronal section of the spinal cord of a WT rat, under the excitation of a TRITC filter and uV light. The gray matter is delimited by a dotted line.

B) Overlapped pictures of a coronal section of a *NeuroD6* rat under the excitation of a TRITC filter and uV light. The gray matter exhibits a high expression of the mCherry, with the characteristic butterfly shape.

4.2.2.2 Visualization in other body organs

Since the integration of the construct can have unexpected results in expression (as seen with the expression of the construct in the secondary visual cortex), the rest of the body was examined to look for unpredicted presence of the mCherry protein. The double transgenic model uses a Site Specific Recombinase (SSR) system that allows the expression of the hDTR to occur only in the tissues where both transgenes are expressed. This extra spatial restriction allows the administration of the toxin systemically, and prevents unwanted phenotypes.

However it is theoretically possible that both constructs could express in organs unexpectedly. The interaction of both constructs in the double transgenic model makes the cells where they are expressed vulnerable to the toxin. Therefore expression in organs other than the desired ones could result in several unexpected phenotypes, which under systemic administration of the toxin could be fatal. Hence tissue samples from heart, liver, kidney and spleen for transgenic lines and wild type animals were harvested. Samples were prepared for histology with a DAPI staining and visualised in order to explore for the presence of mCherry. When examined, no differences between transgenic lines were found in any of the organs, and the mCherry protein was not detected in any of the tissues.

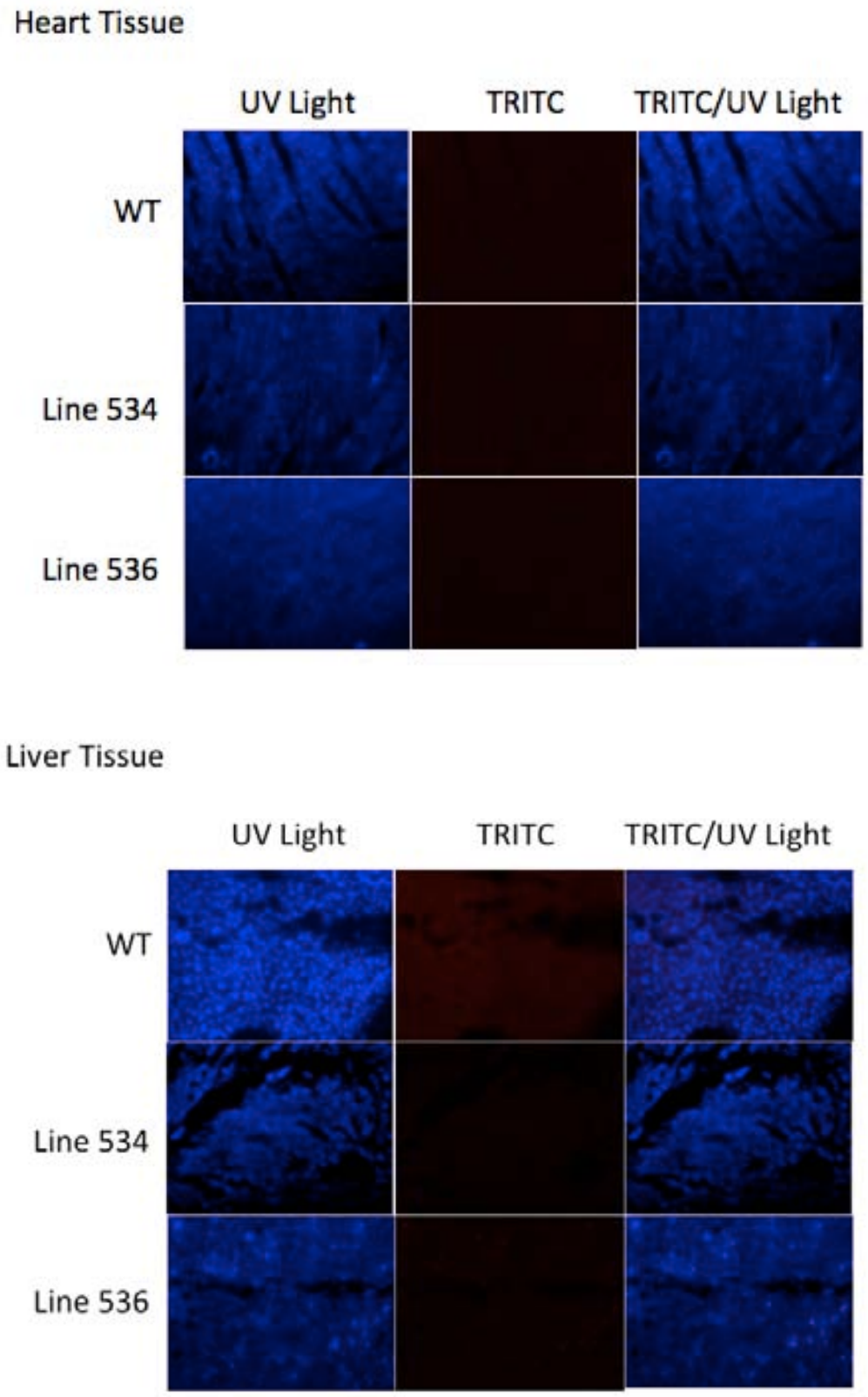

Figure 11: Expression of the mCherry in the heart and the liver. In both organs, a wild type is compared to two different *NeuroD6* lines, and all samples are stained with DAPI. Excitation under a uV light results in the imaging of all cell nuclei. None of the samples emits fluorescence under a TRITC filter. The overlapped images show no mCherry expression.

However, kidney and spleen tissue samples expressed autofluorescence, which was detected by the TRITC excitation. Exciting the tissues under other filters than TRITC shows the fluorescence pattern is not limited to the mCherry emission, as it overlaps with the fluorescence observed under the other filters. The mCherry protein could not be excited under the other filters. Consequently the expressed fluorescence is not linked to the transgene.

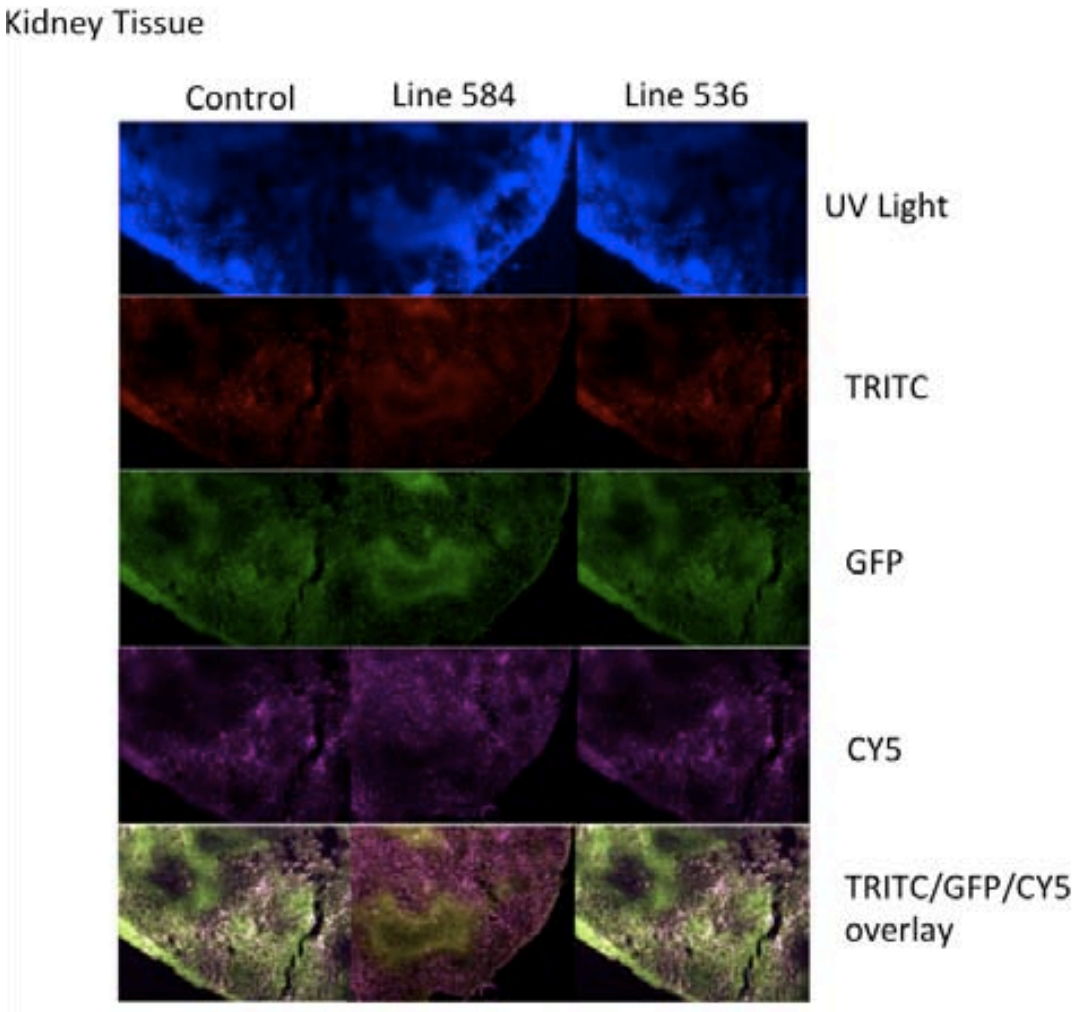

Figure 12: Expression of the mCherry in the kidney. In the left column a wild type is compared to two different *NeuroD6* lines (center and right column). All samples are stained with DAPI. Excitation under a uV light results in the imaging of all cell nuclei. All the samples emit the same fluorescence pattern under a wide variety of filters, including a TRITC filter.

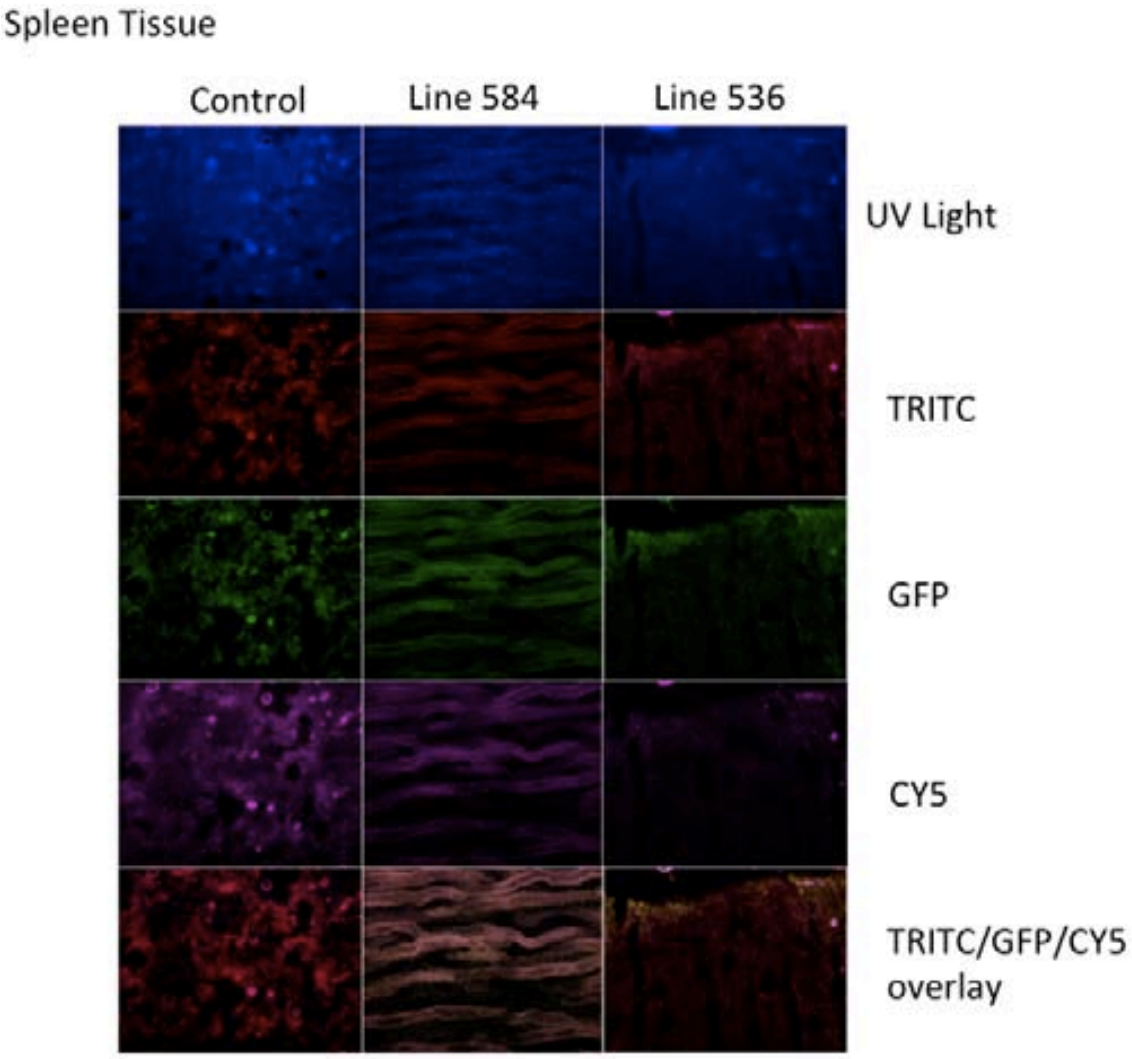

Figure 13: Expression of the mCherry in the spleen. In the left column a wild type is compared to two different *NeuroD6* lines (center and right column). All samples are stained with DAPI. Excitation under a uV light results in the imaging of all cell nuclei. All the samples emit the same fluorescence pattern under a wide variety of filters, including a TRITC filter.

4.3 STUDY 2: VALIDATION OF THE *NEUROD6* TRECK MODEL

In order to validate the TRECK rat model, we bred the *CamkII*α-Flpo and the *NeuroD6*-hDTR rat models together with the aim of producing an experimental group of *NeuroD6* TRECK rat models, which contain both transgenes. The aim of this breeding was to validate the insertion of both transgenes into the genome and validate its expression in the brain, as well as the recombination between the Flpo/FRT SSR system. In this section we describe the experiments to accomplish these goals.

4.3.1. Insertion of both constructs in the rat genome

To assess the insertion of both constructs, the DNA extracted from an ear clip was used to amplify the construct sequence by PCR. The set up is a PCR reaction with three sets of primers targeting the *NeuroD6* construct, the *CamkII*α-Flpo construct and the prolactin gene as a control. The PCR product was visualized and captured using a UV transiluminator (Alpha Innotech Corporation).

A positive band in the three reactions assessed the presence of both transgenes (*NeuroD6* TRECK rat). Following genotyping, *NeuroD6* TRECK, *NeuroD6* and wild type animals were selected for experiments, in order to validate the expression in the brain and the recombination between constructs.

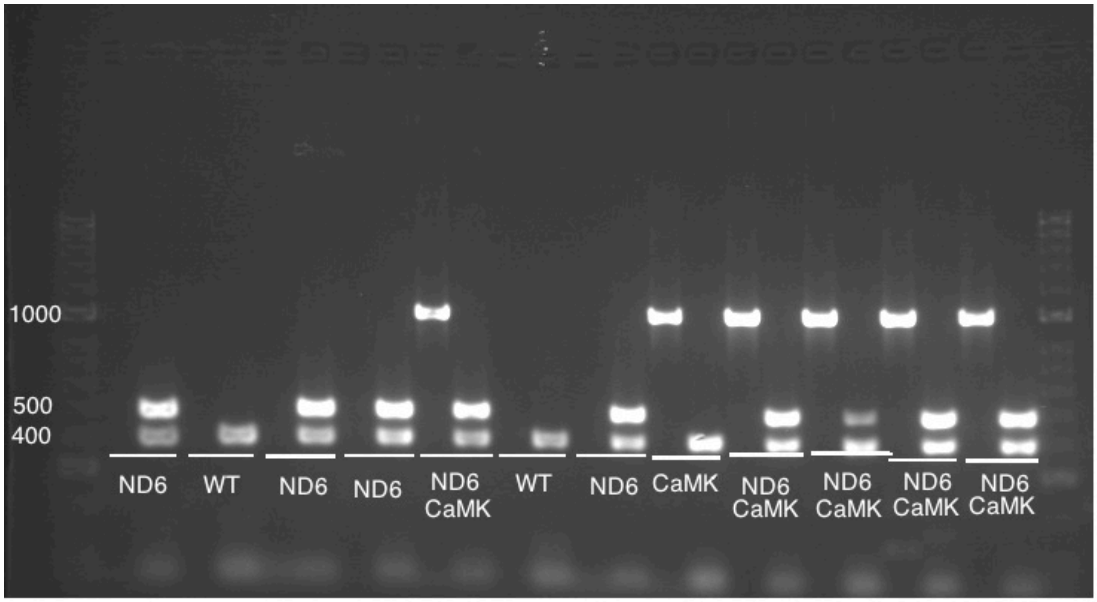

Figure 14: Picture of a gel showing the genotyping of *NeuroD6*/ *CamkII*α-Flpo breeding. The 400 bp product correspond to the Prolactine gene and acts as a positive control which should be amplified in all samples. The 500 bp product correspond to the *NeuroD6* construct amplification. The 1000 bp product is the *CamkII*α-Flpo construct amplification. Animals with the amplification of the three products are double transgenic *NeuroD6* TRECK rats.

4.3.2 Recombination and expression of both transgenes in the brain

In order to assess the recombination of both constructs in the brain, we designed two experiments. The first experiment aims to prove the recombination by PCR size product. The recombination of both constructs should change the size of the *NeuroD6* construct, since after recombination a big part of the construct should be excised. The second experiment focuses in the presence or absence of the mCherry protein as a way of identifying the possible recombination.

4.3.2.1 Assessing recombination using PCR product size

The flpo recombinase is a genetic recombination enzyme, which enables excission/insertion, inversion, translocation, and cassette exchange of genetic material (Gates and Cox, 1988). In the *NeuroD6* TRECK rat, the flpo recombinase interacts with the FRT sites by excising all the sequences between them. The whole *NeuroD6*-hDTR has a size of 3266 bp. By amplifying the construct through a PCR reaction, we can verify the size of the product. If recombination has occurred, the size of the amplified construct after recombination should be smaller (recombined construct) in the tissues where both transgenes are expressed and 3266 bp (non recombined, intact construct) in the rest of the body.

In order to compare the different products, DNA was extracted from heart, liver, hippocampus and ear clips for *NeuroD6* hDTR rats (single transgenic), *NeuroD6* TRECK rats (double transgenic), and wild type littermates. The heart, liver and ear clip DNA should contain the whole construct copies for all the animals except for the wild types. However, the DNA extracted from the hippocampus should contain also recombined construct copies for the double transgenic model.

Animals were given an overdose of Pentobarbitone, and once the absence of a heartbeat was confirmed organs where harvested and frozen by contact. Brain was dissected as a whole and the hippocampus was carefully dissected afterwards while the tissue was frozen. DNA was extracted and several PCR and long-range PCR reactions were set up with the primers to amplify the targeted

sequences. Methods for these experiments are further detailed in the Material and Methods chapter of this thesis.

Two set of primers were designed in order to estimate the size of the construct in the tissues were both transgenes overlap and to compare it with the rest of the tissues. The first set of primers target a fragment from the exon to the hDTR sequence (included). This set of primers, named SPAN, target a fragment that has a size of 2759 bp if the recombination has not occurred and 451 bp if the recombination has been successful.

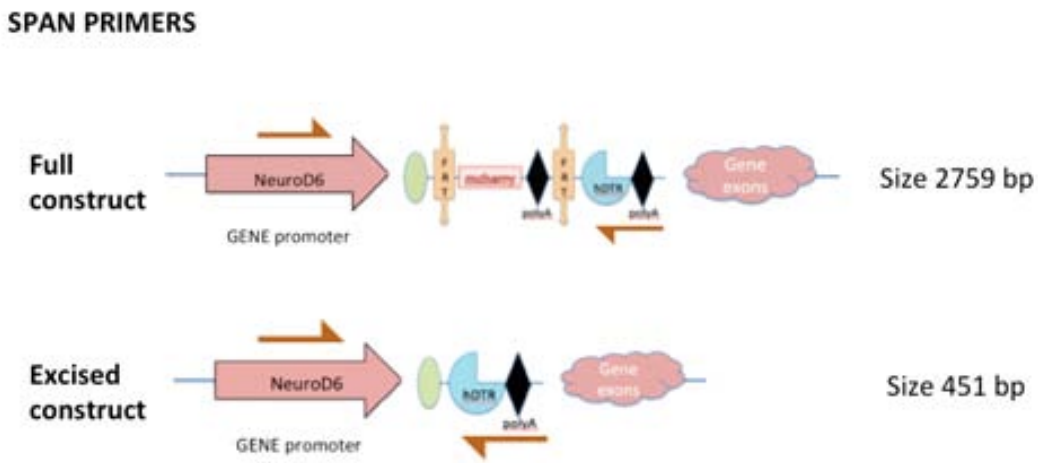

Figure 15: Image showing the *NeuroD6*-hDTR construct before and after the excision with the expected sizes in bp, and the targeting sites of the SPAN primers (orange arrows), from the gene promoter to the hDTR. The full construct has a size of 2759 bp, and the excised construct after the action of the flippase has a size of 451 bp.

The second set of primers target the region comprised between the *NeuroD6* gene promoter and the first exon. This set of primers, named EXON, aims to amplify the intrinsic *NeuroD6* gene (size 105 bp), the recombined construct (924 bp) and the intact construct (3266 bp).

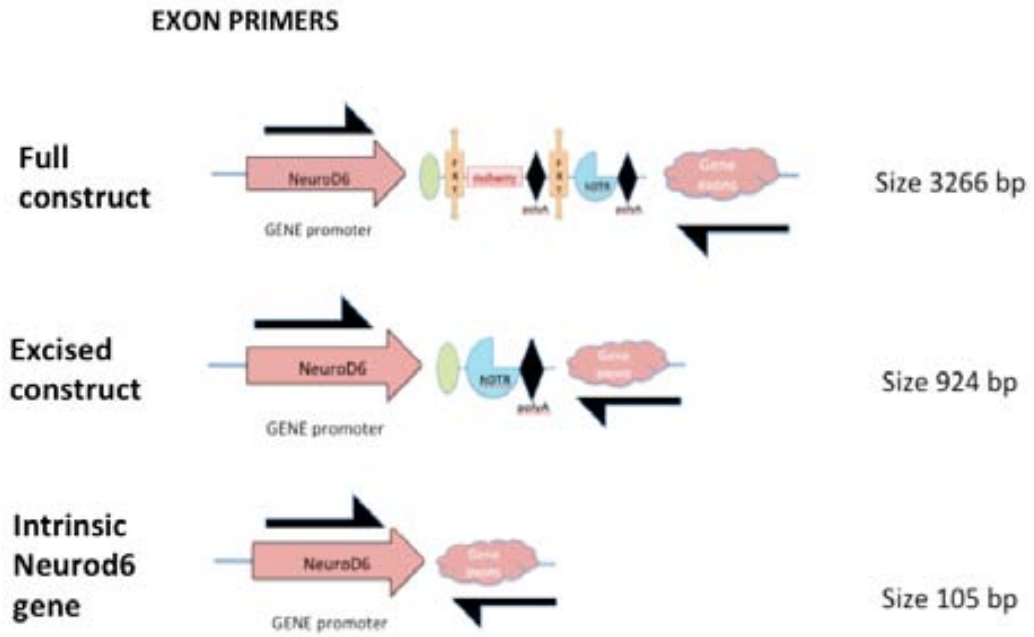

Figure 16: Image showing the *NeuroD6*-hDTR construct before and after the excision with the expected sizes in bp, and the targeting sites of the EXON primers (black arrows), from the *NeuroD6* gene promoter to the gene exons. The full construct has a size of 3266 bp, and the excised construct after the action of the flippase has a size of 924 bp. The intrinsic *NeuroD6* gene amplification product with the EXON primers would be 105 bp.

4.3.2.1.1. Results comparing hippocampus samples

When comparing the hippocampus DNA between double transgenic, single transgenic and wild type animals across both constructs, we consistently observed several unexpected amplified product sizes.

For the SPAN primers, expected sizes were for the recombined product 451 bp and for the intact construct 2759. There is no amplification at 2759 bp but there is amplification between 400 and 600 bp for one of the double transgenic lines and the single transgenic. This amplification cannot correspond to the recombined product, since the single transgenic would not have had

recombination. In addition, there are several unexpected bands at 2500 and 1500 bp for the double transgenic, as well as amplification at 800 and 600 bp, this last one shared by the double transgenic model with the single transgenic which also amplifies at 400 bp.

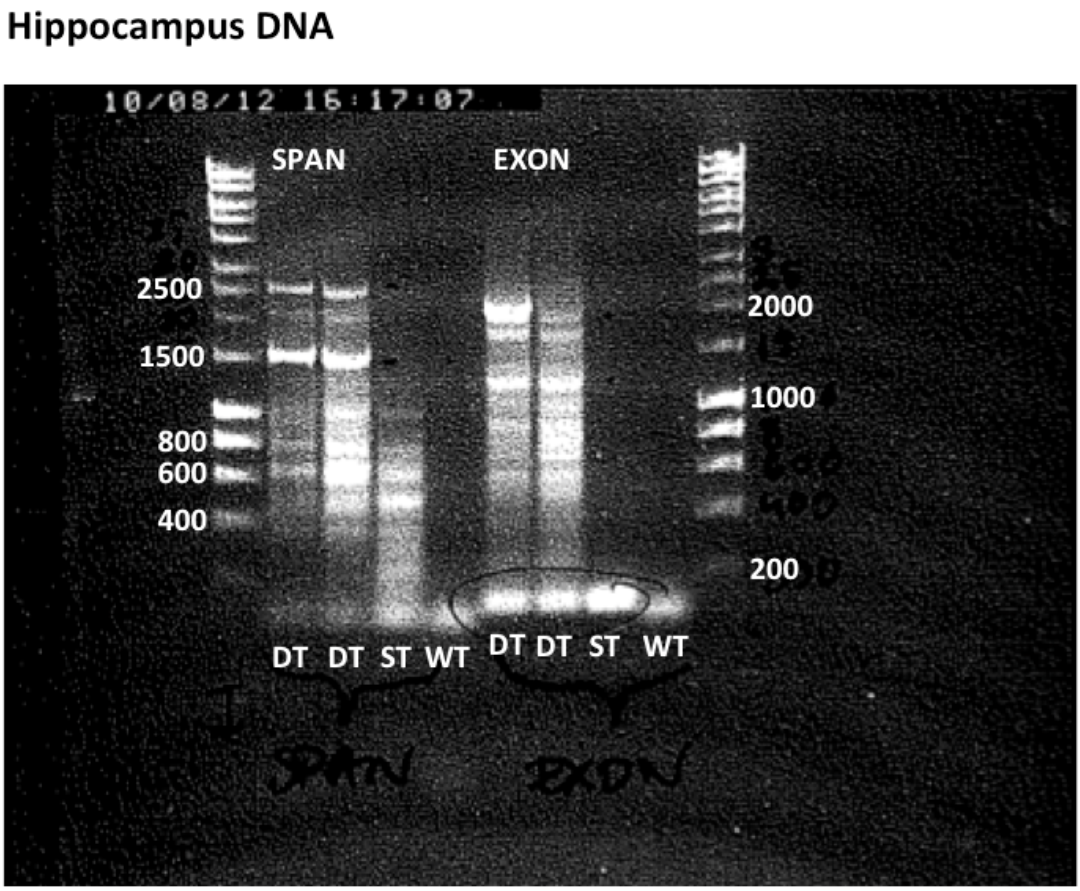

Figure 17: Picture of a gel showing the amplification using the SPAN and EXON primers for DT (double transgenic, *NeuroD6* TRECK rat), ST (single transgenic, *NeuroD6* hDTR rat), WT (wild type littermate).

Regarding the EXON primers, expected products were 3266 bp for intact construct, 924 bp for recombined product and 105 bp for the intrinsic *NeuroD6* gene. The 105 bp product amplifies in all the samples (data not shown clearly in the image but consistent over several replications) but the 924 bp product is not

clearly amplified though there is a faint glowing line, and the whole construct product (3266 bp) is not amplified. As in the previous case, there are also several unexpected amplified size products, at 2000 bp and at 1000 bp (fig. 17).

The fact that none of the expected products is present except for the intrinsic *NeuroD6* gene suggest that the construct is not intact and it might have lost some part of the construct when inserting in the genome. These results are further discussed in the Discussion section of this chapter.

4.3.2.1.2. Results comparing diverse body organs

When comparing for each animal different body organs and its expression, we had trouble amplifying any sequence using the EXON primers. However, the SPAN primers (which target the promoter of the construct up to the hDTR receptor) amplify several size products. For the expected products, only the amplified product between 400 and 600 bp is present, but the fact that it is present in all the body organs as well as in the single transgenic model indicates it is not the expected recombined construct that would have a 451 bp size (fig. 18).

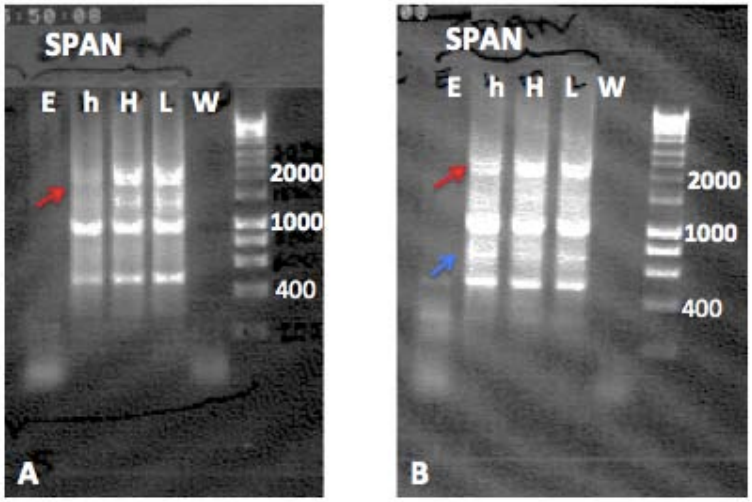

Figure 18: Picture of gels showing the amplification using the SPAN primers in different body samples. E: earclip, h: hippocampus, H: heart, L: liver, W: water. The ear samples show no amplification, probably due to the DNA being extracted to genotype the animals in a previous experiment and being kept for some time which possibly could have degraded.
A) Amplification of a *NeuroD6* TRECK rat DNA for all the body samples previously mentioned. The red arrow points at a missing product in the hippocampus amplification, consistent with recombination of both constructs. The rest of the samples from the same animal have all the bands.
B) Amplification of a single transgenic, *NeuroD6* hDTR rat littermate for all the body samples. The red arrow points at the amplification of the biggest product also in the hippocampus. The blue arrow points at some extra products, which are amplified in this single transgenic animal but not in its double transgenic littermate in the picture on the left.

As per unexpected sizes, there is amplification at 2000 bp and at 1500 bp for all the samples, except for the hippocampus sample in the double transgenic. This difference between organs suggests recombination within the hippocampus. The same happens with a fainter line at 1500 bp. However these size products do not correspond to the full construct, since the construct should be 2759 bp. This suggests (as experiments in section 4.2.1.1 of this chapter) that the construct has not integrated intact, and it might have lost some material.

The results suggest that recombination happens in the hippocampus of the double transgenic rat models that does not occur in any other body organ for the same rat, or in the single transgenic rat models.

In addition to these amplifications, there are some products that appear in the single transgenic models that we do not see in any of the samples for the double transgenic models. This unexpected amplified product has a size between 600 and 800 bp (fig. 18). These results will be further discussed in the discussion section of this chapter.

4.3.2.2 Assessing recombination through presence of mCherry

The mCherry protein is located between the FRT sites in the *NeuroD6* hDTR construct. In a double transgenic model, the expression of the *CamkII*α-Flpo in the brain should excise everything between the FRT sites. Therefore the mCherry protein should not be detectable in the double transgenics. Without recombination the mCherry protein should be visible when exciting the brain tissue at the microscope, analogously as in the *NeuroD6* hDTR single transgenic model. The tissue preparation was the same as described in section 4.2.2 of this chapter and further explained in the Material and Methods chapter. Brains from double transgenic and single transgenic animal were excited under a TRITC filter (pass bandwidth of 656-605 nm) to detect the mCherry protein.

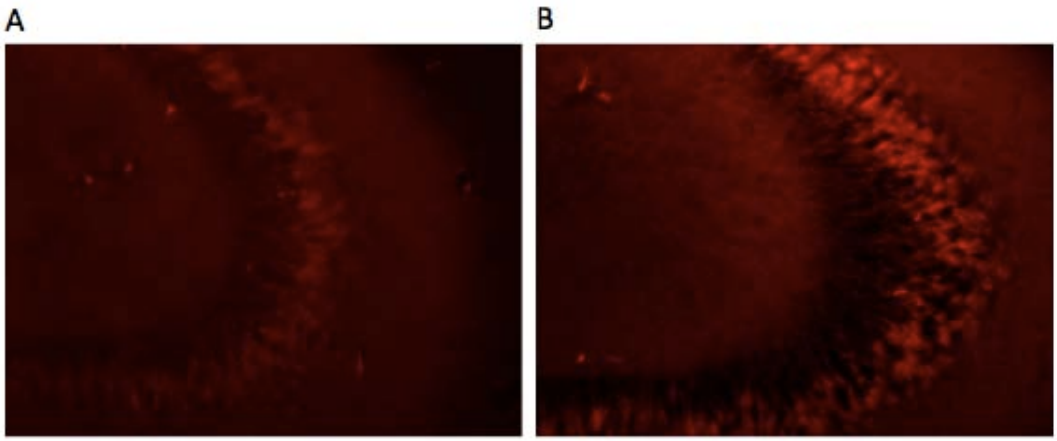

Figure 19: Picture of a detail of the CA3 subfield under a TRITC filter. A) Double transgenic *NeuroD6* TRECK rat. B) Single transgenic *NeuroD6*-hDTR rat.

In all cases animals belonged to the same littermates and when comparing single transgenic rats with double transgenics. The mCherry protein was observed in both rat models (fig. 19). The glowing seemed less intense for the double transgenic than for the single transgenic, but this is merely an anecdotal observation that could not be demonstrated.

4.4. DISCUSSION

The first objective of this chapter is to describe the experiments that validate the *NeuroD6* hDTR model at a genomic level and to demonstrate the insertion of the construct in the rat genome and the germline. It is also one of the goals to assess the expression of the construct at a protein level and the tightness of said expression into the targeted tissues. The experiments demonstrate that the construct has inserted in the germline, and by looking at the mCherry protein

expression, that the construct is expressed at a protein level. The construct is expressed in the expected tissues, but also in some unexpected areas within the brain.

The second objective of the chapter is to validate the recombination between constructs for the *NeuroD6* TRECK model, in order to investigate if the hDTR is expressed in the desired tissue. The results seem to indicate that the construct has integrated but it has a smaller size than expected, which suggests an incomplete BAC integration. There is also evidence of recombination within the hippocampus for the double transgenic rat, however the results of the SPAN and EXON experiments need further exploration.

4.4.1 Validation of the *NeuroD6* hDTR model

The construct integration into the rat genome is demonstrated by PCR amplification, and its integration into the germline is established by being capable of producing offspring that carries the construct. The mCherry protein presence in the brain indicates that the construct is expressed at a protein level. This expression is located where expected according to the literature (Entorhinal cortex, CA1-CA3 of hippocampus and amacrine cells in the retina) and also expressed in areas that we had not anticipated (hilus in the hippocampus, and the secondary visual cortex). Unexpected expression of a construct and variation between lines has been previously reported, as well as differences in cell

populations expressing a transgene (Feng et al. 2000), which makes necessary to explore for unpredicted expression of the construct.

4.4.1.1. Expression in unexpected areas in the brain

The *NeuroD6* gene has a role in the neuronal differentiation process at an embryonic stage (Uittenbogaard, Baxter, and Chiaramello 2010) as well as a role in the differentiation of the amacrine cells in the retina (Kay et al. 2011). Therefore the expression in the secondary visual cortex though unexpected is not unreasonable, and due to the small amount of neurons affected probably not deleterious to the required phenotype.

When observing the images we can see how some pyramidal cells disperse from the CA layer and spread overall the hilus. The expression of the construct in the hilus may support the suggestion that it is a polymorphic zone where the CA and the dentate gyrus blend. In 1934 Lorente de Nó suggested that the neuronal layer in between the fascia dentata should be considered part of the Cornus Ammonis, and named it CA3C and CA4 respectively (as cited in Andersen et al., 2007). However, in an article published in 1978, Amaral analysed the structure and morphology of the layer where the CA pyramidal layer merges with the dentate gyrus. Closer in morphology to the dentate gyrus than to the CA, Amaral argues that the hilus should be considered part of the dentate gyrus, rather than hippocampus proper (Amaral 1978).

4.4.1.2 Autofluorescence in Spleen and Kidneys

Autofluorescence was expected in spleen and kidney for all animals since both organs express it naturally, and it is not related to the construct or the expression of the mCherry protein. Kidneys express intense autofluorescence in the distal tubules of the nephrons as it has been previously reported (Maunsbach 1966; Qian et al. 2011). The red pulp of the spleen is rich in macrophages that exhibit autofluorescence (Ikeda et al. 1985) which can lead to false positives when analizing tissue under the microscope or using flow citometry (Monici 2005; Li et al. 2012). This indicates that the fluorescence is not connected to the mCherry protein and to the construct expression.

None of the body organs were expressing the construct, which makes the *NeuroD6* hDTR a specific model for the study of hippocampal function.

4.4.2. Validation of the *NeuroD6* TRECK rat model

4.4.2.1. Using the EXON and SPAN primers

The results to the experiments described in this chapter indicate that the BAC construct is incomplete, and has only partially integrated into the genome. This is suggested by the size of biggest amplifications achieved with primers that target the beginning and end of the construct (the EXON primers, fig. 17). These

products reach the maximum size of 2500 bp, instead of the 3266 bp predicted. Several other unexpected sizes are amplified suggesting multiple BAC fragments have integrated into the genome.

According to research by Van Keuren and others, in which they generate 707 founders using 70 different BACs, it is not unusual to generate founders with BAC fragments (Van Keuren et al. 2009). In their study, they analise 47 BACs for their complete integration and found out that only 17 of the 47 BACs had all the founders with intact constructs. It has been proven that DNA molecules can randomly break after entering the cell due to size (Bishop and Smith 1989) leading to fragmented transgenes. Moreover the likelihood of having partial BAC integrations has been estimated in 17-36 % (Chandler et al. 2007a; Van Keuren et al. 2009).

It is also possible for the construct to have multiple integrations and at different genomic sites. It has been reported that this multiple-copy BAC insertions usually have at least one full-length monomer (Chandler et al. 2007b). The unexpected amplifications that we observe in our results suggest that the *NeuroD6* hDTR BAC has multiple integrations of fragmented copies of the BAC.

These fragments are all consistent through double transgenic and single transgenic, with the exception of the hippocampus samples on the double transgenic models (fig. 18). The loss of the bigger size product (2000 bp) precisely in the hippocampus of the double transgenic suggests that there is recombination, and that this recombination is specially limited to the

hippocampus as per the action of the Flpo recombinase present in the *CamkII*α-Flpo rat model. This is supported by the fact that the DNA that has been extracted from other organs for the same animal display the 2000 bp product. The loss of product in the hippocampus DNA is not observed in the single transgenic models, where there is no flippase to recombine the constructs (fig. 18). These results suggest that if the 2000 bp product is a fragmented BAC, this fragment at least contains the two FRT sites, and the action of the flippase present in the *CamkII*α-Flpo model is able to excise them.

The fact that only one product disappears when recombining indicates that the rest of products correspond to more than one copy of the BAC, and that they must be fragmented. Despite the fragmentation, the SPAN primers target from the exon of the construct to the hDTR sequence, thus all the fragments amplified contain at least the hDTR sequence. This is of vital importance as if the missing sequence would be the one with the hDTR, it would be impossible to ablate the neurons with the administration of diphtheria toxin in the subsequent experiments.

4.4.2.2 Histological analysis of mCherry expression

The second set of experiments described in the section 4.3.2.2 of this chapter aim to prove the recombination by visualising brain slices on the double transgenic models. If the FRT sites have been excised, there should be no expression of the mCherry protein and no fluorescence would be detected. As there has been loss

of some bands in the PCR product from the hippocampus tissue for the double transgenic, the expected result is no expression of the mCherry fluorescence. Contrarily, all the double transgenic animals express the mCherry protein (fig. 19). However, this does not necessarily mean that there has been no recombination due to the fragmentation and multiple integration of the BAC. This multiple integration suggests that some of the incomplete fragments could contain the sequence for the mCherry protein. Under these circumstances, expressing the mCherry protein does not exclude the possibility of recombination, as multiple fragmented copies of the BAC seem to converge in the same animal. Thus mCherry expression and recombination could coexist in the same hippocampus.

Because a single molecule of the diphtheria toxin in the cell cytosol is capable of induce apoptosis, if the cells in the CA1-CA3 are expressing the hDTR, it seems that the ability of the diphtheria toxin to ablate these cells may be intact.

4.5. CONCLUSION

In conclusion, the *NeuroD6* hDTR model has integrated several copies of the construct with multiple fragmentations. These are expressed at a protein level in the targeted tissues and in two other locations within the brain. The construct is not expressed anywhere else in the rat body, making it an adequate model for the study of hippocampal function. The unexpected areas cover a very small

population of neurons and are assumed not to be deleterious to our desired phenotype.

The *NeuroD6* TRECK model has recombined in the hippocampus, proving the overlapping expression of both constructs. The integration of BAC fragments make the *NeuroD6* TRECK rat model exhibit phenotypes that are related and unique to the *NeuroD6* hDTR model, since some of these several copies may not be able to undergo recombination, as it is the expression of the mCherry protein. Since recombination is proven, the fragmented BAC insertion though not advantageous may not to be detrimental to our model.

These results suggest the double transgenic model can be useful to ablate the CA1-CA3 cells. Further testing is required to estimate the ability of the model to ablate the cells and the functionality of the hDTR.

5. DIPHTHERIA TOXIN EXPERIMENTS

5. DIPHTHERIA TOXIN EXPERIMENTS

In previous chapters we introduced the experiments that tested whether the construct was inserted into the *NeuroD6* model, and if the double transgenic (*NeuroD6* TRECK rat) had a recombined construct. The next step is to validate the ability of the model to ablate neurons. We focused on different experiments administering the diphtheria toxin in order to achieve neuronal death. The aim of this chapter is to describe said experiments and to discuss the ability of the model to ablate neurons.

5.1 INTRODUCTION

Diphtheria toxin (DT) is the exotoxin produced by *Corynebacterium Diphtheriae*. Its toxicity is strictly dependent on being incorporated into the cell cytosol (Yamaizumi et al. 1978). DT has two subunits: DT-A and DT-B. The DT-B subunit binds to the toxin receptor in the cell membrane and incorporates the DT-A subunit by endocytosis. When reaching the cytosol, the DT-A subunit inactivates the polypeptide chain elongation factor 2, inhibiting protein synthesis and causing the cell to die (Pappenheimer et al. 1982; Choe et al. 1992; Sapoznikov and Jung 2008). Once the DT-A is in the cytosol, one single molecule of DT is capable of killing one single cell (Yamaizumi et al. 1978).

The cell receptor for which the DT has affinity is the heparin-binding epidermal-growth-factor-like growth factor (HB-EGF) transmembrane form, which binds with the DT-B subunit of the toxin (Furukawa et al. 2006). However, the murine transmembrane HB-EGF receptor does not offer affinity to the DT-B, preventing the DT-A fragment from reaching the cell cytosol. Consequently, rats and mice are naturally immune to DT, and their cells are at least 10^5 times more resistant to DT than human cells (Saito et al. 2001). The TRECK rat model takes advantage of this difference by expressing the primate HB-EGF transmembrane form in the targeted murine cells and administering the toxin systemically, only affecting the cells with the primate receptor.

However a shortcoming of incorporating this receptor is the increased activity of the EGF (epidermal like growth factor), overexpressed by the additional number of receptors. This overexpression can cause abnormalities in transgenic mice and rats (Furukawa et al. 2006). For this reason, the ND6-hDTR rat model contains a mutated version of the primate receptor developed in Kenji Kohno's laboratory, named I117A/L148V. This receptor differs from the wild type in five amino acids that have been mutated, changing the expression of the receptor in order to eliminate EGF like activity while allowing the binding of diphtheria toxin. The I117A/L148V is resistant to cleavage of the membrane-anchored form for HB-EGF, but its DT sensitivity is almost similar to a wild type receptor (Furukawa et al. 2006).

After proving expression of the construct at a protein level through the mCherry protein, and recombination in the double transgenic and presence of the hDTR at

a genomic level, different experiments with the diphtheria toxin were designed in order to test the activity of the receptor. A review of available literature suggests a wide variety of dosing regimes, from single doses (Pappenheimer et al. 1982; Saito et al. 2001; Wharram et al. 2005; Furukawa et al. 2006) to several mild doses (Buch et al. 2005b; Arruda-Carvalho et al. 2011; Golub et al. 2012; Sonntag et al. 2012), and a wide variety of concentrations ranging from 5ng/kg (Saito et al. 2001) up to 112ug/kg (Arruda-Carvalho et al. 2011) over the course of several administrations. Only one paper in the available literature has performed diphtheria dosing with rats instead of mice (Wharram et al. 2005). Therefore a large variety of doses and administration regimes had to be evaluated in order to estimate the best dose to achieve neuronal death. This chapter aims to describe the experiments we performed and discuss the receptor's capacity to ablate the targeted cells.

5.2 STUDY 3: DIPHTHERIA TOXIN EXPERIMENTS

5.2.1 Experiment 1: Medium dosage testing

The *NeuroD6*-hDTR model allows for systemic dosing as the diphtheria toxin crosses the blood brain barrier (Wharram et al. 2005). The first set of experiments was designed to administer the toxin systemically through an injection in the peritoneal cavity (lower right or left quadrant in the abdomen). This same administration method was reported in several previous articles (Wharram et al. 2005; Arruda-Carvalho et al. 2011; Sonntag et al. 2012) as the

preferred administration method. The volume injected was always 1 ml as recommended in the Handbook of Animal Management and Welfare (Lloyd and Wolfensohn 2003). Given the risks that injecting diphtheria toxin poses to the researchers, all animals were anaesthetised for the procedure.

5.2.1.1 Experimental Design

The experiment tested simultaneously four doses and had four *NeuroD6*-hDTR males and female rats per condition. It has been previously published that gender has no influence in diphtheria toxin dosing (Wharram et al. 2005).

Doses tested were the following: one acute dose of 50 µg/kg, 35 µg/kg, 25 µg/kg and 15 µg/kg. The total injection volume was 1 ml. Animals on the control group received the same injection volume of PBS.

DOSE	VOLUME	TOXIN CONCENTRATION	SUBJECTS
Dose A	1 ml	50ug/kg	4
Dose B	1 ml	35ug/kg	4
Dose C	1 ml	25ug/kg	4
Dose D	1 ml	15ug/kg	4
Control	1 ml	0ug/kg	4

Figure 20: Table showing the dosing regime for the medium dosing experiment. All animals were administered 1 ml volume at different concentrations or PBS in the case of the controls.

Perfusing at different times aimed to establish that the effects of the toxin would be fully observable, and also that the effects would be stable over time. Since the final experimental design aims to include behavioural testing, the experiments would have to accommodate behavioral testing immediately after toxin dosing and before the perfusion, and animals would always be perfused weeks after their dosing.

For this purpose, the range of doses described in this first toxin experiment was performed with four animals per condition. Half of the animals were perfused seven days after their first dosing (two animals per condition). The other half of the animals (n=10) was perfused 28 days after the first dosing.

5.2.1.2 Results

When analysing the brain images, the first thing we wanted to observe was if the administration of the diphtheria toxin had altered the morphology of the CA1-CA3 neuronal layer. Nissl staining uses aniline dye to stain RNA and DNA, and stains neurons and glial cells in a purple-blue colour. This staining allows the observation of cell bodies and the cytoarchitecture of brain structures. We performed Nissl staining using Cresyl Violet to observe the CA1-CA3 sections and an overall image of the cell bodies. When inspecting the brains with the Nissl staining to assess the overall aspect of the brains, no differences were observed between dosed animals and controls (fig. 21). Both at 10X and 20X magnification the CA3 structure looks similar for the wild type control, the double transgenic

rat control and the double transgenic rat with a diphtheria toxin. Regarding thickness, distribution, density and architecture of the neuronal layer, no differences were appreciated.

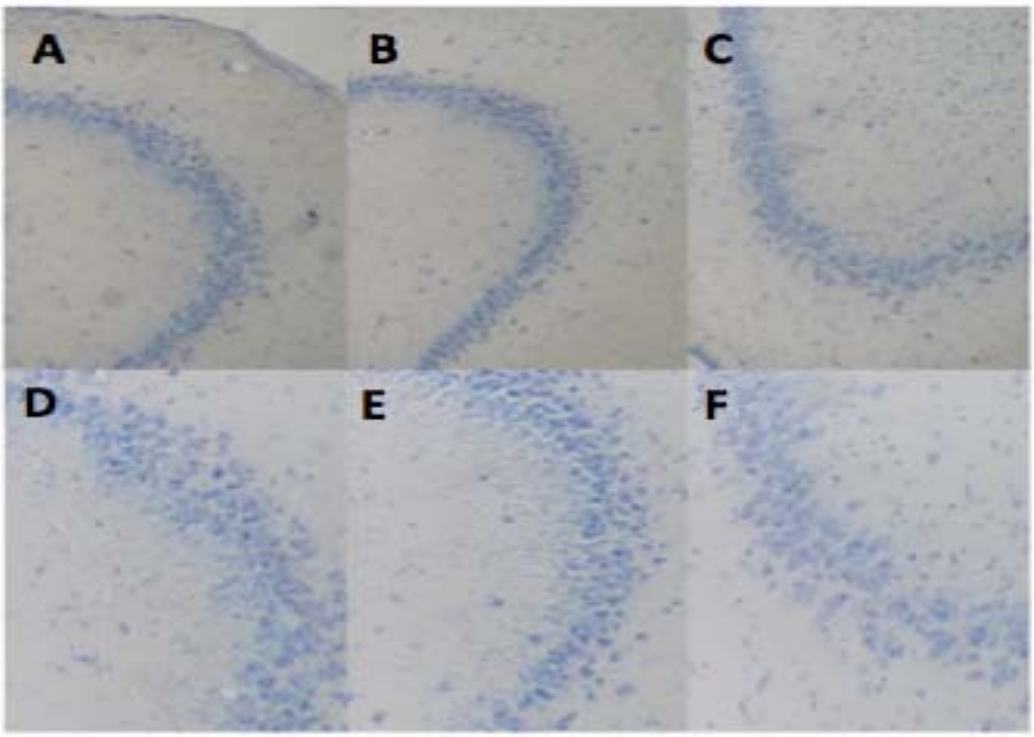

Figure 21: Picture of a Nissl staining of the CA3 subfield at 10x (A, B, C) and 20x magnification (D, E, F). Picture A and D correspond to the highest dose (50 µg/kg), picture B and E correspond to the lowest dose (15 µg/kg) and pictures C and F correspond to the control. In all cases no differences can be observed between the three different doses in the CA3 subfield.

In order to have a better understanding of the effects of the toxin, we counted the neurons labeled with NeuN staining. The NeuN antibody recognizes a neuron-specific nuclear protein in mature neurons in the brain and spinal cord of vertebrates (Sarnat, Nochlin, and Born 1998). Labeling the neurons allows glial cells and other structures to remain in the background.

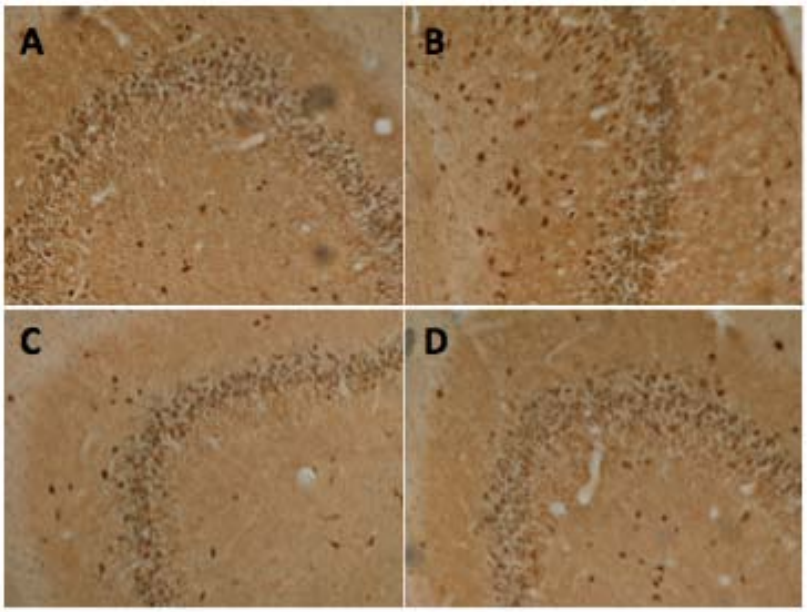

Figure 22: Pictures of CA3 subfields labeled with NeuN antibody, which stains healthy neurons. A: Dose A (50 µg/kg), B: Dose B (35 µg/kg), C: Dose C (25 µg/kg), D: Dose D (15 µg/kg).

This staining allowed the counting of healthy neurons in the brain slices in order to compare between dosing regimes, and between dosed animals and controls. Two random slides per animal were analysed using the Image J analysis software (Fiji). The counting was done blind to the experimental set up, except for perfusion day. However no differences can be observed between groups, or between controls and dosed animals (fig. 22). The analysis of variance, with data from 40 brain slices shows there is no significant difference in the number of neurons present in the hippocampus after any of the doses tested (n=40, $F_{5,34}$= 0.31, p= 0.90). It also shows none of the doses has a different effect than the control dose.

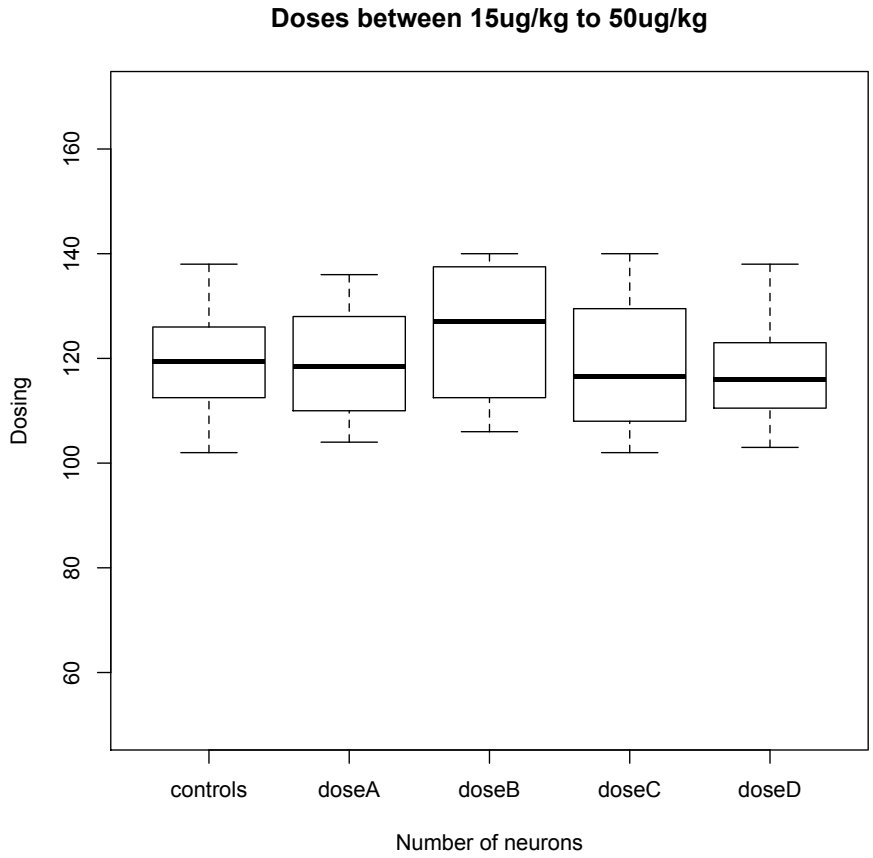
Doses between 15ug/kg to 50ug/kg
Dosing
60
80
100
120
140
160
controls
doseA
doseB
doseC
doseD
Number of neurons

H3

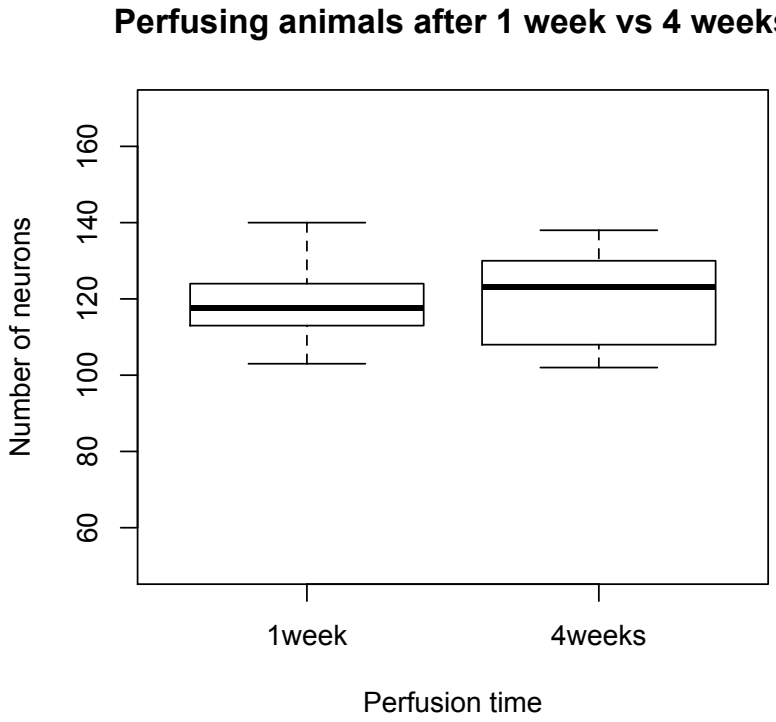
Perfusing animals after 1 week vs 4 weeks
Number of neurons
60
80
100
120
140
160
1week
4weeks
Perfusion time

H0

the available literature is 50 µg/kg for an acute dosing (Saito et al. 2001; Furukawa et al. 2006) and 112 µg/kg as total amount given after a week of daily low dosing (Arruda-Carvalho et al. 2011).

Four double transgenic rats were given a single low dose of 4µg/kg and four double transgenic rats were given a single high dose of 120µg/kg. Four double transgenic rats were injected with PBS to provide a control.

DOSE	VOLUME	TOXIN CONCENTRATION	SUBJECTS
Dose E	1 ml	120 µg/kg	4
Dose F	1 ml	4 µg/kg	4
Control	1 ml	0 µg/kg	4

Figure 25: Table showing the dosing regime for the acute dosing experiment. All animals were administered 1 ml volume at different concentrations or PBS in the case of the controls.

5.2.2.2 Results

Animals were perfused after a week and brains were processed as described in the previous experiment. In order to analyse the data, NeuN staining was performed to be able to count the cells in 24 brain slices corresponding to the three different dosing regimes.

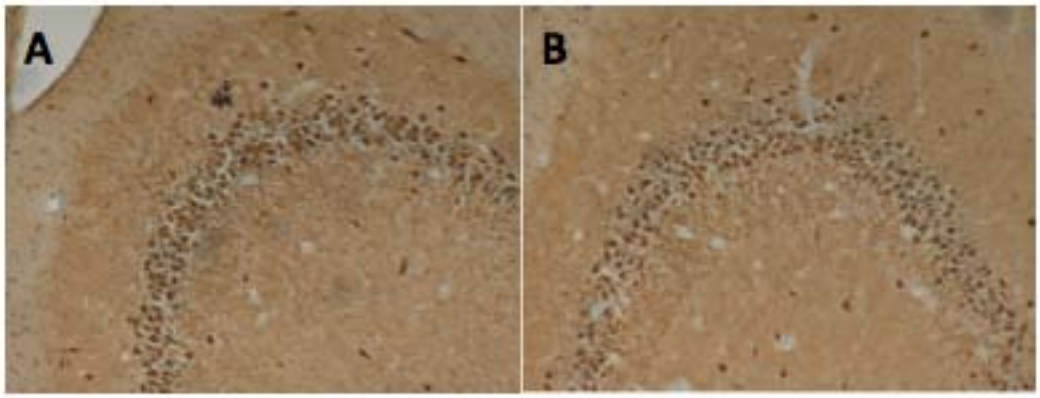
A
B

Acute high and low diphtheria dosing
Number of neurons
60
80
100
120
140
160
controls
doseE
doseF
Dosing

5.2.3 Experiment 3: Toxin infusion

In order to test the administration of the toxin we designed another experiment, which administered the toxin subcutaneously via an osmotic mini pump. Osmotic mini pumps infuse substances at a stable rate achieving a constant dosing by osmosis. The mini pump implantation is a simple surgical procedure, which consists in inserting the mini pump through a scapular incision to be placed caudally in the dorsum (full surgery procedures are detailed in the Material and Methods chapter of this thesis).

The mini pumps were loaded with a dose of 120 μg/kg to be infused during 14 days giving a daily dose of 8.5 μg/kg at a rate of 0.35μg/kg per hour. Four double transgenic rats and two controls underwent mini pump implantation to infuse diphtheria toxin or PBS accordingly. Animals were perfused after 14 days and brains were processed identically to all the other experiments.

5.2.3.1. Results

In order to assess if there was any neuronal death when administering the toxin via osmotic mini-pump, a TUNEL fluorescein staining was performed in the tissue. The staining revealed a normal CA1-CA3 structure, with no changes in the neuronal layer or cell morphology. No neuronal death was detected in any case (fig. 30, in section 5.2.5 of this chapter).

5.2.4 Experiment 4: Lower and more frequent dosing

To test if it was more effective to give the same dose in lower but more frequent doses, four double transgenic animals were subjected to the same amount of toxin but in different dosing regimes. Two of the animals received daily 10 µg/kg injections; whereas two other animals received two 20 µg/kg doses with one day break in between, with the total dose being in all cases 40 µg/kg. Control received daily PBS injections for four days (fig. 28).

DOSE	Day 1	Day 2	Day 3	Day 4	TOTAL DOSE
Dose A (2 subjects)	10 µg/kg	10 µg/kg	10 µg/kg	10 µg/kg	40 µg/kg
Dose B (2 subjects)	20 µg/kg	---	20 µg/kg	---	40 µg/kg
Control (2 subjects)	PBS	PBS	PBS	PBS	0

Figure 28: Table showing the dosing regime for the mild daily and alternate days dosing experiment. All animals were administered 1 ml volume at different concentrations or PBS in the case of the controls.

In order to detect neuronal death, we performed a Fluorojade C staining. This staining is a polyanionic fluorescein staining which selectively and specifically binds to degenerating neurons. Fluorojade C binds to degenerating neurons independently of the trauma, however the target mechanism is unknown

(Schmuck and Kahl 2009). Using Fluorojade C, we aimed to label the neurons that were degenerating after diphtheria dosing.

5.2.4.1 Results

No differences between the samples of controls and cases were found in the Fluorojade C staining (fig. 29), since we could not distinguish any labeling in any cell. Despite a high background in all the images, all the cell bodies in the brain were equally visible and there was no labeling in any of the structures of the CA1-CA3 or anywhere else in the brain.

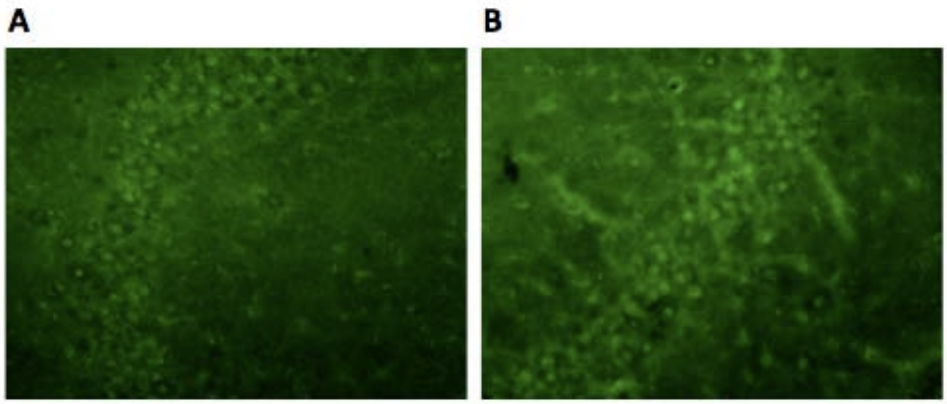

Figure 29: Picture of a CA3 subfield stained with Fluorojade C for the mild and daily dosing regime experiment. A) dosing regime A (daily dosing). B) dosing regime B (alternate days dosing).

We performed a Fluorescein staining with a positive control as described in section 3.2.6 of this chapter to corroborate the results obtained with the Fluorojade C staining (data not shown). The results are consistent through both stainings, with no labeling for degenerating neurons in any of the experimental doses tested in this experiment.

5.2.5. Histological analyses with fluorescein staining

To further the analysis, an extra staining was performed for all the experiments previously reported in order to confirm the absence of neuronal death. This was intended to bring some consistency in the analysis of all the samples with a positive control.

With this aim, we performed a TUNEL fluorescein staining. During apoptosis, genomic DNA strands break and consequently generate fragments of low molecular weight DNA. The In Situ Cell Death staining uses TUNEL technology to label low molecular weight DNA strands. This allows the detection of individual apoptotic cells and the precise labeling of apoptotic neurons. We aimed to label the neurons undergoing apoptosis after the diphtheria dosing.

In order to have a positive control, we used the Bel/Bel mouse model. This mouse model has an onset of neuronal death from day P18-19 (Oliver et al. 2011). The neuronal death occurs when cerebellar neurons become apoptotic. The tissue from Bel/Bel mice used in this experiment was kindly provided by Dr. Peter Oliver (University of Oxford).

To assess if the tissue preparation was interfering with the results, three different conditions were tested for the TUNEL fluorescein staining. Slides were either:

A) Incubated with a Protease K treatment (20 µg/ml in 10 mM Tris/Hcl, ph: 7.4-8) in a humid environment at 21-37°C during twenty minutes. Then rinsed with PBS two times for five minutes and followed a common staining step.
B) Permeabilisation solution: 0.1% Triton X-100 in 0.1% sodium citrate freshly prepared for 8 minutes. Then rinsed with PBS two times for five minutes and followed a common staining step.
C) Microwave radiation: slides were immersed in an antigen solution (2.94 gr of sodium citrate in 500 µl of concentrated hydrochlorid acid) microwaved at 450 W for five minutes. Then rinsed with PBS two times for five minutes and followed a common staining step.

No differences could be seen between any of these pre-steps (data not shown), and the staining did not label any neurons for the *NeuroD6* TRECK rat samples, but did label all the positive controls (fig. 30) . The TUNEL fluorescein staining reported no neuronal death after diphtheria dosing; irrespective of administration route, dose concentration, dosing rate, or perfusion time.

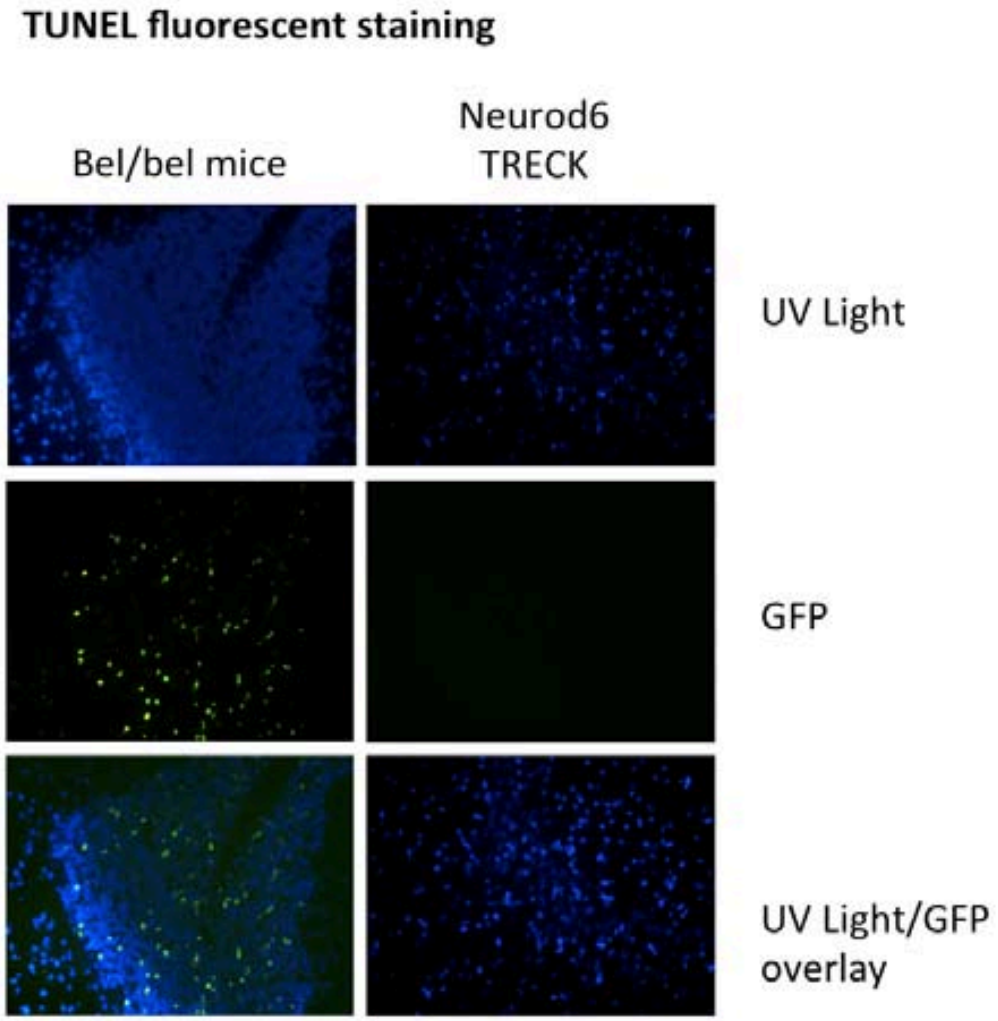

Figure 30: Picture showing the CA3 subfield in the *NeuroD6* TRECK rat (right column) and the cerebellum of Bel/bel mice (left column), both with a TUNEL fluoresceing staining and mounted with DAPI. Cells which are apoptopic get labelled and are visualised under a GFP filter with a bright green. The images on the third row are the overlapped images with the uV light and GFP excitation. There are no *NeuroD6* TRECK rat cells which are apoptotic.

5.3. DISCUSSION

The toxin experiments reported in this chapter aimed to achieve neuronal death in the cells expressing the hDTR. Consequently the designed experiments included previously tested dosing regimes in the literature. Additionally, they

also add a higher dose than ever reported before as well as diverse administration regimes. To analyse the samples and to detect the potential neuronal death, three different tissue treatments were tested as well as several stainings. The analysis focuses on the biochemical changes in the cell induced by apoptosis rather than the morphological changes. Finally a staining was performed for all the samples with a positive control for comparison. The stainings use biochemical signals to label the degenerating neurons to be visualised in the microscope, or the healthy neurons to be counted.

However it was not possible to achieve any neuronal death irrespective of administration route, dose concentration, dosing rate, or perfusion time. In this section I discuss the possible limitations to these experiments and suggest future work in order to tackle them.

5.3.1 Toxin administration route and rate

It has long been established that diphtheria toxin crosses the blood brain barrier, which allows systemic dosing (Pappenheimer et al. 1982). The available literature suggests injection as the preferred administration route for diphtheria toxin, with successful results when administered in the peritoneal cavity in rats (Wharram et al. 2005), or in mice (Buch et al. 2005c; Arruda-Carvalho et al. 2011; Sonntag et al. 2012). Therefore the experiments used the same administration route as suggested in these papers.

However, the acute dose via intraperitoneal injection toxin administration showed no effect. Since administering the toxin in a lower but more frequent dose manner had successfully increased the ablation rate in some experiments with mice (Buch et al. 2005c), two alternative administration method experiments were designed.

In the first one, administration of the toxin was via slow-release mini-pump infusion during 14 days. The mini-pump releases the toxin subcutaneously, which has not been used in diphtheria toxin dosing before, but the use of mini-pumps has proven a successful administration route for substances that can cross the blood brain barrier and have successfully ablated neurogenesis in the hippocampus in previous works (Groves et al. 2013b).

Secondly we tested if daily injections or injections every second day could achieve neuronal death. Some experiments have reported an administration regime where the diphtheria is given via an intraperitoneal injection at daily low doses (Buch et al. 2005c; Arruda-Carvalho et al. 2011) or at low doses every second day (Golub et al. 2012; Sonntag et al. 2012).

Both of these administration routes and frequency regimes did not prove more successful than the intraperitoneal acute injection. No neuronal death was observed in any of the conditions; despite testing all the administration regimes that prove successful in other reported works.

5.3.2 Toxin dose concentration

The literature reports a wide variety of dosing concentrations to achieve cell ablation using the hDTR receptor in mice. Dosing in rats it has been reported only in one article, which has an hDTR model for podocyte depletion. The experiment described dose ranges from 10ng/kg up to 5 μg/kg for the case subjects and 50μg/kg for the control subjects. This rat model causes podocyte depletion and consequent nephropathy, which caused death in every transgenic rat dosed 50ng/kg and beyond (Wharram et al. 2005). However, other mice models administer doses range from 5ng/kg (Saito et al. 2001) up to 112μg/kg (Arruda-Carvalho et al. 2011).

Two aspects make the *NeuroD6* TRECK rat dosing able to start with higher doses than those described in the work of Wharram and colleagues (Wharram et al. 2005). First, the mutated version of the hDTR (I117A/L148V) that is incorporated in our model, has a decreased sensitivity to diphtheria toxin compared to that of the wild type (Furukawa et al. 2006). Therefore a higher dose might be necessary for the mutated version of the hDTR to reach the same efficacy than the wild type hDTR. Secondly, the *NeuroD6* TRECK rat phenotype would not lead to a lethal consequence even if all the cells in the CA1-CA3 were ablated, since the loss of neurons in CA1-CA3 is not incompatible with life. Complete podocyte ablation however, leads to nephropathy and consequently to renal failure. Considering our phenotype is not life threatening, our diphtheria toxin experiments started with a dosing range slightly superior to most of the experiments with a range from 0.35μg/kg per hour up to 50μg/kg per dose.

Taking into account that we could test a higher concentration, we tested a dose of 120μg/kg. This dose is higher than any other dosing reported by the literature in rodents, whether they were transgenic or controls. The highest reported acute dose administered in rats and mice is 50μg/kg (Saito et al. 2001; Wharram et al. 2005; Furukawa et al. 2006) and the highest dose as the total amount given after a week of daily low dosing is 112μg/kg (Arruda-Carvalho et al. 2011). Furthermore, the experiments that use the mutant version of the hDTR achieve successful cell death with dosing around 500ng/kg (Furukawa et al. 2006). Other work reports that 50μg/kg is a dosing two orders of magnitude higher than required to kill wild type hDTR cells (Saito et al. 2001). Therefore our tested range of doses should have been more than sufficient to achieve neuronal death. This suggests that our doses should have been effective in killing the cells expressing the hDTR.

5.3.3 Perfusion time

In the only article available describing diphtheria dosing to rats in other to achieve cell death with an hDTR model, complete cell depletion was achieved at day seven after the dosing (Wharram et al. 2005). Other experiments in mice report death of the transgenic mice after an acute dose in forty hours (Saito et al. 2001), or complete cell ablation when perfusing after eight and thirty days (Golub et al. 2012), and after eight weeks and six months (Sonntag et al. 2012).

In our experiments, we tested three different perfusion times: seven, fourteen and twenty-eight days after the first dosing. It is expected that the effects of the toxin would have been already visible by any of the three perfusion times tested in our experiments. This suggests that the absence of an effect cannot be attributed to the time in which we perfused the animals.

5.3.4 Assessment of apoptosis

Apoptosis causes several morphological and biochemical changes in the cell. Morphologically, some of the changes include cell shrinkage, cytoplasmic condensation and membrane blebbing (Clarke 1990; Charriaut-Marlangue et al. 1996). These morphological changes can be assessed performing stainings that help visualise the appearance of the cell, such as the Nissl staining. However, morphological analyses can be ambiguous, and are very dependent on the staining, image quality, and an experienced researcher.

The biochemical changes associated with apoptosis include the internucleosomal DNA to cleavage into small fragments (Kumamoto 1997). Biochemical labeling discriminates between apoptotic and healthy neurons using dyes and fluorescence to label these nick DNA fragments, detecting a biochemical signal of apoptosis.

The analysis focuses in the biochemical labeling. As all of the tissue was fixed with 4% paraformaldehyde, we used three different tissue preparation methods

(microwave radiation, incubation and permeabilisation) to rule out the possibility of a tissue fixation problem as suggested in the literature (Negoescu et al. 1996). The TUNEL fluorescein staining confirmed the presence of a signal in the positive controls for the three different tissue treatments, but not in these experimental samples. This indicates the tissue preparation allowed for the staining to access the tissue adequately, and is not responsible for the lack of positive signal.

TUNEL fluorescein has been widely used and if correctly used it should only give a positive signal to the last stages of apoptotic neurons (Negoescu et al. 1996). The only reported case of TUNEL fluorescein mislabeling is a false positive result in the cases where necrosis is present in the sample. The labeling can sometimes give a positive signal of apoptosis since it can not distinguish between random DNA cleavage from necrosis (Loo and Rillema 1998). However in the experiments there is no positive signal at all. Given the presence of a positive control, the histology assessment seems to indicate that the absence of a positive signal is a sign of absence of apoptosis in any of the dosing experiment results.

5.3.5. Limitations

It is important to note that there are several limitations to our experiments, mostly linked to the nature of the toxin work. The biggest limitation is that we are not certain the toxin was active since we do not have access to a positive control. It was not possible to obtain a transgenic rat or mice model that has

been previously validated to use as a positive control. In order to avoid undesirable effects, cautionary measures were taken when manipulating the toxin. For instance, the reconstitution and storage protocol was discussed with researchers that have successfully used the same toxin (Dr. Maithe Arruda Carvalho, Mount Sinai Hospital, personal communication). A new vial was used for every single experiment, and the reconstituted toxin was used within twenty-four hours. The toxin was always kept according to the manufacturer instructions (Sigma), and the spare toxin was discarded. While it is unlikely that the toxin was ineffective in every experiment, the lack of a positive control makes it impossible to be certain about the toxin effectiveness.

When examining the experiments, and despite having tried all the doses that have successfully ablated neurons in other laboratories, it can also be considered that we have not exhausted all the possible dosing ranges. It is theoretically possible that the *NeuroD6* TRECK rat model may require a higher dose or different administration than those tested in our experiments. However there are a number of limitations that should be considered towards the feasibility of the experimental design if higher doses were required due to the risks associated with diphtheria toxin. The first limitation is that the human lethal dose of diphtheria toxin is 100ng/kg, which makes a 6-7µg/ml dose able to kill a human with a weight of 60-70 kg. It is difficult to work with a model that requires dosing in such high quantities, posing serious risks and constraints to experimental work.

In our case, we tackle these risks by immunisation of the researchers and using anaesthesia when administering the toxin. The use of anaesthesia intends to minimise the struggle of the animal when being injected, which increases if the animal is exposed to repeated dosing (Dr. Andrew Thompson, Biological Safety Officer at University of Oxford, personal communication). However this protective measure is a further limitation if very high and continuous doses are required. Furthermore, it has been reported that isoflurane exposure affects behavioural testing (Culley et al. 2004) and if extended, the exposure causes a long term impairment of spatial memory tasks (Culley et al. 2004; Loepke et al. 2009). The effects that isoflurane has in spatial memory tasks, which are hippocampal dependent, would confound when testing the effects of neuronal ablation in the *NeuroD6* TRECK rat model, if that were finally achieved.

Another important limitation is that we have not proved the expression of the hDTR at a protein level in the *NeuroD6* TRECK rat model. It has been reported that in rodents, transgenic expression of an hDTR renders the diphtheria toxin resistant cells sensitive to the toxin, providing a system for cell ablation (Sapoznikov and Jung 2008). The expression of the mutant hDTR, which is identical to the one present in the *NeuroD6* construct, has been also reported capable of inducing neuronal death (Furukawa et al. 2006). But despite extensive toxin testing, our experiments have never achieved neuronal death. If the receptor is not expressed at a protein level, it cannot incorporate the toxin into the cell cytosol. In the experiments described in the *NeuroD6* TRECK rat chapter, we have proved expression of the construct at a protein level in the neuron's membrane through the mCherry protein, which is visible in the brain. The

recombination between both constructs excising the STOP cassette was also validated at a genetic level, a primer design that specifically targets the hDTR receptor. This proves that after the recombination, the hDTR receptor was present at a genomic level. However we never proved the genomic hDTR was translated into RNA and later expressed at a protein level in the membrane of the cell. These experiments are necessary to have a full understanding of our results.

5.3.6. Future work

Future work will tackle the expression of the hDTR in the *NeuroD6* TRECK rat model. This would provide a deeper understanding of the results obtained in the experiments with diphtheria dosing. If the hDTR is not expressed at a protein level, the model renders unable to ablate the neurons. If the hDTR is expressed, then different options could be considered regarding the diphtheria toxin dosing. However, as discussed previously in this chapter, if other dosing regimes are necessary for the neuronal ablation the practicality of the model would be in question. Diphtheria toxin work poses a series of difficulties and increases the measures and protocols that the animals and experimenters have to be subjected to, complicating the testing and the practicality of the model if doses have to be very elevated and continuous.

5.4 CONCLUSION

Overall the results indicate that the lack of neuronal death might be either related to the lack of hDTR expression in the neuronal membrane or to a toxin preparation/dosing protocol that escaped our testing range. Further work will be required to specifically validate the nature of the hDTR expression in the *NeuroD6* TRECK rat model, and if it proves expressed, the diphtheria toxin experiments could be reconsidered. However the nature of the testing developed in this thesis with the diphtheria toxin is comprehensive and extensive. If the hDTR is expressed and we have not achieved neuronal ablation, the feasibility of the model as a practical tool to elucidate hippocampal behaviour should be in question.

6. PARENT-OF-ORIGIN EFFECTS IN THE HS RATS

6. PARENT OF ORIGIN EFFECTS IN THE COMPLEX TRAITS IN THE HS RAT

6.1 MISSING HERITABILITY OF COMPLEX TRAITS

6.1.1. Introduction

Heritability is the proportion of phenotypic variance due to genetic effects. This can be estimated for a disease or physiological measure by using family and twin studies, or in general populations of individuals with equal degrees of relatedness by mixed models (Visscher et al. 2006), described below. The latter are of particular importance in the analysis of complex polygenic traits, where many loci contribute to trait variation. For example, in humans (and rats) height is a polygenic trait. Its heritability is estimated as about 80% in a study of 3375 pairs of human siblings. The estimate was obtained by using a mixed model in which the genetic similarity between individuals was estimated from genome-wide SNP data (Visscher et al. 2006), and is consistent with classic observations on height from family and twin studies (Silventoinen et al. 2003).

Estimates of heritability can be obtained without knowledge of the causal variants. This is fortunate since in general only a small fraction of heritability can be explained by the loci detected in a genome wide association study (GWAS). Thus, in a meta-analysis that identified hundreds of variants associated with

height collected from 180 GWAS in 133,653 individuals, the loci identified could only explain 10% of the total variation, roughly 13% of the heritability (Lango Allen et al. 2010). This missing heritability is observed across a variety of complex diseases: a meta-analysis of several GWAS for complex diseases calculated the percentage of heritability that the identified loci explain and heritability estimated by family or twin studies as it stood in 2011 (So et al. 2011).

Disease	**Heritability (h^2)**	**Number of GWAS loci**	**Heritability explained by GWAS loci**	**% of h^2 explained**
Alzheimer's	0.79	4	0.18	23%
Bipolar disorder	0.77	5	0.02	3%
Breast Cancer	0.53	13	0.07	13%
Crohn's disease	0.55	32	0.07	13%
Prostate Cancer	0.50	27	0.15	31%
Schizophrenia	0.81	4	0.00	0%
SLE (lupus)	0.66	23	0.09	14%

Figure 31: Table collecting seven complex diseases, their heritability estimates, number of loci found in GWAS up to 2011 and the percentage of heritability explained by the findings in the GWAS. (So et al. 2011)

Several explanations have been proposed for the missing heritability problem (Maher 2008; Manolio et al. 2009; Eichler et al. 2010). Proposed causes include the presence of many common causal variants of low effect size (Bodmer and Bonilla 2008; Gibson 2012), rare and low-frequency causal variants with large effects (Cirulli and Goldstein 2010; Johansen et al. 2010; Gibson 2012), copy-

number variants (Bodmer and Bonilla 2008; Zhang et al. 2010), and epistasis (Haig 2011; Hemani, Knott, and Haley 2013).

6.1.2. Parent of Origin Effects

Here we investigate another proposed cause, namely parent of origin effects (POE). An allele has a parent of origin effect if its influence on a phenotype depends on whether it was inherited from the mother or the father. Related to POE are maternal and paternal effects, where the maternal or paternal expression of an allele affects the phenotype of the offspring regardless of whether it is transmitted.

The difficulty of establishing parent of origin effects in humans lays in the need of a substantial data set which contains not only genotypic and phenotypic information from hundreds (or thousands) of individuals but also from their parents. Yet the use of several GWAS datasets allowed to identify imprinting of the DLK1-MEG3 gene which confers paternal but not maternal inherited risk for diabetes type 1 (Wallace et al. 2010). In a study using data from the Icelandic population susceptibility variants were discovered to confer risk for the disease only if inherited from a specific parent in cancer, and confer risk or reduce it depending on the parent of origin in type 2 diabetes (Kong et al. 2009). The percentage of heritability in type 2 diabetes due to the parent of origin effect was estimated in 10-13% (Kong et al. 2009).

Another study identified the imprinting of the IGF2 (insulin-like growth factor II) in humans after being demonstrated that the gene was imprinted in mice and only the paternal gene copy is expressed (Giannoukakis et al. 1993). The work done in mice has allowed the identification of a few imprinted genes, such as the Grb10 that shows to modulate certain emotional behaviours (Garfield et al. 2011) or the identification of genomic regions showing imprinting effect patterns in their inheritance (Wolf et al. 2008). More recently, the work with an HS mice population has identified a parent-of-origin effect in the heritability of complex traits, and has shown that many mouse QTLs have parent-of-origin effects as well (Mott et al. 2014). These results are particularly interesting if we take into account that the 91 analysed traits that showed a POE effect in their heritability are traits that configure complex disease models such as obesity, hypertension, diabetes and anxiety.

6.1.3. Coping style

The pro-active coping style is characterised by active responses directed to address the aversive situation, either to confront stressful stimuli or to increase the distance between the stressful stimuli and the individual (Benus et al. 1991). The pro-active coping style has been associated with increased exploratory behaviour (Wechsler 1995; Steimer and Driscoll 2003; MacKenzie et al. 2009; Coppens et al. 2013), aggressive behaviour (Dingemanse et al. 2004; Koolhaas 2008), and struggling (Schouten and Wiegant 1997; Steimer and Driscoll 2003; Jaap M. Koolhaas et al. 2007). In opposition, the reactive coping style is defined

by inactivity and disengagement when in an aversive situation, and only reacting if absolutely necessary. The reactive coping style has been associated with non-aggressive behaviour (Dingemanse et al. 2002; Koolhaas et al. 2007), absence of responses (Engel and Schmale 1972; Steimer and Driscoll 2003; Koolhaas 2008), immobility and extended latency (Schouten and Wiegant 1997; von Holst 1998; Steimer and Driscoll 2003; MacKenzie et al. 2009).

6.1.4. Emotional characterisation of the HS rats

The HS rats have shown to have an emotional profile characterised by anxious and fearful responses in several experiments in our laboratory, in conditioned and unconditioned anxiety tests such as the elevated zero maze, classically-conditioned freezing and the acquisition of two-way active avoidance in the shuttle box (Lopez-Aumatell et al. 2008; Vicens-Costa et al. 2011).

They also present a reactive coping style defined by immobility and lack of activity in the forced swimming test (fig. 32), not only comparable but superior to the RLA-I strain (Díaz-Morán et al. 2012), which has been selected for generations for their anxious behaviour versus the RHA-I strain (Steimer, Fleur, and Schulz 1997; Driscoll et al. 1998; Escorihuela et al. 1999; Fernández-Teruel et al. 2002b; Steimer and Driscoll 2003b; Coppens et al. 2013).

Immobility and struggling scores of the three groups of rats in both forced swimming sessions

	RHA-I	RLA-I	N/Nih-HS
Immobility 15'	408.2 ± 69.6	413.0 ± 74.9	659.2 ± 48.5*
Struggling 15'	134.4 ± 34.6	120.8 ± 22.13	47.4 ± 12.8*
Immobility 5'	46.2 ± 11.7	115.9 ± 28.1**	169.8 ± 15.5**
Struggling 5'	157.8 ± 17.0	78.8 ± 18.4**	33.5 ± 6.2*

Figure 32: Results comparing the struggling and the immobility of a cohort of HS rats with RHA-RLA rats in the two sessions of the forced swimming test. *p < 0.05 vs both RHA-I and RLA-I groups, **p < 0.05 vs RHA-I group (one-way ANOVA). "Immobility15" and "Struggling15": measures (s) from the first 15-min swimming session. "Immobility5" and "Struggling5": measures (s) from the second 5-min swimming session. (Díaz-Morán et al. 2012)

The behavioural tests (two-way active avoidance, elevated zero-maze and novel-cage "open-field-like" activity) have been previously analysed for this HS rats dataset with a obliquely-rotated factor analyses applied to the main variables from the three behavioral tests (López-Aumatell et al. 2011). This factorial analysis shows a first factor that contains related variables from the two tests, which are consistent with those that can assess a passive-active coping style (fig. 33).

Remarkably, our QTL study on these HS rats has shown a QTL influencing some of those coping style related phenotypes (e.g. latencies in the response in the shuttle box session). This QTL has helped identify a candidate gene, named *Catenin delta-2*, which is known to be involved in hippocampal plasticity and context-conditioned fear (Baud et al. 2014).

	Factor 1	Factor 2
Elevated "zero-maze"		
Entries into open sections	0.71	-
Number of SAPs	0.75	-
Two-way shuttlebox avoidance conditioning		
Time spent freezing trials 1-5	-0.50	-
Avoid40+ITC40	0.44	-
Automated novel-cage activity		
Distance travelled min 0-5	-	0.86
Distance travelled min 25-30	-	0.87
Eigenvalues	1.68	1.41
% of accumulated explained variance:	28.1	51.6
Correlation between factors = 0.13		

Figure 33: Two-factor solutions from obliquely-rotated factor analyses applied to the main variables from the three behavioral tests in the HS rats of this dataset. Oblique two-factor solution (Direct Oblimin) with the 6 most relevant variables. Only loadings with absolute values ≥ 0.30 are shown (López-Aumatell et al. 2011). SAP: stretch attendance postures, AVOID40+ITC40: avoidances+intertrial crossings in the whole 40 trial shuttlebox session, "Time spent freezing trials 1-5": context-conditioned freezing during the frist 5 intertrial intervals of the shuttle box session.

6.1.5. Aim

If POE explains a component of the heritability in complex diseases in mice, the same effect could exist in other organisms. The aim of this chapter is to assess if parent-of-origin effects can explain any of the heritability of complex traits in the HS rats as it has been recently observed in the HS mice (Mott et al. 2014). Since the phenotypic data includes conditioned and unconditioned fear and anxiety measures, the analysis focuses on the behavioural traits to investigate if there is a parent-of-origin effect in the behavioural measures associated with different coping styles.

6.2. ESTIMATING POE HERITABILITY IN THE HS RATS

6.2.1. The HS rats study

In order to study the genetic basis of several complex traits, genotypic and phenotypic data was collected from 1407 HS rats. This study is in many ways similar to the HS mouse study (Valdar et al 2006) in that a large number of phenotypes were measured on a population of outbred animals descended from known inbred strains. The phenotyped animals exhibit varying degrees of relatedness, comprising a large number of sibships. Quantitative Trait Loci (QTL) were mapped in both populations by first reconstructing the genome of each animal as a heterozygous mosaic of founder haplotypes and then testing at the locus in question, if the effects of the haplotypes on the phenotype differed.

In the HS Rats 355 QTLs for 160 phenotypic measures were mapped at a false discovery rate of 10%. This lead to the identification of 35 causal genes (Baud, 2013a). On average across all the traits, the combined variance explained by the mapped QTLs explained 42% of the estimated heritability of each phenotype (Baud, 2013a), leaving over half of the genetic variance unexplained (Fig. 34).

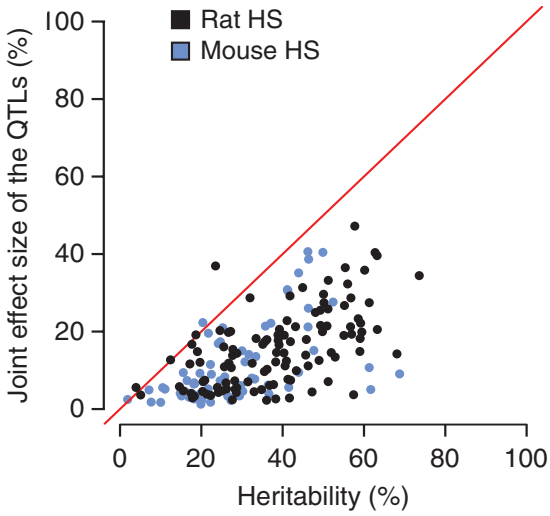
Rat HS
Mouse HS
Joint effect size of the QTLs (%)
Heritability (%)
0
20
40
60
80
100

and experimenter. Covariates such as cage are surrogates for maternal effects, as it is a measure of shared environment and can be confounded with parent-of-origin (Hager, Cheverud, and Wolf 2008). Previous evidence shows that such covariates have a significant effect on behavioural phenotypes in conditioned and unconditioned fear tests (Valdar, Solberg, Gauguier, Cookson, et al. 2006; López-Aumatell et al. 2011).

21 phenotypes were discarded because they were measured on fewer that 200 rats in our data subset. The rest of the data was analysed. A full report on the breeding scheme, testing sequence, phenotypic measures, covariates and number of rats phenotyped for each trait is available in the Material and Methods and the Appendix section of this thesis.

6.2.2.1 Behavioural measures

The behavioural testing comprised unconditioned and conditioned anxiety and fear tests, measuring anxiety/fearfulness (elevated zero-maze and novel-cage activity), context-conditioned freezing and two-way active avoidance acquisition (shuttle box). The measures take into account measures for latency to response, exploration of a new environment, spontaneous activity, conditioned freezing and avoidance acquisition.

6.2.3. Estimating Parent-of -origin heritabilities

We first summarise the method presented in (Mott 2014) to estimate heritability due to parent-of-origin. This is an extension of the mixed model methodology widely used to estimate heritability. Let us suppose that phenotypic and genotypic information is available for a population with different degrees of relatedness (eg the HS rats). In the standard mixed model parent of origin effects are ignored and instead we estimate the components of phenotypic variance attributable to additive genetic effects and to the environment. This is summarised by the mixed model matrix equation

$$V = I\sigma_e^2 + K\sigma_g^2 \qquad (1)$$

in which the matrix V is the phenotypic covariance matrix between individuals. The matrix K summarises the pairwise genetic relationships between the individuals in the population (and is estimated from the genotypes), and I is the identity matrix. The coefficients σ_e^2 and σ_g^2 are the environmental and additive genetic variances. These coefficients are estimated by fitting the equation (1) to the phenotype data, using a software such as GCTA (ref). We then estimate the additive heritability as the fraction of variance accounted for by genetic effects

$$h^2 = \frac{\sigma_g^2}{\sigma_e^2 + \sigma_g^2}$$

Here we wish to take into account parent of origin effects. We do this by splitting the additive genetic similarity matrix K into two matrices

$$K = K^{+} + K^{-}$$

by noting that shared alleles must either descend from parents of the same sex or from parents of the opposite sex (Mott et al. 2014). These kinship matrices summarize the allele sharing for individuals. This is illustrated in Figure 35, which shows the inheritance of alleles a, A at a SNP for four offspring in two sibships. In this example we have made the parents homozygous for different alleles so that the parental origin of each allele in their offspring is unambiguous. In this pedigree the four individuals share the same alleles but with different parental origins. If we analyse the descent of these alleles, individuals 1 and 2 have inherited the alleles from a parent of the same sex (female for a and male for A), and so:

$$K^{+}_{1,2} = 2$$

$$K^{-}_{1,2} = 0$$

Whereas if we take individuals 2 and 3, they share the same alleles but inherited from parents that do not have the same sex (female parent of origin for individual 2 and male parent of origin for individual 3 for the allele a, and male parent of origin for individual 2 and female parent of origin for individual 3 for the allele A), and therefore:

$$K^{+}_{2,3} = 0$$

$$K^{-}_{2,3} = 2$$

In this example we are only considering a single SNP. In reality, we estimate the kinship differently but the same principles apply. The main differences are that we work in terms of the eight founder haplotypes of the HS averaged across all autosomes, and we standardise the kinship matrices so that the diagonal elements of the combined kinship matrix K are all 1. Full details are given in the methods of (Mott el al 2014).

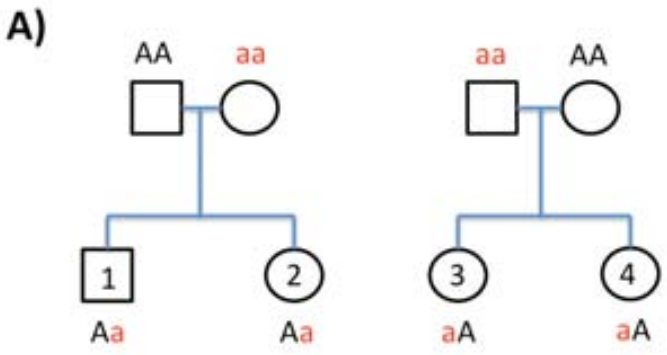

B)

	1	2	3	4
1	—	K_+ =2 K_- =0	K_+ =0 K_- =2	K_+ =0 K_- =2
2		—	K_+ =0 K_- =2	K_+ =0 K_- =2
3			—	K_+ =2 K_- =0
4				—

Figure 35: A) Pedigree in which four individuals (1, 2, 3 and 4) share the same alleles but the alleles descend from different parents. B) Table that attributes a value to the kinship matrices according to whether the shared allele descends from parents of the same sex (K^{+}) or parents from the opposite sex (K^{-}).

To take into account parent-of-origin effects, the phenotypic covariance is now modeled as

$$V = I\sigma_e^2 + K^+\sigma_{g+}^2 + K^-\sigma_{g-}^2 \qquad (2)$$

Where σ_e^2 is the environmental variance, σ_{g+}^2 is the variance attributed to a common parent of origin, and σ_{g-}^2 is the variance attributed to opposite parent of origin. Using these kinship matrices, heritabilities can be estimated using GCTA (Yang et al. 2011).

$$h_+^2 = \sigma_+^2/(\sigma_+^2 + \sigma_-^2 + \sigma_e^2)$$

$$h_-^2 = \sigma_-^2/(\sigma_+^2 + \sigma_-^2 + \sigma_e^2)$$

If there is no differences between parent-of-origin and non-parent of origin effects then $\sigma_{g+}^2 = \sigma_{g-}^2$ since then the model (2) becomes identical to the usual model (1).

6.3. RESULTS

6.3.1 Parent-of-Origin Effects in Heritability

Applying GCTA to 199 phenotypes (Yang et al. 2011) we estimated fractions of phenotypic variation h_+^2 and h_-^2, attributable to each component of the variance.

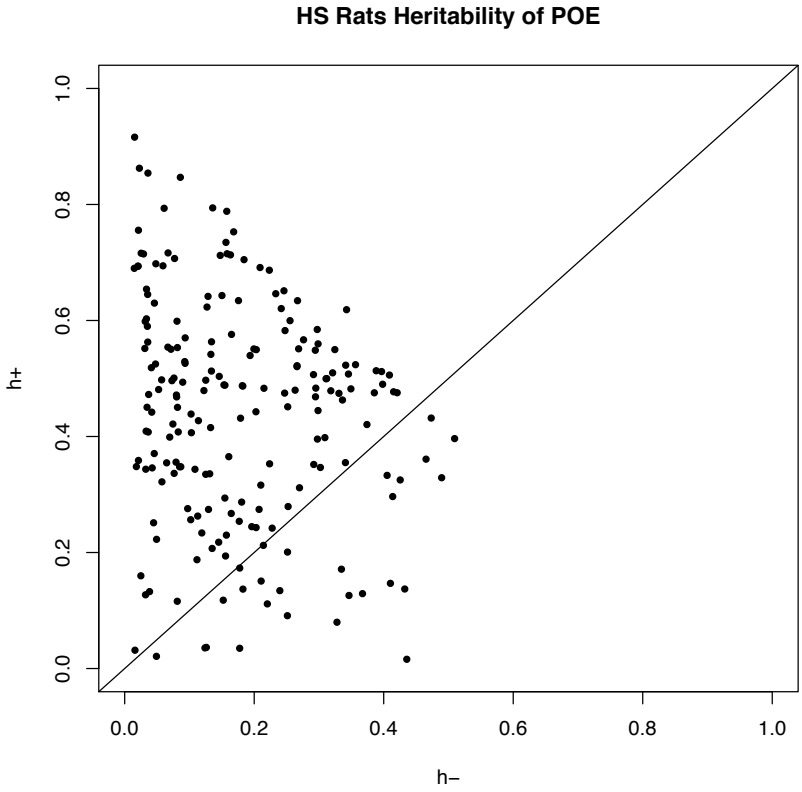

Figure 36: Heritability estimates of 199 traits measured in HS rats. Each black dot represents one trait. The y axis represents h^2_+, the x axis represents h^2_-. The diagonal is the line of equality between the heritabilities where $h^2_+ = h^2_-$.

In 86% of the traits examined (172 out of 199), $h^2_+ > h^2_-$ (fig. 36). The medians are 0.474 and 0.155 respectively with a median ratio $h^2_+/h^2_- = 2.66$. The average standard errors of the medians are 0.133 for h^2_+ and 0.172 for h^2_-. The full results are in Appendix 11.1. of this thesis. These results are consistent with those found in HS mice.

6.3.2 Confounding with family structure and analysis of parental effects

Parent-of-origin effects are confounded with parental effects, since siblings will share more alleles that derive from common parents than non-siblings. Parental effects can express as parent-of-origin effects and must be accounted for when studying heritability of complex traits (Spencer 2009). If we classify the HS individuals according to whether they are siblings or not siblings (figure 37), we can observe the distribution of shared alleles is much more similar in K^-. Siblings and not siblings shared a similar amount of alleles if they descend from parents of the opposite sex. Whereas for the distribution of K^+, siblings share substantially more alleles than not siblings for alleles that descend from parents of the same sex.

If parents are unrelated to each other then the expected distribution of K- for siblings and non-siblings should be equal, as was observed for HS mice (Mott et al 2014). However, in the rats we see that whilst the distributions for siblings and non-siblings are much closer together for K-, they are not identical. The reason for this is probably that the rats selected for mating were more closely related than would be expected if they were chosen at random (e.g. due to cousin matings).

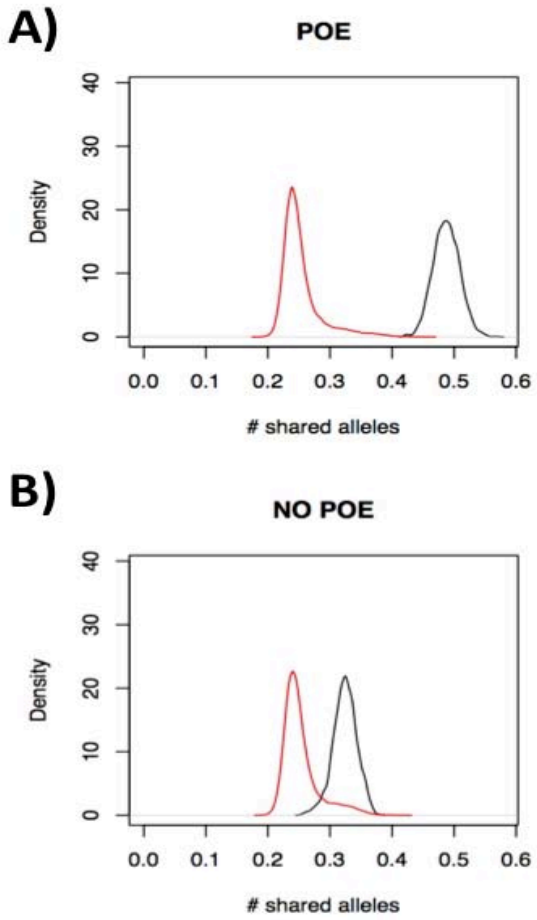

Figure 37: Distribution of parent-of-origin components of kinship between HS rats for siblings (black) and nonsiblings (red). A) Distribution of the elements for the kinship matrix K^{+}. B) Distribution of the elements for the kinship matrix K^{-}.

6.3.3 Heritability of behavioural phenotypes

6.3.3.1 Parent-of-origin effects

The behavioural testing includes the elevated zero maze, the novel-cage activity test, context-conditioned freezing and the two-way active avoidance test. In total there are 45 measures corresponding to the behavioural phenotypes in our data.

The measures distribute towards the lowest $h^2_{+\_}$ values (fig. 38). This indicates the phenotypic variation in the behavioural measures in our sample is more dependent on environmental than genetic factors, or is subject to greater experimental noise.

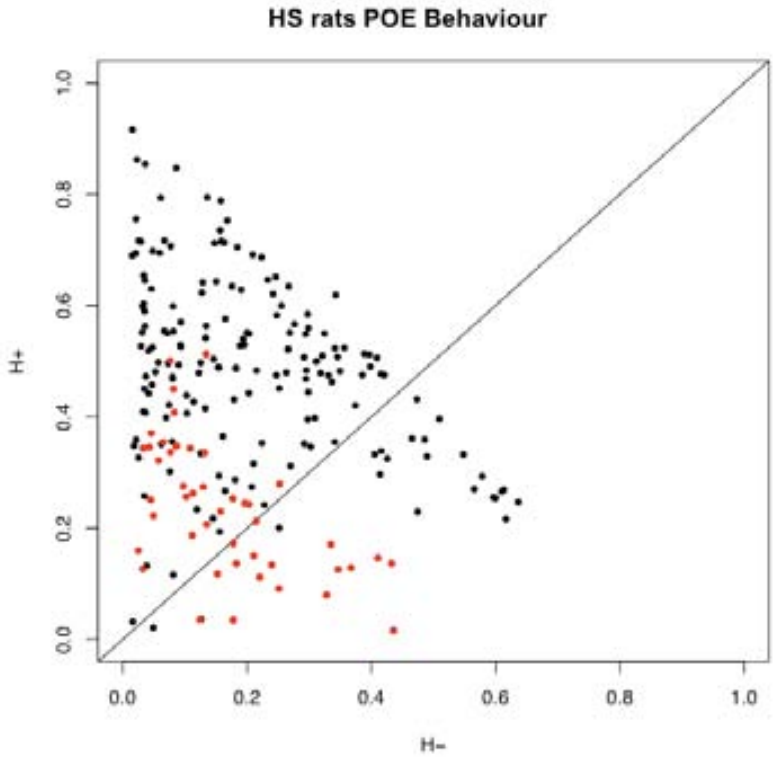

Figure 38: Heritability estimates for 199 traits in the HS rats. Every dot represents a trait, red for behavioural measures, black for the rest of the phenotypes. The y axis represents h^2_+, the x axis represents h^2_-. The diagonal is the line of equality between the heritabilities where $h^2_+ = h^2_-$.

In 57% of the behavioural traits examined (26 out of 45 measures), $h^2_+ > h^2_-$. The medians are $h^2_+ = 0.242$ and $h^2_- = 0.131$ with a median ratio of $h^2_+/h^2_- = 1.68$ and the average standard errors of the medians had values of 0.122 and 0.171 respectively. Full results are in the Appendix 11.2. of this thesis.

6.3.3.2 Parental effects

Complex traits and in particular behavioural phenotypes are susceptible to environmental effects (Valdar, Solberg, Gauguier, Cookson, et al. 2006; López-Aumatell et al. 2011). These covariates, such as maternal effects can be confounded with parent-of-origin (Hager, Cheverud, and Wolf 2008). However if all the heritability that can be attributed to the parental-of-origin effects were due to maternal effects, all the behavioural phenotypes would show a skewed strong maternal heritability versus paternal heritability. For all the 199 traits, the parental heritability medians are 0.323 for maternal heritability with an average standard error of 0.165, and 0.295 for the paternal heritability with an average standard error of 0.164. The median ratio of maternal heritability/paternal heritability = 1.08.

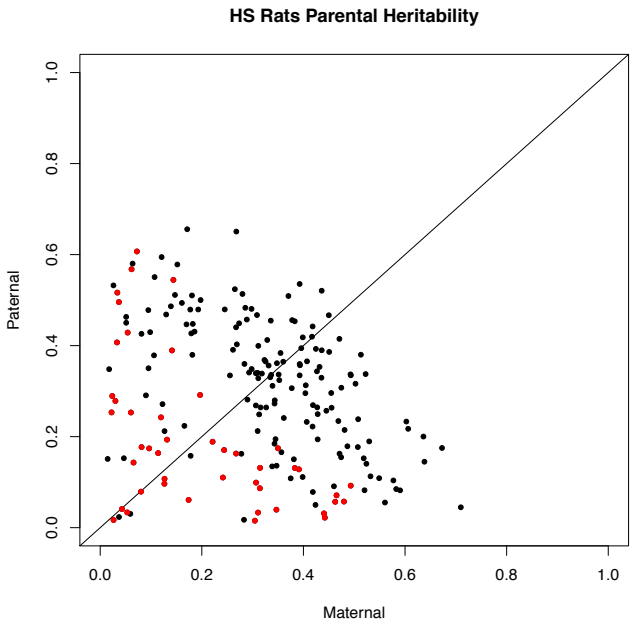

Figure 39: Parental heritability estimates for 199 traits in the HS rats. Every dot represents a trait, red for behavioural measures, black for the rest of the phenotypes. The y axis represents paternal heritability, the x axis represents maternal heritability. The diagonal is the line of equality between the heritabilities where maternal heritability = paternal heritability effects.

6.3.3.3. Parent-of-origin effects in the heritability of passive-active coping style

In order to determine if coping styles heredity had a parent-of-origin component, we selected the behavioural measures most relevant to coping style: latency to enter the open section and number of entries into the open section in the elevated zero maze, context-conditioned freezing and latency to escape to the other compartment in the shuttle box.

All the measures but one (9 out of the 10 measures) have a $h^2_+ > h^2_-$ (fig. 40). The medians are $h^2_+ = 0.305$ and $h^2_- = 0.130$ with a median ratio of $h^2_+/h^2_- = 3.19$ and the average standard errors of the medians had values of 0.134 and 0.183 respectively.

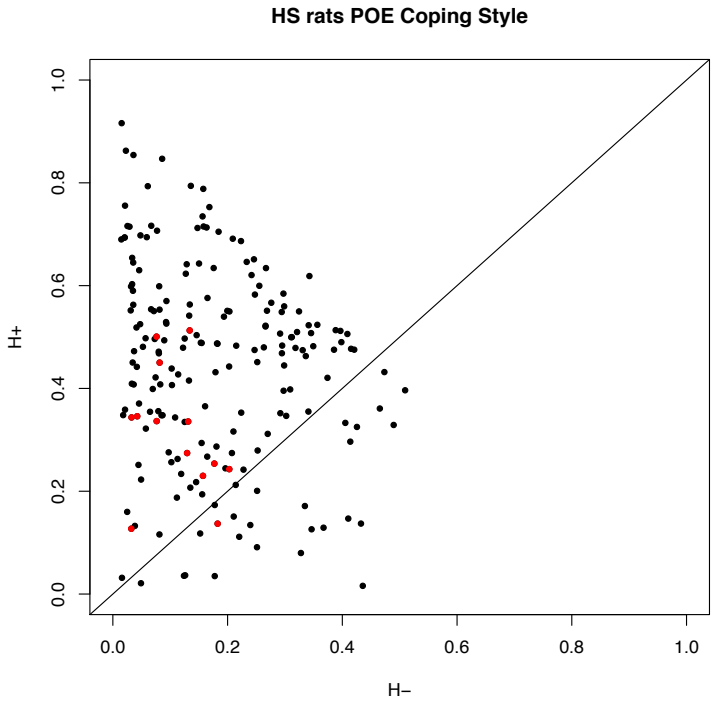

Figure 40: Heritability estimates for 199 traits in the HS rats. Every dot represents a trait, red for behavioural measures corresponding to coping styles, black for the rest of the phenotypes. The y axis represents h^2_+, the x axis represents h^2_-. The diagonal is the line of equality between the heritabilities where $h^2_+ = h^2_-$.

6.4. DISCUSSION

The results here presented constitute the first investigation regarding the POE in the heritability of complex traits in rats, using an heterogeneous stock as done in other previous work (Mott et al. 2014).

6.4.1 Parent of origins in the HS population: mice and rats

Similarly to the results for the HS mice, most of the complex traits in the HS rats exhibit a parent-of-origin effect. The heritability values are similar for the HS mice and the HS rats ($h^2_+/h^2_- = 2.04$, $h^2_+/h^2_- = 2.66$ respectively). However, the average standard errors of the medians are 0.133 for h^2_+ and 0.172 for h^2_- for the HS rats, whereas the HS mice the values are 0.058 and 0.078 respectively. With an HS rat sample of 798 individuals versus the 1389 individuals analysed in HS mice, the difference in the sample size impacts in the accuracy of the heritability estimates for the HS rats.

Despite eliminating from our analysis any phenotypic measure that had less than 200 measurements, there is a wide variability in the measurements in our samples (Appendix 11.1), which explains the size of the average errors of the medians. Improving the power of the analysis by accessing a bigger sample should provide with better estimates of the parent-of-origin effects, and should

be taken into account for future work if analysing HS models or other organisms. Due to the sample size limitation it has also not been possible to map POE QTLs, as it was done in the HS mice (Mott et al. 2014). It will be interesting to investigate human populations where the genotypes of parents are available, for example some twin studies such as (Bell and Spector 2011), to see if the same patterns of heritability are observed. If so, this would explain some of the missing heritability observed in GWAS.

6.4.2 Parent-of-origin is confounded

In (Mott et al. 2014) it was shown that, for a SNP in Hardy-Weinberg equilibrium with an allele frequency p, siblings share on average $2p(1-p)$ more alleles via parents of the same sex compared to unrelated non-siblings. Allele-sharing from parents of the opposite sex is the same for siblings and non-siblings and is equal to $2(p^2 + (1-p)^2)$. However, in our data showed in figure 37, siblings and non siblings share different amount of alleles for $K\_$. This could not be possible if the parents are unrelated to each other. A plausible explanation is that parents are more related that would be expected at random, due either to the selection of individuals to have their parents genotyped or due to some sort of failure in the rotational breeding scheme, e.g. matings between uncles and nieces.

The fact that parent-of-origin allele sharing tracks sibship membership means the effects are confounded with family structure. Maternal effects are a form of

shared environment and therefore they would be confounded too as environmental variance. However, a multiple regression has been applied to the phenotypes to generate residuals free of effects, and despite there is always the possibility of residual cofounding, it seems reasonable to assume that not all the heritability observed to parent-of-origin effects can be attributable to shared environments.

6.4.3 Parent-of-origin effects in the behavioural measures and in the heritability of coping styles

It is not surprising that the behavioural measures show the lowest phenotypic variation attributable to genetic effects among all the other measures tested in these experiments (Figure 39). In the HS mice, gene-environment effects have been estimated more frequent and greater than the main genetic effect in behavioural and physiological phenotypes (Valdar, Solberg, Gauguier, Cookson, et al. 2006). Behavioural phenotypes have a strong component of environmental variance and covariates account for an important portion of the variation (López-Aumatell et al. 2011). Thus it is reasonable that the phenotypic variation attributable to genetic effects is lower in behavioural phenotypes than in other measures. The results show there is a parent-of-origin effect in the heritability of 54% of the examined behavioural measures.

The analysis indicates that 9 out of the 10 traits examined for heritability of the coping style pattern response show $h^2_+ > h^2_-$. The measures selected to analyse

coping style were selected for their ability to indicate differences between a reactive and a pro-active coping style. Differences between the measures we have analysed have previously been correlated with differences in coping style (Escorihuela et al. 1999; Steimer and Driscoll 2003; Lopez-Aumatell et al. 2008; Díaz-Morán et al. 2012; Coppens et al. 2013).

The factorial analysis shown for the behavioural data in the introduction of this chapter (Figure 33) includes another measure traditionally included in the coping style studies: the avoidance acquisition in the shuttle box. Avoidance acquisition has been used to assess coping style in previous works and is predicted by freezing (Vicens-Costa et al. 2011) and correlates with other measures such as latency to escape and entries to the open section of the elevated zero maze (Fernández-Teruel et al. 1991; Escorihuela et al. 1999; Lopez-Aumatell et al. 2008; López-Aumatell et al. 2009; Vicens-Costa et al. 2011; Coppens et al. 2013; Díaz-Morán et al. 2012). However, we decided not to include the avoidance acquisition in the shuttle box due to the measurement used. The data from the shuttle box was loaded into a computer that measures acquisition by the ability to escape to the next compartment during the light and tone phase and before the shock administration. However it does not discriminate between struggling and actively searching for an exit and immobility. That is, a rat that spends most of this phase immobile and escapes at the last second is counted in the same manner than a rat that is actively pursuing an escape and escapes at the last second. That is essentially the difference between a reactive and a pro-active coping style. It is proven that reactive coping style can elicit an escape depending on the appraisal of the situation by the animal and the quality and duration of the

stressor (von Holst 1998). Therefore the analysis includes only those measures that inform precisely about coping style.

6.4.4. Conclusion

Our results suggest there is a large component of the heritability that can be attributed to parent-of-origin effects in rats. This result replicates what has been previously reported in mice (Mott et al. 2014) and constitutes the first evidence of parent-of-origin effects component in the heritability of multiple complex traits in rats such as behavioural traits. However, because parent-of-origin effects are confounded with family, some of the variance explained by parent-of-origin may be due to shared environments.

7. CONCLUSIONS AND LIMITATIONS

7. CONCLUSIONS AND LIMITATIONS

The present work aimed to study behaviour using the rat as a model with two very different approaches: one interventional and one observational. The interventional approach aimed to study hippocampal behaviour using a transgenic rat model. The observational approach aimed to analyse genotypic and phenotypic data (including hippocampus-dependent behavioral traits) that had been collected in order to establish components in complex traits heritability in a rat heterogeneous stock. Each approach uses experiments and tests in order to fulfill the objectives of the thesis described in the Aims section. The results of the experiments are outlined and thoroughly discussed in each chapter. Here, I summarize the main conclusions that we can extract from the experiments and tests, as well as their limitations.

7.1 THE INTERVENTIONAL APPROACH: THE *NEUROD6* TRECK RAT MODEL

The main goal in the generation of the *NeuroD6* TRECK rat model was to have a neuronal ablation rat model that targets the Cornus Ammonis in order to have a unique model to dissect hippocampus-dependent behaviour. The model has to be thoroughly characterised to fully understand its feasibility as a behavioural model. The hypothesis that neuronal ablation of the CA1-CA3 layer would affect changes in hippocampus-dependent tasks remains unaccomplished due to the

results obtained in the experiments described in this thesis. The aims for this study are listed below with its main results summarised.

i) The *NeuroD6* construct is inserted in the rat genome and expresses in the targeted areas.

The experiments presented in this thesis confirm the insertion of the *NeuroD6* construct in the rat genome and in the rat germline. They also confirm the expression of the construct at a protein level. This expression is located where expected according to the literature (Entorhinal cortex, CA1-CA3 of hippocampus and amacrine cells in the retina) and also expressed in areas that we had not anticipated and are not reported in the literature (hilus in the hippocampus, and the secondary visual cortex). Unexpected expression of a construct and variation between lines has been previously reported, as well as differences in cell populations expressing a transgene (Feng et al. 2000), which makes it necessary to explore unpredicted expression of the construct. The construct is not expressed anywhere else in the rat body, crucial for an adequate model to study hippocampal function.

ii) There are multiple fragmented copies of the BAC inserted in the rat genome.

The results of experiments described in this thesis indicate that the BAC construct is incomplete, and has only partially integrated into the genome. This is suggested by the unexpected size of the amplifications achieved with primers that target the beginning and end of the construct (the EXON primers). Several other unexpected sizes are amplified suggesting multiple BAC fragments have integrated into the genome. The unexpected amplifications observed in our

results suggest that the *NeuroD6* hDTR BAC has multiple integrations of fragmented copies of the BAC.

Despite the fragmentation, the SPAN primers target from the exon of the construct to the hDTR sequence, thus all the fragments amplified contained at least the hDTR sequence. The presence of the mCherry protein, under these circumstances, did not exclude the possibility of recombination, as multiple fragmented copies of the BAC seem to converge in the same animal. Thus mCherry expression and recombination could coexist .

iii) There is recombination of the constructs in the *NeuroD6* TRECK rat.

The loss of the biggest amplification product (2000 bp) in the hippocampus of the double transgenic suggests that recombination occurred, and that the recombination is limited to the hippocampus as per the action of the Flpo recombinase present in the *CamkII*α-Flpo rat model. This loss of product does not happen in the other organs for the double transgenic model, and it does not happen anywhere in the single transgenic model. These results suggest that if the 2000 bp product is amplifying a fragmented BAC, the fragment at least contains the two FRT sites, and the action of the flippase present in the *CamkII*α-Flpo model is able to excise them.

iv) Our toxin experiments were not capable of causing neuronal death irrespective of administration route, dose concentration, dosing regime and perfusion time.

The toxin experiments reported in this thesis aimed to achieve neuronal death in the cells expressing the hDTR. Our experiments included previously tested dosing regimes in the literature and a higher dose than ever reported before, with a range from 0.35μg/kg per hour up to 120μg/kg per dose. Other work reports that 50μg/kg is a dosing two orders of magnitude higher than required to kill wild type hDTR cells (Saito et al. 2001). Regarding perfusion time, we tested three different conditions: seven, fourteen and twenty-eight days after the first dosing. All of these perfusion times prove to be sufficient to see an effect in the published literature. Several alternatives were also tested for administration route: intraperitoneal injections and mini-pump dosing. Finally, different stainings and methods were used to quantify and analyse the presence or absence of an effect in our experiments. It was not possible to replicate the results of previous work with these experiments and our experiments did not achieve any neuronal death irrespective of administration route, dose concentration, dosing rate, or perfusion time.

The hypothesis remains untested, as the capability of the model to ablate the CA1-CA3 neuronal layer and its feasibility as a practical behavioural tool in question. The main limitation of our work is the lack of a positive control for the toxin and the uncertainty of the hDTR expression at a protein level. Future work will tackle first the validation of the expression of the hDTR at a protein level, and if proven positive the toxin experiments should be revaluated.

7.2. THE OBSERVATIONAL APPROACH: POE IN THE HERITABILITY OF COMPLEX TRAITS

The aim of the observational approach was to analyse genotypic and phenotypic data to study if the heritability of complex traits in the HS rats had a parent-of-origin effect. The secondary objective was to assess if behavioural phenotypes and specifically the coping styles heritability have a parent-of-origin effects component.

i) The heritability of complex traits in the HS rats has a parent-of-origin component.

The majority of complex traits analysed in this thesis (86%) shows a parent-of-origin effect, confounded with parental effects. The analysis of the parental effect demonstrates the HS rats of our sample are more closely related than expected if they were chosen at random. The data available is close to 600 measures (one per individual) per phenotype in most cases but lower in some phenotypes, increasing the SE median values. However the results obtained could not be possible without a genuine parent-of-origin effect.

ii) Behavioural phenotypes and particularly coping styles heritability have a parent-of-origin effect.

A high percentage (57%) of behavioural phenotypes display a parent-of-origin component in their heritability. The heritability of coping styles also has a

parent-of-origin component in almost all the measures analysed (nine out of ten).

The hypothesis of the heritability of complex traits in the HS rats is validated as the analysis demonstrates a parent of origin effect component. This further suggests other organisms could also have a POE effect in their heritability of complex traits, and partially explains some of the missing heritability seen in the HS rats.

Finding mechanisms and effects that explain part of the missing heritability helps us understand heritability of complex traits. Missing heritability is attributed to multiple effects. Nonetheless POE does explain a component of the heritability of a number of complex traits in the HS mice (Mott et al. 2014) and in the HS rats. An exploration of its effects in other organisms would allow us to ascertain how common is this effect in the heritability of complex traits.

In the natural habitat survival depends on adopting the best strategy when facing a threat. The best strategy depends entirely of the nature of the threat. If an animal appears to see a predator, an active escape can be as successful as hiding immobile without being noticed. In a study in a natural bird population coping style was found to fluctuate across years within great tits. The study found that reactive coping style birds had better chances to survive in 1999, but in the year 2000 pro-active coping style birds had a better survival ratio, only to be reversed again in the year 2001 (Dingemanse et al. 2004). Therefore the existence of two opposite response patterns ensures the survival of those who

display a certain response, and the survival of the population depends on having individuals displaying different responses to the same threat. It seems plausible that coping styles would be highly heritable if there is a need for variability in the coping styles of a population to guarantee its survival.

The Swiss sublines of Roman high and low avoidance (RHA/I and RLA/I) inbred rats exhibit opposite pattern responses to stressful situations. These two strains have been subjected to several generations of selective breeding in order to increase an extreme phenotypic response to such stressful situations. The HS rats have an emotional profile similar to the RLA rats in their pattern responses to stressful situations (Lopez-Aumatell et al. 2008; López-Aumatell et al. 2009; Díaz-Morán et al. 2012). The RLA rats exhibit a reactive coping style, while the RHA rats have a pro-active coping style (Steimer, Fleur, and Schulz 1997; Steimer and Driscoll 2003; Díaz-Morán et al. 2012; Coppens et al. 2013). This phenotypic response is strictly dependent on the animal strain (Steimer and Driscoll 2003).

Our future work includes validation of the parent-of-origin effects in coping styles by generating and F1 crossing of the RHA and RLA. By forming groups with a paternal RHA and a maternal RLA and the opposite breeding scheme, we aim to phenotype their descendants and investigate if a certain parental composition has any effect in their coping style.

7.4. FINAL CONCLUSIONS

The work presented in this thesis stretches between the disciplines of molecular biology, behavioural neuroscience and statistical genetics. While these fields are quite distinct, it is possible and attractive to merge different approaches to investigate scientific problems. Each of the fields brings a set of techniques, which provide complementing tools to investigate the relationship between brain, genes and function.

The time constraints associated with doctoral work have limited the scope of the thesis. For instance, studies with living models extend the timeline of experiments when taking into account breeding, maintenance of colonies and generation of experimental animals. Work with a lethal toxin requires the implementation of several protocols and security measures before any work can be done. Future work will help elucidate the questions that have been raised with the experiments here presented.

8. MATERIAL AND METHODS

8. MATERIAL AND METHODS

In this chapter we list all materials, apparatus and methods used for the realisation of the tests and experiments of this doctoral work.

8.1 INTERVENTIONAL APPROACH: VALIDATION OF THE *NEUROD6* TRECK RAT MODEL MATERIAL AND METHODS

All of the procedures described in this thesis regarding the interventional project were done under UK Home Office personal and project licenses, and following the UK Home Office Code of Practice under the ASPA Act 1986 for Animal Management and Welfare. All the laboratory and animal procedures followed the Health and Safety protocols and guidelines in accordance of University of Oxford. Animals were bred and maintained in the Biomedical Services at the University of Oxford, under UK Home Office personal and project licenses, and in accordance of University of Oxford guidelines.

8.1.1. Molecular methods

8.1.1.1 Genotyping

8.1.1.1.1. DNA extraction

Earclips were collected for each animal, and DNA was extracted from ear clips using the Nucleon Genomic DNA Extraction Kit from Gen-Probe. Ear clips were digested overnight with a Proteinase K solution at 55 °C, and then vortexed and spinned with a resin. The pellet was discarded and the resultant solution was centrifuged with 99% isopropanol and washed with 70% ethanol. Pellets were allowed to air dry at room temperature for an hour before rehydrating over night in the shaker.

All DNA samples were checked for quality and concentration using a Nanodrop spectophotometer from Thermo Scientific, and diluted to reach a concentration of 10ng/ul.

When extracting DNA from other organs (heart, liver, brain) samples were processed using the same protocol and kit, but increasing the amount of resin accordingly to the size of the tissue.

8.1.1.1.2 PCR amplification

8.1.1.1.2.1 Primer Sequences

Primers were designed using 'Primer3' software and ordered from MGW Eurofins Operon (Ebersberg, Germany).

NeuroD6 Construct:

fw 5'-AGG ATC TCC TGT CAT CTC ACC TTG CTC CTG-3'

rv 5'-AAG AAC TCG TCA AGA AGG CGA TAG AAG GCG-3'.

CamkIIα-Flpo construct:

fw 5'-AGA ATG TGG CAC CCA CTA GC-3'

rv 5'-TCT TCT TGC TGT GGC TGT TG-3'.

Prolactine:

fw 5’- GCT TCT GAG CAA TGA CAC CA- 3’

rv 5’-ATT CCA GGA GTG CAC CAA AC-3’.

Span:

fw 5’- GCT TTA ACG CCA CTC CAT GT- 3’

rv 5’- GAA CTG CAG CCA GAA AGA GC- 3’.

Exon:

fw 5’- ACA CTT TAA AAA CTG TGC TGG C- 3’

rv 5’- CTG GGA TTC GGG CAT TAC GA- 3’

8.1.1.1.2.2. Short Range PCR Protocol

The standard PCR protocol for genotyping was performed in a 96 well plate in a PTC-225 DNA Engine Tetrad. The PCR the components used were Taq PCR Master Mix Kit of QIAGEN:

1.0 µl template DNA at 10 ng/µl, 2.0 µl primer solution at 10 mM, 2.0 µl dNTP at 8 mM, 1.2 µl $MgCl_2$ at 25 mM, 0.1 µl Hot Star Taq Polymerase (QIAGEN), 11.7 µl ddH_2O.

PCR program unless stated otherwise was used as follows:

95°C for 10 minutes; 95 °C for 30 seconds; 14 cycles of 63 °C for 30 seconds, minus 0.5 °C per cycle, 72 °C for 1 minute; 28 cycles of 95 °C for 30 seconds, 55 °C for 30 seconds, 72 °C for 1 minute; 72 °C for 7 minutes and 15 °C for ever.

8.1.1.1.2.3. Long Range PCR Protocol

In order to amplify long sequences, a long range PCR protocol was used to ensure amplification of big products. The long range PCR protocol was performed in a 96 well plate in a PTC-225 DNA Engine Tetrad. The PCR the components used were the QIAGEN long range PCR mix:

12.5 µl template DNA at 10 ng/µl, 5.0 µl primer solution at 10 mM, 2.5 µl dNTP at 8 mM, 5.0 µl Buffer containing $MgCl_2$ at 25 mM, 0.4 µl QIAGEN long range enzyme mix, 24.6 µl ddH_2O.

The long range PCR programm starts at 93°C for 3 minutes; 93°C for 15 seconds; 62°C for 30 seconds; 68°C for 10 minutes; 30 cycles of 93°C for 15 seconds, 62°C for 30 seconds and 68°C for 10 minutes; and 4°C for ever.

8.1.1.1.2.4 Electrophoresis

Gel electrophoresis was used to assess the PCR product amplification. The PCR products ran on a 3%, 2%, 1.5%, 1% and 0.8% agarose gel containing Ethidium bromide (0.5ug/ml). DNA bands were separated by electrophoresis, at 120-200 mV for 20-60 minutes. Bands were visualized and captured using a UV transiluminator (Alpha Innotech Corporation).

8.1.1.2 Toxin Preparation

Diphtheria Toxin is a potent exotoxin. The minimal lethal dose in humans is less than or equal to 100ng/kg when injected intramuscularly in an unimmunized adult. Therefore proof of immunization was required before any work was carried on with the handling and preparation of the Diphtheria Toxin, and special measures were taken to avoid accidents. Diphtheria Toxin from Corynebacterium Diphtheriae (Sigma Aldrich) was reconstituted using sterile water to reach concentration of 1mg/ml and then diluted into sterile PBS to reach the desired concentration for each dosing. The reconstituted toxin was used within 24 hours and kept at a 10°C temperature at all times.

8.1.1.3 Osmotic Mini Pump Priming

From six to sixteen hours before mini-pump implantation, mini-pumps were primed in saline. We used the model 2ML4 from ALZET Osmotic Pumps. Keeping a septic environment at all times, the mini-pumps were filled with toxin using a filling needle provided with the kit. When completely full, the cap was inserted

and they were submerged into sterile saline solution and kept at 10°C temperature.

8.1.2 Animal Proceedures

8.1.2.1 Breeding and Colony Management

Animals were group-housed in standard open top cages with bedding and a cardboard tube for enrichment. Food and water were available ad libitum, and lighting was kept on a 12 hour cycle with lights coming on at 7am.

The *NeuroD6* hDTR rat and the *CamkII*α-Flpo breeders of each transgenic strain bred with Sprague-Dawley wild type females and males of circa ten weeks of age, caged by pairs. Each litter was ear clipped in order to be genotyped to assess the presence of the construct at maximum 21 days of age. Transgenic animals were selected either for breeding or experimental purposes.

8.1.2.2 Toxin Dosing

8.1.2.2.1 Injection and anesthesia

To minimise the chances of needle stick injuries with the diphtheria toxin rats where anaesthetised. Rats were placed in an induction chamber with Isoflurane at a concentration of 2.0-3.0% for induction. Then they were transferred to a

facemask and maintained at a 0.25-2.0% concentration until loss of righting and flexing reflex. When immobilised, a trained researcher placed the rat comfortably in its back in an upright position. Holding it by the tail an injection was administered in the peritoneal cavity (lower left or right quadrant of the abdomen) and animals were left to recover and returned to their cages.

8.1.2.2.2 Subcutaneous pump implantation surgery

Osmotic pumps allow the delivery of substances in vivo safely in a very controlled manner. We implanted the 2ML4 pump model (ALZET), designed to deliver at a ratio of 2.5 µl/hr during 4 weeks. The pump was implanted subcutaneously in the dorsum, slightly caudal to the scapulae.

Pre-Operative care: Rats were placed in an anesthetic induction box with Isoflurane until induced assessed by righting reflex, and then moved to a facemask to keep them anesthetized during the whole process. Depth of the anesthetic is assessed by loss of flexion reflex and by respiration, and when reached rats were administered 0.1 ml of Metacam via subcutaneous injection prior to the procedure. The incision site and and a large square around it was shaved and cleaned with hibiscrub.

Surgery: A round bladed size 10 scalpel was used to make a 1.75-2 cm mid scapular incision at a medial/lateral orientation. Once the skin was clean cut, blunted scissors were inserted and pushed caudally in the dorsum and slowly opened to blunt dissect the skin and muscle layers until a 2.5 cm wide and 8 cm

long subcutaneous pocket was created. Once the pocket was shaped, an osmotic pump was introduced cap first and located at the end of the pocket, as far away as the incision site as possible by manipulating the skin. The incision wound was brought together to its original position and closed using surgical staples (Leica Biosystems). The wound was cleaned from blood, and sprayed with Opsite wound film spray. Rats were weighted and recovered in a warm chamber for a minimum of 30-40 minutes.

Post-operative care: Rats were checked for signs of discomfort and their weight was monitored daily for 7 days. The mini pumps were manipulated by hand to ensure free mobility under the skin. Staples were removed 12-14 days post surgery.

8.1.2.3 Perfusion and organ harvesting

8.1.2.3.1 Perfusion

All animals received an i.p. injection of Pentobarbitone (300 mg/kg) to reach a deep anesthetic state. Access to the thoracic cavity allowed to clamp the aorta and access to the heart to transcardially perfuse it with a continuous stream of saline (0.9 %, 4 °C). A butterfly needle was stick into the left ventricle, while making an incision into the atrium. Five minutes of saline washing was followed by a 4% paraformaldehyde solution in PBS using an automated perfusion pump. When sufficiently perfused (assessed by upper body stiffness, and light

coloration of liver), brains and organs were extracted and allowed to post fixe for 24 hours on a 4% paraformaldehyde solution at 4 °C. Brains were cryoprotected by immersion of PBS with 30% of sucrose until equilibrated.

8.1.2.3.2 Fresh tissue harvesting

Animals received an i.p. injection of Pentobarbitone (300mg/kg). When absence of heartbeat was confirmed, the thoracic cavity was accessed to harvest different organs such as lungs, heart, kidneys, liver and spleen. The brain was separately harvested. Tissue is immediately frozen by contact with dry ice and kept in eppendorfs at -80°C or wrapped in aluminium foil.

The dissection of the brain is done sectioning the interhemispheric fissure to access the hippocampus.

8.1.3 Histology

8.1.3.1 Tissue preparation: slicing and slide mounting

A freezing microtom was used to slice the brains and organs in a coronal plane at a thickness of 40 µm. Slices were washed in PBS and then preserved as free-floating sections in antifreeze stored at -20 °C.

To mount the slides, slices were washed in PBS and then located in the slide. Slides were left to air-dry overnight.

8.1.3.2 Inmunohistochemistry and Stainings

8.1.3.2.1. Dapi Counterstaining

Except for the Nissl, the Fluorojade C and the NeuN staining, all the fluorescent inmunohistochemistry and stainings have a counterstaining with DAPI.
Fluorescent DAPI: 4 µl of Vectashield (Vector Laboratories) mounting media with DAPI was pippeted per brain or organ slice, carefully covered with the coverslips, and sealed with nail varnish. Slides are protected from light at all times and were allowed to dry overnight.

8.1.3.2.2 Nissl Staining

Slides were immersed in water three times, and placed in a Nissl staining solution for 1 minute. They were washed in water three more times and then background staining was removed by washing them in a series of increased ethanol concentrations: 50%, 75%, and 95% for 20 seconds each and a final wash of 100% ethanol. Slides were placed in three successive histoclear bathes for fixing for 15 minutes (5 minutes each), mounted with DPX medium, and sealed with nail varnish.

8.1.3.2.3 NeuN Antibody staining

The NeuN antibody staining was performed on the brain sections using Anti-NeuN antibody Neuronal marker from Abcam (1:3000). The sections were permeabilised with Triton-X and then transferred and blocked with serum for one hour. Sections were then incubated with the primary antibody at 1:3000 for two hours at 21°C in humid conditions. The secondary antibody used was goat polyclonal to rabbit IgG conjugated to biotin, at (1:200). In certain experiments, some of the slides where followed with a Nissl staining, or mounted in DPX medium and sealed with nail varnish.

8.1.3.2.4 Fluoro-Jade staining

The protocol was an optimised version to use with Fluoro-Jade B from Millipore: The slides were immersed in a series of baths: 100 % EtOH for 3 minutes, 70% EtOH for 1 minute and then dH_2O for 1 minute. Slides were transferred to a 0,06% solution of $KMnO_4$ (potassium permanganate), gently shacking during 14 minutes to ensure even exposure and rinsed with H_2O during one minute.

After that, the following steps were performed in the dark. Slides were immersed in Fluorojade B staining solution (0.01% stock solution of Fluorojade B added to 0.1% of acetic acid vehicle, to reach 0.0004% concentration) during 30 minutes. To rinse, they were washed into a dH_2O bath for 1 minute and repeated the dH_2O bath 2 times. Slides were allowed to dry in the dark overnight. Once slides were dry, and still in the dark, they were rinsed in xylene for 2 minutes 3 times, and

mounted with DPX media and a coverslip. Slides were maintained always in the dark and at a 10°C.

8.1.3.2.5 Tunel Fluorescent Staining

For the fluorescein Tunel Staining we used the In Situ Cell Death detection Kit from Roche Pharmaceuticals. Slides were rinsed in PBS for 2 minutes, and then samples were divided in three groups and processed differently:

A) Incubated with a Protease K treatment (20 ug/ml in 10 mM Tris/Hcl, ph: 7.4-8) in a humid environment at 21-37°C during twenty minutes. Then rinsed with PBS two times for five minutes and followed the common staining step.
B) Permeabilisation solution: 0.1% Triton X-100 in 0.1% sodium citrate freshly prepared for 8 minutes. Then rinsed with PBS two times for five minutes and followed the common staining step.
C) Microwave radiation: slides were immersed in an antigen solution (2.94 gr of sodium citrate in 500 µl of concentrated hydrochlorid acid) microwaved at 450 W for five minutes. Then rinsed with PBS two times for five minutes and followed the common staining step.

Some wild type slides were treated to become positive control slides with a pre staining step: Incubated with DNAse recombinant (1000U/ml of DNAse I diluted in 50 µl of Bovine Serum Albumina at 20mg/ml reconstituted in 50 mM Tris HCl and 950 µl of 5 mM Tris HCl, ph: 7.5) during 10 minutes at 15-25 °C.

In a second experiment to analyse all samples the positive slides were from bel/bel mice brain tissue kindly provided by Dr. James Oliver.

Common staining step: All slides were retrieved from the PBS bath and incubated in TUNEL staining reaction mix for 75 minutes at 37°C in the dark. They were washed with PBS three times and covered with Vectorshield DAPI mounting media and a coverslip, and kept in the dark at all times.

8.1.4 Microscopy, image capture and image analysis

The slides with a Nissl and NeuN staining were processed with a Nikon Eclipse E600 microscope to obtain the images, which were captured with a Nikon camera.

For all the fluorescence images, the microscope used to obtain the images is a Nikon TE2000 Inverted Microscope. The software to process image capture and processing is NIS-elements, using a Hamamatsu Orca C4742-95 camera to capture them.

The mCherry protein has an excitation and emission maxima of 587 nm and 610 nm. The slices preparation included a vector shield mounting media with DAPI, which would allow to the DNA in the nucleus of the cell to get stained by it and emit fluorescence. Therefore, DAPI filter (blue emission colour, violet excitation,

pass bandwith of 310-330 nm) and TRITC filter (red emission colour, green excitation, pass bandwith of 565-605nm) were used to capture fluorescence.

8.1.5. Image processing and Cell counting

When comparing several experimental conditions, we used the number of healthy neurons to see if there are any differences. The staining used for the counting was the antibody NeuN staining. All brains were sliced at a 30 µm. Two random slides per animal were analysed using the Image J analysis software (Fiji). The number of neurons in the CA3 region was counted in a 20x magnification image using the counting and labeling plugins of the software. The CA3 region was defined by the natural curvature of the CA3 region. The counting was done blind to the experimental set up, except for perfusion day.

8.2. THE OBSERVATIONAL APPROACH: POE IN THE HERITABILITY OF COMPLEX TRAITS MATERIAL AND METHODS

All the procedures described regarding the observational project were carried out in accordance with Spanish legislation on the Protection of Animals Used for Experimental and Other Scientific Purposes and the European Community's Council Directive (86/609/EEC) on this subject. The experimental protocol was

approved by the Autonomous University of Barcelona ethics committee (permit CEEAH 697).

8.2.1. Animals and breeding scheme

The HS rats follow a rotational outbreeding scheme involving 40 different families. The scheme is implemented as follows: Given a population of 2m individuals, split equally between the sexes, couples are put into cages labeled 1–m. Cages labeled are assigned 1′–m′ for the next generation. The female from cage 1 is mated with the male from cage 2, and their offspring are placed in cage 1′. Similarly, the female from cage k is mated with the male from cage k + 1 (or the male from cage 1 if k = m) and offspring placed in cage k′, and so on for all remaining k. The procedure is repeated for each generation.

8.2.2. Behavioural testing

The HS rats were approximately eight weeks old at the beginning of the behavioural testing, which stretched for two weeks, with one week separation between each tests.

8.2.2.1. Elevated Zero Maze

The maze comprised an annular platform (105 cm diameter; 10 cm in width)

made of black plywood and elevated to 65 cm above the ground level. It had two open sections (quadrants) and two enclosed ones (with walls 40 cm in height). The subject was placed in an enclosed section facing the wall. The apparatus was situated in a black testing room, dimly illuminated with red fluorescent light, and the behavior was videotaped and measured outside the testing room. Latency to enter into an open section, time spent in the open sections, number of entries in the open sections, number of stretched attend postures, and number of defecation boluses were measured for 5 min.

8.2.2.2. Actimmetry (automated novel-cage activity)

The apparatus (Panlab) consisted of a horizontal surface (50 × 50 cm) provided with photobeams that detect movement and measure it automatically, loading the data in a computer. The subjects were placed in transparent Plexiglas cages (40 × 40 × 40 cm). They were situated in a white fluorescent (60 W) illuminated chamber. Spontaneous horizontal activity was measured for the first 5 min (ACT-DIST5; measure of novelty-induced—open filed-like—activity) and for the last 5 min (ACT-DIS30; as a measure of habituated activity) of a 30-min session.

8.2.2.3. Two-way active shuttle-box avoidance acquisition

Active avoidance acquisition sessions were performed in three identical shuttle boxes (Letica Instruments), each one placed in independent sound-attenuating

boxes consisting of two equal-sized compartments (25 × 25 × 28 cm) connected by an opening (8 × 10 cm). Rats were allowed a 4-min period of familiarization to the box. Immediately after that period, a 40-trial session/rat was administered, each trial consisting of a 10-sec CS (conditioned stimulus; 2400 Hz, 63-dB tone plus a 7-W small light) followed after termination by a 20-sec US (unconditioned stimulus; scrambled 0.7-mA foot shock) delivered through the grid floor. Crossings to the other compartment during the CS (avoidances) or US (escapes) switched off the stimuli and were followed by a 60-sec intertrial interval. The data is detected and loaded into a computer automatically, except the context-freezing which is measured by a researcher.

8.2.3 Other phenotypic measures

Intraperitoneal Glucose Tolerance Test (IPGTT)

Conscious rats in the post absorptive state were injected intraperitoneally with a solution of glucose (2g / kg body weight.). Blood samples were collected for glucose reading before glucose injection and 30, 60 and 120 minutes afterwards by tail tipping. Blood glucose concentration was determined using a glucose meter (Accucheck, Roche Diagnostics, Welwyn Garden City, UK). Cumulative glycemia (AUC_G) was calculated as the increment of the values of plasma glucose during the IPGTT. Incremental plasma glucose values above baseline integrated over 120 min, after an injection of glucose, were used to calculate the index of glucose tolerance (DeltaG).

Blood pressure

Systolic blood pressure was measured by tail plethysmography in conscious, restrained animals as previously described 3,4. Briefly, rats were pre-warmed for 15 min at 30°C for tail artery vasodilation. Rats were then wrapped in a cloth for restraint and an inflatable cuff placed on their tail along with a piezoceramic transducer (Hartmann & Braun type 2). Pulse detection was visualised as a function of pressure and displayed using Microsoft Windows compatible software. An average of 6-8 pressure readings were taken for each rat per sitting.
Haematology Blood (350µl/sample) was collected from the lateral tail vein of anesthetized rats into a tube pretreated with the anticoagulant EDTA-2K (Sangüesa), immediately after the rats were injected with emulsified myelin oligodendrocyte glycoprotein (MOG, used to induce Experimental Autoimmune Encephalomyelitis), and stored cold until used. Full blood count measures were acquired by an automatic hemocytometer (ADVIA 120 Hematology analyzer from Bayer, Siemens Diagnostics).

Basal immunology

Blood was collected from the lateral tail vein of anesthetized rats immediately after they were injected with emulsified MOG, into a heparinized tube (500µl/sample) and stored cold until used. A total of 20 µl blood was added per well in duplicate to 96 well v-bottom polypropylene plates (BD Falcon). Staining with fluorescently labeled monoclonal antibodies (MAb) was performed on non-lysed whole blood for 20 min in the cold. MAbs were diluted in EDTA-FACS buffer (calcium- and magnesium-free PBS-D supplemented with 1% FCS, 10mM

EDTA and 0.01% sodium azide) to predetermined optimal concentrations. The MAbs used were purchased from BD Pharmingen (San Diego, CA): CD45 (OX-1 FITC), RT1-B (OX-6 PE), CD45RA (OX-33 Pe-Cy5), abTCR (R73 biotin and PerCP/APC), CD8a (OX-8 FITC), CD25 (OX-39 PE/APC), CD4 (OX-35 APC/Pe-Cy5), CD28 (JJ319 FITC), RT1-A (OX-18 PE), pan-granulocyte (HIS-48 biotin/Fitc). Streptavidine (SA) -APC was used as a secondary reagent. The stained blood was incubated and washed twice at RT for 10 min in a hypertonic potassium buffer containing 8.26g ammonium chloride and 0.037g EDTA per dm3/ RBC lysis buffer, immediately after incubation with streptavidin. Washed cells were resuspended and incubated for 20 min at RT in a 2% phosphatebuffered formaldehyde solution and thereafter washed twice in EDTA-FACS buffer. Acquisition was performed on a four-color BD FACS Calibur for the first four batches and thereafter on a BD SORP LSRII Analytic Flow Cytometer, no later than 6 days post-staining. The data was analyzed with FlowJo (Tree Star Inc., Ashland, OR).

Induction and Clinical Evaluation of Experimental Autoimmune Encephalomyelitis (EAE)

EAE is a highly reproducible model of multiple sclerosis with a robust clinical score scale 5,6. Recombinant rat myelin oligodendrocyte glycoprotein (MOG), amino acids 1–125 from the N terminus, was expressed in E. coli and purified to homogeneity by metal chelate affinity chromatography 7 and ion exchange chromatography. MOG for the entire HS cohort was produced in 3 batches. Rats were anesthetized with isoflurane (Servicios Genéticos Porcinos) and immunized subcutaneously in the dorsal tail base with 200 μL inoculum

containing MOG (females 50-65 µg and males 120-155 µg) in phosphate buffered-saline (PBS; Life Technologies) emulsified 1:1 with Freund's adjuvant (Sigma-Aldrich) containing 200 µg Mycobacterium tuberculosis (H37 RA, Sigma-Aldrich). Signs of EAE and body weight were monitored daily from day 9 until day 28 postimmunization (p.i.). The scale for EAE scoring was as follows: 0 = healthy; 1 = tail weakness or tail paralysis; 2 = hind leg paresis or hemiparesis; 3 = hind leg paralysis or hemiparalysis; 4 = tetraplegy, urinary, and/or fecal incontinence; and 5 = death. If severe disease (score 4) was observed for two consecutive days, the rats were sacrificed for ethical reasons. Duration of EAE was defined as the number of days with signs of disease including days after rats died/were sacrificed. Cumulative scores were defined as the sum of all scores received during the experiment including days after rats died/were sacrificed. Weight loss is a sub phenotype of EAE, which may depend on inflammation-mediated effects or the inability to hydrate and eat properly. WL reflects sub-clinical disease and is a quantitative trait considered to correlate well with EAE disease course. WL0 was defined as (weight at day 0 p.i. - minimum weight during the experiment)/weight at day 0 p.i.) and WL9 was defined as (weight at day 9 p.i. - minimum weight during the experiment)/weight at day 9 p.i.).

Tissue dissection

Rats were euthanized by exsanguination under isofluorane anesthesia. Blood was obtained from cardiac puncture, and then the heart was dissected out and weighed. Thereafter the ears, abdominal aorta, liver, and bones were dissected in parallel whenever possible. Other tissues were collected for future studies (thymus, brain, pituitary, spinal cord, spleen, kidneys, adrenal glands, tail). Blood

was kept at room temperature for 4 hours, then at 4°C for 4 hours until it was centrifuged, the heart and liver were snap frozen in a tube in liquid nitrogen, the ears and abdominal aorta were immersed in buffered formalin, and the bones kept on ice until stored at -20°C.

Serum biochemistry

Blood was centrifuged at 2000rpm for 20 minutes at 4°C, and the serum was separated, aliquoted and stored at -80°C. Serum was analysed on a AU400 Analyser.

Internal elastic lamina ruptures

Abdominal aorta (AA) and the proximal 1 cm of the left common iliac artery (IA) were dissected out, rapidly rinsed in saline and fixed by immersion in buffered formalin. En face preparations of the unperfused AA and the attached left IA were then made. Under a dissecting microscope, arteries were cleaned, opened longitudinally and pinned out, luminal surface uppermost. The luminal surface was stained with orcein and hematoxylin to show the internal elastic lamina (IEL) and the nuclei respectively. After staining, arteries were dehydrated, unpinned, cleared and mounted on slides for microscopic observation. With this technique, as previously described 9, ruptures appear as dark grey transverse bands due to absence of the internal elastic lamina, which stains pink, and the intense staining of underlying smooth muscle cell nuclei, which are not stained in areas where the IEL is present. Ruptures were then quantified at a final magnification of x 40. For each individual, the total number of IEL ruptures in the AA and IA were recorded and each rupture was graded on a semi-quantitative

scale according to its size in the circumferential direction, using a grid in the eyepiece. A final score was calculated taking into account the size of the ruptures. Thus the degree of IEL rupture in each AA and IA was expressed as a number of ruptures per artery, or as a score indicating the severity of the phenomenon. For each rat, global values were also obtained by adding those for AA and IA.

Bone Phenotyping

For bone density and structure, femurs were placed in plastic tubes filled with 70% ethyl alcohol and centered in the gantry of a Norland Stratec XCT Research SA+pQCT (Stratec Electronics, Pforzheim, Germany). Slice measurements of 0.26 mm thickness and a voxel size of 0.07 mm were taken at the midshaft, distal femur and perpendicularly through the femoral neck. For each slice, the Xray source was rotated through 180º of projection. Volumetric BMD (vBMD; mg/cm3), cross sectional area (CSA; mm2) and polar moment of inertia (Ip; mm4) were measured from the pQCT images. Density thresholds of 500 and 900 were used to identify mineralized bone. The femur BMC (g) was measured using DXA (PIXImus mouse densitometer, Lunar Corp., WI, USA). The femoral neck width (NW; mm) was measured in the anterior-posterior direction using digital calipers. For bone biomechanics, femurs were tested in three-point bending by positioning them on the lower supports of a three-point bending fixture and applying load at the midpoint using a material testing machine (Alliance RT/5, MTS Systems Corp., Eden Prairie, USA). Force and displacement measurements were collected every 0.05 second. From the force vs. displacement curves, work to failure (W; in mJ) was calculated in TestWorks software.

Wound healing

At 7 weeks of age a 2-mm hole was made in the center of the cartilaginous part of one ear using a metal ear punch. At sacrifice, the whole ear was placed in buffered formalin. To calculate the area of the hole, the ear was first trimmed so that it could be placed flat between two slides, and scanned. The hole was delimited and the area calculated using ImageJ.

8.2.4. Data analysis

8.2.4.1. Phenotypes and Genotypes

Phenotypes were transformed to residuals to eliminate covariates that were significantly associated, such as sex, batch, cage and experimenter using boxcox and quantile normalisation. All the information on genotypes and further mapping information is available in the Supplementary Text and Figures of the HS rats paper (Baud, 2013b).

9. BIBLIOGRAPHY

9. BIBLIOGRAPHY

Abbott, A. (2004) "Laboratory Animals: The Renaissance Rat." *Nature* 428, no. 6982: 464–66. doi:10.1038/428464a.

Aitman TJ., Critser JK., Cuppen E., Dominiczak A., Fernandez-Suarez XM., Flint J, Gauguier D, et al. (2008) "Progress and Prospects in Rat Genetics: a Community View." *Nature Genetics* 40, no. 5: 516–22. doi:10.1038/ng.147.

Imranul A, Koller DL, Sun Q, Roeder RK, Cañete T, Blázquez G, López-Aumatell R, et al. (2011): "Heterogeneous Stock Rat: a Unique Animal Model for Mapping Genes Influencing Bone Fragility." *Bone* 48, no. 5 1169–77. doi:10.1016/j.bone.2011.02.009.

Albright TD., Jessell TM, Kandel ER, Posner MI. (2000) "Neural Science: a Century of Progress and the Mysteries That Remain." *Neuron* 25, no. 1: S1–S55.

Amaral, D G. (1978) "A Golgi Study of Cell Types in the Hilar Region of the Hippocampus in the Rat." *The Journal of Comparative Neurology* 182, no. 4 Pt 2: 851–914.

Amaral, D. G., Witter M.P. (1995) *Hippocampal Formation, Paxinos G., The Rat Nervous System, , 443-493*. Academic Press, San Diego, n.d.

Amaral, DG., Ishizuka N, Claiborne B. (1990) "Chapter 1 Chapter Neurons, Numbers and the Hippocampal Network." In *Progress in Brain Research*, edited by J. Zimmer and O. P. Ottersen J. Storm-Mathisen, Volume 83:1–11. Understanding the Brain Through the Hippocampus the Hippocampal Region as a Model for Studying Brain Structure and Function. Elsevier. http://www.sciencedirect.com/science/article/pii/S0079612308612376.

Amaral DG., Scharfman HE, Lavenex P. (2007) "The Dentate Gyrus: Fundamental Neuroanatomical Organization (dentate Gyrus for Dummies)." *Progress in Brain Research* 163: 3–22. doi:10.1016/S0079-6123(07)63001-5.

Andersen P, R. Morris, D. Amaral, T. Bliss, O'Keefe J . (2007*) The Hippocampus Book*. Oxford University Press, New York, n.d.

Annese J, Schenker-Ahmed NM, Bartsch H, Maechler P, Sheh C, Thomas N, Kayano J, et al. (2014) "Postmortem Examination of Patient H.M.'s Brain Based on Histological Sectioning and Digital 3D Reconstruction." *Nature Communications* 5 doi:10.1038/ncomms4122.

Antonarakis SE., Beckmann JS. (2006) "Mendelian Disorders Deserve More Attention." *Nature Reviews Genetics* 7, no. 4 :277–82. doi:10.1038/nrg1826.

Arruda-Carvalho M, Sakaguchi M, Akers KG, Josselyn SH, Frankland PW.(2011) "Posttraining Ablation of Adult-Generated Neurons Degrades Previously Acquired Memories." *The Journal of Neuroscience* 31, no. 42 :15113–27. doi:10.1523/JNEUROSCI.3432-11.2011.

Badano JL., Katsanis N. (2002) "Beyond Mendel: An Evolving View of Human Genetic Disease Transmission." *Nature Reviews Genetics* 3, no. 10 : 779–89. doi:10.1038/nrg910.

Bannerman D. M, Grubb M, Deacon RMJ, Yee BK, Feldon J, Rawlins J. N. P. (2003) "Ventral Hippocampal Lesions Affect Anxiety but Not Spatial Learning."

Behavioural Brain Research 139, no. 1–2 : 197–213. doi:10.1016/S0166-4328(02)00268-1.

Bannerman D. M, Rawlins J. N. P, McHugh S. B, Deacon R. M. J, Yee B. K, Bast T, Zhang W. -N, Pothuizen H. H. J, Feldon J. (2004) "Regional Dissociations Within the Hippocampus—memory and Anxiety." *Neuroscience & Biobehavioral Reviews* 28, no. 3 : 273–83. doi:10.1016/j.neubiorev.2004.03.004.

Bannerman, D. M., Yee B. K., Good M. A., Heupel M. J., Iversen S. D., Rawlins. J. N. (1999) "Double Dissociation of Function Within the Hippocampus: a Comparison of Dorsal, Ventral, and Complete Hippocampal Cytotoxic Lesions." *Behavioral Neuroscience* 113, no. 6: 1170–88.

Bannerman DM., Bus T, Taylor A, Sanderson DJ, Schwarz I, Jensen V, Hvalby Ø, Rawlins JNP, Seeburg PH, Sprengel R. (2012) "Dissecting Spatial Knowledge from Spatial Choice by Hippocampal NMDA Receptor Deletion." *Nature Neuroscience* 15, no. 8 : 1153–59. doi:10.1038/nn.3166.

Bannerman DM., Sprengel R, Sanderson DJ, McHugh SB, Rawlins JNP, Monyer H, H. Seeburg PH. (2014) "Hippocampal Synaptic Plasticity, Spatial Memory and Anxiety." *Nature Reviews Neuroscience* 15, no. 3 : 181–92. doi:10.1038/nrn3677.

Baud A., Rat Genome Sequencing and Mapping Consortium. "Combined Sequence-based and Genetic Mapping Analysis of Complex Traits in Outbred Rats." *Nature Genetics* 45, no. 7 (July 2013): 767–75. doi:10.1038/ng.2644.

Begum F, Ghosh D, Tseng GC, Feingold E.(2012) "Comprehensive Literature Review and Statistical Considerations for GWAS Meta-analysis." *Nucleic Acids Research*, gkr1255. doi:10.1093/nar/gkr1255.

Bell JT., Spector TD. (2011) "A Twin Approach to Unraveling Epigenetics." *Trends in Genetics* 27, no. 3 : 116–25. doi:10.1016/j.tig.2010.12.005.

Benus R. F., Bohus B, Koolhaas JM, van Oortmerssen GA. (1991) "Heritable Variation for Aggression as a Reflection of Individual Coping Strategies." *Experientia* 47, no. 10 : 1008–19. doi:10.1007/BF01923336.

Bertelsen A., Harvald B., Hauge. M. (1977) "A Danish Twin Study of Manic-depressive Disorders." *The British Journal of Psychiatry* 130, no. 4 : 330–51. doi:10.1192/bjp.130.4.330.

Bishop JO, Smith P (1989). "Mechanism of Chromosomal Integration of Microinjected DNA." *Molecular Biology & Medicine* 6, no. 4 : 283–98.

Bodmer W, Bonilla C. (2008) "Common and Rare Variants in Multifactorial Susceptibility to Common Diseases." *Nature Genetics* 40, no. : 695–701. doi:10.1038/ng.f.136.

Bouchard TJ, Loehlin JC. (2001) "Genes, Evolution, and Personality." *Behavior Genetics* 31, no. 3 : 243–73. doi:10.1023/A:1012294324713.

Boucher W., Cotterman CW. (1990) "On the Classification of Regular Systems of Inbreeding." *Journal of Mathematical Biology* 28, no. 3 : 293–305. doi:10.1007/BF00178778.

Broadbent NJ., Squire LR, Clark RE. (2004) "Spatial Memory, Recognition Memory, and the Hippocampus." *Proceedings of the National Academy of Sciences of the United States of America* 101, no. 40: 14515–20. doi:10.1073/pnas.0406344101.

Brockschnieder D, Pechmann Y, Sonnenberg-Riethmacher E, Riethmacher D. (2006) "An Improved Mouse Line for Cre-induced Cell Ablation Due to Diphtheria Toxin A, Expressed from the Rosa26 Locus." *Genesis* 44, no. 7 : 322–27. doi:10.1002/dvg.20218.

Buch T, Heppner FL, Tertilt C, Tobias J. A., Heinen J., Kremer M, Wunderlich FT, Jung S, Waisman A. (2005) "A Cre-inducible Diphtheria Toxin Receptor Mediates Cell Lineage Ablation after Toxin Administration." *Nature Methods* 2, no.6 : 419–26. doi:10.1038/nmeth762.

Burgess N, Maguire EA, O'Keefe J. (2002) "The Human Hippocampus and Spatial and Episodic Memory." *Neuron* 35, no. 4 : 625–41. doi:10.1016/S0896-6273(02)00830-9.

Burmeister M, McInnis MG, Zöllner S. (2008) "Psychiatric Genetics: Progress Amid Controversy." *Nature Reviews Genetics* 9, no. 7 : 527–40. doi:10.1038/nrg2381.

Bush D, Barry C, Burgess N. (2014) "What Do Grid Cells Contribute to Place Cell Firing?" *Trends in Neurosciences*. Accessed doi:10.1016/j.tins.2013.12.003.

Busjahn A., Faulhaber H. D., Freier K., Luft F. C. (1999) "Genetic and Environmental Influences on Coping Styles: a Twin Study." *Psychosomatic Medicine* 61, no. 4: 469–75.

Cannon WB. (1915) "Bodily Changes in Pain, Hunger, Fear and Rage: An Account of Recent Researches into the Function of Emotional Excitement.," http://psycnet.apa.org/psycinfo/2004-15415-000.

Caspi A, Moffitt TE. (2006) "Gene–environment Interactions in Psychiatry: Joining Forces with Neuroscience." *Nature Reviews Neuroscience* 7, no. 7: 583–90. doi:10.1038/nrn1925.

Cha J-H, Chang MY, Richardson JA, Eidels L. (2003) "Transgenic Mice Expressing the Diphtheria Toxin Receptor Are Sensitive to the Toxin." *Molecular Microbiology* 49, no. 1 : 235–40. doi:10.1046/j.1365-2958.2003.03550.x.

Chandler KJ., Chandler RL, Broeckelmann EM, Hou Y, Southard-Smith EM, Mortlock DP. (2007) "Relevance of BAC Transgene Copy Number in Mice: Transgene Copy Number Variation Across Multiple Transgenic Lines and Correlations with Transgene Integrity and Expression." *Mammalian Genome* 18, no. 10: 693–708. doi:10.1007/s00335-007-9056-y.

Charriaut-Marlangue C., Margaill I., Represa A., Popovici T., Plotkine M., Ben-Ari Y. (1996) "Apoptosis and Necrosis After Reversible Focal Ischemia: An In Situ DNA Fragmentation Analysis." *Journal of Cerebral Blood Flow & Metabolism* 16, no. 2 : 186–95. doi:10.1097/00004647-199603000-00002.

Chelly J, Khelfaoui M, Francis F, Chérif B, Bienvenu T. (2006) "Genetics and Pathophysiology of Mental Retardation." *European Journal of Human Genetics* 14, no. 6 : 701–13. doi:10.1038/sj.ejhg.5201595.

Chen H, Kohno K, Gong Q. (2005) "Conditional Ablation of Mature Olfactory Sensory Neurons Mediated by Diphtheria Toxin Receptor." *Journal of Neurocytology* 34, no. 1–2 :37–47. doi:10.1007/s11068-005-5046-8.

Cheung T, Cardinal RN. (2005) "Hippocampal Lesions Facilitate Instrumental Learning with Delayed Reinforcement but Induce Impulsive Choice in Rats." *BMC Neuroscience* 6, no. 1 : 36. doi:10.1186/1471-2202-6-36.

Choe S, Bennett MJ, Fujii G, Curmi P, Kantardjieff KA, Collier RJ, Eisenberg D. (1992) "The Crystal Structure of Diphtheria Toxin." *Nature* 357, no. 6375: 216–22. doi:10.1038/357216a0.

Cirulli ET., Goldstein DB. (2010)"Uncovering the Roles of Rare Variants in Common Disease through Whole-genome Sequencing." *Nature Reviews Genetics* 11, no. 6 : 415–25. doi:10.1038/nrg2779.

Clarke PG. (1990) “Developmental Cell Death: Morphological Diversity and Multiple Mechanisms.” *Anatomy and Embryology* 181, no. 3 : 195–213. doi:10.1007/BF00174615.

Coca AF., Russell EF., Baughman WH. (1921)“The Reaction of the Rat to Diphtheria Toxin With Observations on the Technic of the Roemer Method of Testing Diphtheria Toxin and Antitoxin.” *The Journal of Immunology* 6, no. 6: 387–98.

Coppens CM., de Boer SF., Steimer T, Koolhaas JM. (2013) “Correlated Behavioral Traits in Rats of the Roman Selection Lines.” *Behavior Genetics* 43, no. 3: 220–26. doi:10.1007/s10519-013-9588-8.

Crawley JN. (1999) “Behavioral Phenotyping of Transgenic and Knockout Mice: Experimental Design and Evaluation of General Health, Sensory Functions, Motor Abilities, and Specific Behavioral Tests.” *Brain Research* 835, no. 1: 18–26. doi:10.1016/S0006-8993(98)01258-X.

Culley DJ., Baxter MG, Crosby CA, Yukhananov R, and Crosby G. (2004) “Impaired Acquisition of Spatial Memory 2 Weeks After Isoflurane and Isoflurane-Nitrous Oxide Anesthesia in Aged Rats:” *Anesthesia & Analgesia*, 1393–97. doi:10.1213/01.ANE.0000135408.14319.CC.

Culley DJ., Baxter MG, Crosby CA, Yukhananov R, and Crosby G. (2004) “Long-term Impairment of Acquisition of a Spatial Memory Task Following Isoflurane–Nitrous Oxide Anesthesia in Rats:” *Anesthesiology* 100, no. 2 : 309–14. doi:10.1097/00000542-200402000-00020.

Davidson T L, Jarrard LE. (2004) “The Hippocampus and Inhibitory Learning: a ‘Gray’ Area?” *Neuroscience and Biobehavioral Reviews* 28, no. 3 : 261–71. doi:10.1016/j.neubiorev.2004.02.001.

Davies W, Isles A, Smith R, Karunadasa D, Burrmann D, Humby T, Ojarikre O, et al. (2005) “Xlr3b Is a New Imprinted Candidate for X-linked Parent-of-origin Effects on Cognitive Function in Mice.” *Nature Genetics* 37, no. 6 : 625–29. doi:10.1038/ng1577.

Deng W, Aimone JB, Gage F. (2010) “New Neurons and New Memories: How Does Adult Hippocampal Neurogenesis Affect Learning and Memory?” *Nature Reviews Neuroscience* 11, no. 5 : 339–50. doi:10.1038/nrn2822.

Díaz-Morán, S. (2013) “What Can We Learn on Rodent Fearfulness/anxiety from the Genetically Heterogeneous NIH-HS Rat Stock?” *Open Journal of Psychiatry* 03, no. 02 (2013): 238–50. doi:10.4236/ojpsych.2013.32022.

Díaz-Morán S, Palència M, Mont-Cardona C, Cañete T, Blázquez G, Martínez-Membrives E, López-Aumatell R, et al. (2013) “Gene Expression in Amygdala as a Function of Differential Trait Anxiety Levels in Genetically Heterogeneous NIH-HS Rats.” *Behavioural Brain Research* 252 : 422–31. doi:10.1016/j.bbr.2013.05.066.

Díaz-Morán S, Palència M, Mont-Cardona C, Cañete T, Blázquez G, Martínez-Membrives E, López-Aumatell R, Tobeña A, Fernández-Teruel A. (2012) “Coping Style and Stress Hormone Responses in Genetically Heterogeneous Rats: Comparison with the Roman Rat Strains.” *Behavioural Brain Research* 228, no. 1: 203–10. doi:10.1016/j.bbr.2011.12.002.

Dingemanse NJ, Both C, Drent PJ, van Oers K, van Noordwijk AJ. (2002) “Repeatability and Heritability of Exploratory Behaviour in Great Tits from the Wild.” *Animal Behaviour* 64, no. 6 :929–38. doi:10.1006/anbe.2002.2006.

Dingemanse NJ., Both C, Drent PJ, Tinbergen JM. (2004) "Fitness Consequences of Avian Personalities in a Fluctuating Environment." *Proceedings of the Royal Society B: Biological Sciences* 271, no. 1541 : 847–52.

Doeller CF., Barry C, Burgess N. (2010) "Evidence for Grid Cells in a Human Memory Network." *Nature* 463, no. 7281 : 657–61. doi:10.1038/nature08704.

Drent, Pieter J, van Oers K, van Noordwijk AJ. (2003) "Realized Heritability of Personalities in the Great Tit (Parus Major)." *Proceedings of the Royal Society B: Biological Sciences* 270, no. 1510 : 45–51. doi:10.1098/rspb.2002.2168.

Driscoll, P., Escorihuela R. M., Fernández-Teruel A., Giorgi O., Schwegler H., Steimer Th., Wiersma A., et al. (1998) "Genetic Selection and Differential Stress Responses: The Roman Lines/Strains of Rats." *Annals of the New York Academy of Sciences* 851, no. 1 : 501–10. doi:10.1111/j.1749-6632.1998.tb09029.x.

Eichenbaum, H. (2011) *The Cognitive Neuroscience of Memory: An Introduction*. Oxford University Press. doi:10.1038

Eichler EE., Flint J, Gibson G, Kong A, Leal SM, Moore JH, Nadeau JH. (2010) "Missing Heritability and Strategies for Finding the Underlying Causes of Complex Disease." *Nature Reviews Genetics* 11, no. 6 : 446–50. doi:10.1038/nrg2809.

Engel, G. L., Schmale A. H. (1972) "Conservation-withdrawal: a Primary Regulatory Process for Organismic Homeostasis." *Ciba Foundation Symposium* 8 : 57–75.

Escorihuela R. M, Fernández-Teruel A, Gil L, Aguilar R, Tobeña A, Driscoll P. (1999) "Inbred Roman High- and Low-Avoidance Rats: Differences in Anxiety, Novelty-Seeking, and Shuttlebox Behaviors." *Physiology & Behavior* 67, no. 1 : 19–26. doi:10.1016/S0031-9384(99)00064-5.

Fanselow MS., Dong HW. (2010) "Are the Dorsal and Ventral Hippocampus Functionally Distinct Structures?" *Neuron* 65, no. 1 : 7–19. doi:10.1016/j.neuron.2009.11.031.

Farley FW., Soriano P, Steffen LS, Dymecki SM. (2000) "Widespread Recombinase Expression Using FLPeR (Flipper) Mice." *Genesis* 28, no. 3–4 : 106–10. doi:10.1002/1526-968X(200011/12)28:3/4<106::AID-GENE30>3.0.CO;2-T.

Feng G, Mellor RH, Bernstein M, Keller-Peck C, Nguyen QT, Wallace M, Nerbonne JM, Lichtman JW, Sanes JR. (2000) "Imaging Neuronal Subsets in Transgenic Mice Expressing Multiple Spectral Variants of GFP." *Neuron* 28, no. 1 : 41–51. doi:10.1016/S0896-6273(00)00084-2.

Fernández-Teruel A., Escorihuela R. M, Núñez J. F., Zapata A., Boix F., Salazar W., and Tobeña A. (1991) "The Early Acquisition of Two-way (shuttle-box) Avoidance as an Anxiety-mediated Behavior: Psychopharmacological Validation." *Brain Research Bulletin* 26, no. 1: 173–76. doi:10.1016/0361-9230(91)90205-X.

Fernández-Teruel A, Escorihuela RM, Gray JA, Aguilar R, Gil L, Giménez-Llort L, Tobeña A, et al. (2002) "A Quantitative Trait Locus Influencing Anxiety in the Laboratory Rat." *Genome Research* 12, no. 4 : 618–26. doi:10.1101/gr.203402.

Fisher, R. A. (1919) "XV.—The Correlation Between Relatives on the Supposition of Mendelian Inheritance." *Earth and Environmental Science Transactions of the Royal Society of Edinburgh* 52, no. 02 : 399–433. doi:10.1017/S0080456800012163.

Fitzgerald PJ., Barkus C, Feyder M, Wiedholz LM, Chen YC, Karlsson RM, Machado-Vieira R, et al. (2010) "Does Gene Deletion of AMPA GluA1 Phenocopy Features of Schizoaffective Disorder?" *Neurobiology of Disease* 40, no. 3 : 608–21. doi:10.1016/j.nbd.2010.08.005.

Flint, J. (2003)"Analysis of Quantitative Trait Loci That Influence Animal Behavior." *Journal of Neurobiology* 54, no. 1: 46–77. doi:10.1002/neu.10161.

Flint, J. (1999) "The Genetic Basis of Cognition." *Brain* 122, no. 11 : 2015–32. doi:10.1093/brain/122.11.2015.

Flint J, Corley R, DeFries JC, Fulker DW, Gray JA, Miller S., Collins, AC. (1995) "A Simple Genetic Basis for a Complex Psychological Trait in Laboratory Mice." *Science*. http://psycnet.apa.org/psycinfo/1996-16518-001.

Flint J, Kendler KS. (2014) "The Genetics of Major Depression." *Neuron* 81, no. 3 : 484–503. doi:10.1016/j.neuron.2014.01.027.

Flint J, Monaco AP. (2006) "Focus on Behavioural Genetics." *European Journal of Human Genetics* 14, no. 6: 647–48. doi:10.1038/sj.ejhg.5201599.

Flint J, Mott R. (2001) "Finding the Molecular Basis of Quatitative Traits: Successes and Pitfalls." *Nature Reviews Genetics* 2, no. 6 : 437–45. doi:10.1038/35076585.

Flint J, Munafò M. (2014) "Schizophrenia: Genesis of a Complex Disease." *Nature* 511, no. 7510 : 412–13. doi:10.1038/nature13645.

Flint J, Munafò M. (2008) "Forum: Interactions Between Gene and Environment:" *Current Opinion in Psychiatry* 21, no. 4 : 315–17. doi:10.1097/YCO.0b013e328306a791.

Flint J, Valdar W, Shifman S, Mott R. (2005) "Strategies for Mapping and Cloning Quantitative Trait Genes in Rodents." *Nature Reviews Genetics* 6, no. 4: 271–86. doi:10.1038/nrg1576.

Foster DJ, Wilson MA. (2006) "Reverse Replay of Behavioural Sequences in Hippocampal Place Cells During the Awake State." *Nature* 440, no. 7084: 680–83. doi:10.1038/nature04587.

Frankland PW., O'Brien C, Ohno M, Kirkwood A, Silva AJ. (2001) "α-CaMKII-dependent Plasticity in the Cortex Is Required for Permanent Memory." *Nature* 411, no. 6835: 309–13. doi:10.1038/35077089.

Furukawa N, Saito M, Hakoshima T, Kohno K. (2006) "A Diphtheria Toxin Receptor Deficient in Epidermal Growth Factor–Like Biological Activity." *Journal of Biochemistry* 140, no. 6 :831–41. doi:10.1093/jb/mvj216.

Garcia-Falgueras A., Castillo-Ruiz M.M., Put T., Tobeña A., Fernández-Teruel A. (2012) "Differential Hippocampal Neuron Density Between Inbred Roman High- (low Anxious) and Low-avoidance (high Anxious) Rats." *Neuroscience Letters* 522, no. 1 : 41–46. doi:10.1016/j.neulet.2012.06.011.

Garfield AS., Cowley M, Smith FM, Moorwood K, Stewart-Cox JE, Gilroy K, Baker S, et al. (2011) "Distinct Physiological and Behavioural Functions for Parental Alleles of Imprinted Grb10." *Nature* 469, no. 7331: 534–38. doi:10.1038/nature09651.

Gates CA, Cox MM. (1988) "FLP Recombinase Is an Enzyme." *Proceedings of the National Academy of Sciences of the United States of America* 85, no. 13: 4628–32.

Gershenfeld HK., Paul SM. (1997) "Mapping Quantitative Trait Loci for Fear-like Behaviors in Mice." *Genomics* 46, no. 1 : 1–8. doi:10.1006/geno.1997.5002.

Giannoukakis N, Deal C, Paquette J, Goodyer CG, Polychronakos C. (1993) "Parental Genomic Imprinting of the Human IGF2 Gene." *Nature Genetics* 4, no. 1: 98–101. doi:10.1038/ng0593-98.

Gibbs RA, Weinstock GM , Metzker ML, Muzny DM, Sodergren EJ, Scherer S, Scott G. (2004) "Genome Sequence of the Brown Norway Rat Yields Insights into Mammalian Evolution." *Nature* 428, no. 6982: 493–521. doi:10.1038/nature02426.

Gibson, G. (2012) “Rare and Common Variants: Twenty Arguments.” *Nature Reviews Genetics* 13, no. 2 : 135–45. doi:10.1038/nrg3118.

Giraldo P, Montoliu LL. (2001) “Size Matters: Use of YACs, BACs and PACs in Transgenic Animals.” *Transgenic Research* 10, no. 2 (April 1, 2001): 83–103. doi:10.1023/A:1008918913249.

Golub, J. S., Tong L., Ngyuen T. B., Hume C. R., Palmiter R. D., Rubel E. W, Stone J. S. (2012) “Hair Cell Replacement in Adult Mouse Utricles after Targeted Ablation of Hair Cells with Diphtheria Toxin.” *Journal of Neuroscience* 32, no. 43: 15093–105. doi:10.1523/JNEUROSCI.1709-12.2012.

Good M, de Hoz L, Morris RG. (1998) “Contingent Versus Incidental Context Processing During Conditioning: Dissociation after Excitotoxic Hippocampal Plus Dentate Gyrus Lesions.” *Hippocampus* 8, no. 2 : 147–59. doi:10.1002/(SICI)1098-1063(1998)8:2<147::AID-HIPO7>3.0.CO;2-I.

Gould E, McEwen BS, Tanapat P, Galea LAM, Fuchs E. (1997) “Neurogenesis in the Dentate Gyrus of the Adult Tree Shrew Is Regulated by Psychosocial Stress and NMDA Receptor Activation.” *The Journal of Neuroscience* 17, no. 7 : 2492–98.

Gray J. A., McNaughton N. (2000) *The Neuropsychology of Anxiety: An Enquiry into the Functions of the Septo-hippocampal System*. Oxford University Press, Oxford, n.d.

Gray, JA. (1982) “The Neuropsychology of Anxiety: An Enquiry into the Functions of the Septo-hippocampal System.,” http://doi.apa.org/psycinfo/1992-98224-000.

Green AE., Munafò MR, DeYoung CG, Fossella JA, Fan J, Gray JR. (2008) “Using Genetic Data in Cognitive Neuroscience: From Growing Pains to Genuine Insights.” *Nature Reviews Neuroscience* 9, no. 9 : 710–20. doi:10.1038/nrn2461.

Gross, C. G. (1987) “Early History of Neuroscience.” *Encyclopedia of Neuroscience* 2 : 843–46.

Group, Psychiatric GWAS Consortium Bipolar Disorder Working. (2011) “Large-scale Genome-wide Association Analysis of Bipolar Disorder Identifies a New Susceptibility Locus Near ODZ4.” *Nature Genetics* 43, no. 10: 977–83. doi:10.1038/ng.943.

Groves JO., Leslie I, Huang GJ, McHugh SB, Taylor A, Mott R, Munafò M, Bannerman DM, Flint J. (2013) “Ablating Adult Neurogenesis in the Rat Has No Effect on Spatial Processing: Evidence from a Novel Pharmacogenetic Model.” *PLoS Genet* 9, no. 9 : e1003718. doi:10.1371/journal.pgen.1003718.

Hafting T, Fyhn M, Molden S, Moser MB, Moser EI. (2005) “Microstructure of a Spatial Map in the Entorhinal Cortex.” *Nature* 436, no. 7052: 801–6. doi:10.1038/nature03721.

Hagan, J. J., Salamone J. D., Simpson J., Iversen S. D., Morris R. G. M. (1988) “Place Navigation in Rats Is Impaired by Lesions of Medial Septum and Diagonal Band but Not Nucleus Basalis Magnocellularis.” *Behavioural Brain Research* 27, no. 1 : 9–20. doi:10.1016/0166-4328(88)90105-2.

Hager R, Cheverud JM, Wolf JB. (2008) “Maternal Effects as the Cause of Parent-of-origin Effects That Mimic Genomic Imprinting.” *Genetics* 178, no. 3 : 1755–62. doi:10.1534/genetics.107.080697.

Haig D. (2011) “Does Heritability Hide in Epistasis Between Linked SNPs?” *European Journal of Human Genetics* 19, no. 2 : 123. doi:10.1038/ejhg.2010.161.

Hansen C., Spuhler K. (1984) “Development of the National Institutes of Health Genetically Heterogeneous Rat Stock.” *Alcoholism, Clinical and Experimental Research* 8, no. 5 : 477–79.

Hawrylycz MJ., Lein ES, Guillozet-Bongaarts AL, Shen EH, Ng L, Miller JA, van de Lagemaat LN, et al. (2012) "An Anatomically Comprehensive Atlas of the Adult Human Brain Transcriptome." *Nature* 489, no. 7416 : 391–99. doi:10.1038/nature11405.

Hemani G, Knott S, Haley C. (2013) "An Evolutionary Perspective on Epistasis and the Missing Heritability." *PLoS Genetics* 9, no. 2 . doi:10.1371/journal.pgen.1003295.

Henry JP, Stephens PM. (1977) *Stress, Health, and the Social Environment: A Sociobiologic Approach to Medicine*. Springer-Verlag New York.

Henze DA., Buzsáki G. (2007) "Hilar Mossy Cells: Functional Identification and Activity in Vivo." In *Progress in Brain Research*, edited by Helen E. Scharfman, Volume 163:199–810. The Dentate Gyrus: A Comprehensive Guide to Structure, Function, and Clinical Implications. Elsevier. http://www.sciencedirect.com/science/article/pii/S007961230763012X.

Hettema JM., Neale MC, Kendler KS. (2001) "A Review and Meta-Analysis of the Genetic Epidemiology of Anxiety Disorders." *American Journal of Psychiatry* 158, no. 10 : 1568–78. doi:10.1176/appi.ajp.158.10.1568.

Hettema J, Neale M, Myers J, Prescott C, Kendler K. (2006) "A Population-Based Twin Study of the Relationship Between Neuroticism and Internalizing Disorders." *American Journal of Psychiatry* 163, no. 5: 857–64. doi:10.1176/appi.ajp.163.5.857.

Hirschhorn JN., Lohmueller K, Byrne E, Hirschhorn K. (2002) "A Comprehensive Review of Genetic Association Studies." *Genetics in Medicine* 4, no. 2 : 45–61. doi:10.1097/00125817-200203000-00002.

Holmes, RK. (2000) "Biology and Molecular Epidemiology of Diphtheria Toxin and the *Tox* Gene." *The Journal of Infectious Diseases* 181, no. s1 : S156–S167. doi:10.1086/315554.

Huerta PT, Sun LD, Wilson MA, Tonegawa S. (2000) "Formation of Temporal Memory Requires NMDA Receptors Within CA1 Pyramidal Neurons." *Neuron* 25, no. 2 : 473–80. doi:10.1016/S0896-6273(00)80909-5.

Ikeda H, Tauchi H, Shimasaki H, Ueta N, Sato T. (1985) "Age and Organ Difference in Amount and Distribution of Autofluorescent Granules in Rats." *Mechanisms of Ageing and Development* 31, no. 2 : 139–46. doi:10.1016/S0047-6374(85)80024-5.

IoannidiS JPA., Thomas G, Daly MJ. (2009) "Validating, Augmenting and Refining Genome-wide Association Signals." *Nature Reviews. Genetics* 10, no. 5: 318–29. doi:10.1038/nrg2544.

Ishizuka N, Cowan WM, Amaral DG. (1995) "A Quantitative Analysis of the Dendritic Organization of Pyramidal Cells in the Rat Hippocampus." *The Journal of Comparative Neurology* 362, no. 1 : 17–45. doi:10.1002/cne.903620103.

Jang KL., Thordarson DS, Stein MB, Cohan SL, Taylor S. (2007) "Coping Styles and Personality: A Biometric Analysis." *Anxiety, Stress & Coping* 20, no. 1 : 17–24. doi:10.1080/10615800601170516.

Jarrard LE. (1993) "On the Role of the Hippocampus in Learning and Memory in the Rat." *Behavioral and Neural Biology* 60, no. 1 : 9–26. doi:10.1016/0163-1047(93)90664-4.

Jinde S, Zsiros V, Jiang Z, Nakao K, Pickel J, Kohno K, Belforte JE, Nakazawa K. (2012) "Hilar Mossy Cell Degeneration Causes Transient Dentate Granule Cell Hyperexcitability and Impaired Pattern Separation." *Neuron* 76, no. 6 : 1189–1200. doi:10.1016/j.neuron.2012.10.036.

Johannesson M, Lopez-Aumatell R, Stridh P, Diez M, Tuncel J, Blázquez G, Martinez-Membrives E, et al. (2009) "A Resource for the Simultaneous High-resolution Mapping of Multiple Quantitative Trait Loci in Rats: The NIH Heterogeneous Stock." *Genome Research* 19, no. 1 : 150–58. doi:10.1101/gr.081497.108.

Johansen CT., Wang J, Lanktree MB, Cao H, McIntyre AD, Ban MR, Martins RA, et al. (2010) "Excess of Rare Variants in Genes Identified by Genome-wide Association Study of Hypertriglyceridemia." *Nature Genetics* 42, no. 8 : 684–87. doi:10.1038/ng.628.

Jordan WH., Young JK, Hyten MJ, Hall DG. (2011) "Preparation and Analysis of the Central Nervous System." *Toxicologic Pathology* 39, no. 1 : 58–65. doi:10.1177/0192623310391480.

Kallmann JF. (1946) "The genetic theory of schizophrenia: An Analysis of 691 Schizophrenic Twin Index Families." *American Journal of Psychiatry* 103, no. 3 : 309–22.

Kamboh, M. I., Demirci F. Y., Wang X., Minster R. L., Carrasquillo M. M., Pankratz V. S., Younkin S. G., et al. (2012) "Genome-wide Association Study of Alzheimer's Disease." *Translational Psychiatry* 2, no. 5 : e117. doi:10.1038/tp.2012.45.

Kawamata M, Ochiya T. (2010) "Generation of Genetically Modified Rats from Embryonic Stem Cells." *Proceedings of the National Academy of Sciences* 107, no. 32 : 14223–28. doi:10.1073/pnas.1009582107.

Kay JN., Voinescu PE, Chu MW, Sanes JR. (2011) "Neurod6 Expression Defines New Retinal Amacrine Cell Subtypes and Regulates Their Fate." *Nature Neuroscience* 14, no. 8 : 965–72. doi:10.1038/nn.2859.

Kempermann G, Wiskott L, Gage FH. (2004) "Functional Significance of Adult Neurogenesis." *Current Opinion in Neurobiology* 14, no. 2 : 186–91. doi:10.1016/j.conb.2004.03.001.

Kitchin, RM. (1994) "Cognitive Maps: What Are They and Why Study Them?" *Journal of Environmental Psychology* 14, no. 1 :1–19. doi:10.1016/S0272-4944(05)80194-X.

Kjelstrup KG., Tuvnes FA, Steffenach HA, Murison R, Moser EI, Moser MB. (2002) "Reduced Fear Expression after Lesions of the Ventral Hippocampus." *Proceedings of the National Academy of Sciences* 99, no. 16 : 10825–30. doi:10.1073/pnas.152112399.

Kong A, Steinthorsdottir V, Masson G, Thorleifsson G, Sulem P, Besenbacher S, Jonasdottir A, et al. (2009) "Parental Origin of Sequence Variants Associated with Complex Diseases." *Nature* 462, no. 7275 : 868–74. doi:10.1038/nature08625.

Koolhaas J. M. (2008) "Coping Style and Immunity in Animals: Making Sense of Individual Variation." *Brain, Behavior, and Immunity*, Personality and Disease, 22, no. 5 (July 2008): 662–67. doi:10.1016/j.bbi.2007.11.006.

Koolhaas J. M., de Boer S. F., Coppens C. M., Buwalda B. (2010) "Neuroendocrinology of Coping Styles: Towards Understanding the Biology of Individual Variation." *Frontiers in Neuroendocrinology* 31, no. 3 : 307–21. doi:10.1016/j.yfrne.2010.04.001.

Koolhaas JM., de Boer S. F., Buwalda B, van Reenen K. (2007) "Individual Variation in Coping with Stress: a Multidimensional Approach of Ultimate and Proximate Mechanisms." *Brain, Behavior and Evolution* 70, no. 4 : 218–26. doi:10.1159/000105485.

Korte S M, Koolhaas JM, Wingfield JC, McEwen BS. (2005) "The Darwinian Concept of Stress: Benefits of Allostasis and Costs of Allostatic Load and the Trade-offs in

Health and Disease." *Neuroscience and Biobehavioral Reviews* 29, no. 1 :3–38. doi:10.1016/j.neubiorev.2004.08.009.
Koyner J, Demarest K, McCaughran J, Cipp L, Hitzemann R. (2000) "Identification and Time Dependence of Quantitative Trait Loci for Basal Locomotor Activity in the BXD Recombinant Inbred Series and a B6D2 F2 Intercross." *Behavior Genetics* 30, no. 3 : 159–70. doi:10.1023/A:1001963906258.
Krysko DV., Berghe TV, Parthoens E, D'Herde K, Vandenabeele P. (2008) "Chapter 16 Methods for Distinguishing Apoptotic from Necrotic Cells and Measuring Their Clearance." In *Methods in Enzymology*, Volume 442:307–41. Programmed Cell Death, General Principles for Studying Cell Death. Academic Press, http://www.sciencedirect.com/science/article/pii/S007668790801416X.
Kumamoto, H. (1997) "Detection of Apoptosis-related Factors and Apoptotic Cells in Ameloblastomas: Analysis by Immunohistochemistry and an in Situ DNA Nick End-labelling Method." *Journal of Oral Pathology & Medicine* 26, no. 9 : 419–25. doi:10.1111/j.1600-0714.1997.tb00242.x.
L T., McKernan MG, Jarrard LE. (1993) "Hippocampal Lesions Do Not Impair Negative Patterning: A Challenge to Configural Association Theory." *Behavioral Neuroscience* 107, no. 2 :227–34. doi:10.1037/0735-7044.107.2.227.
Lander E. S., Schork N. J. (1994) "Genetic Dissection of Complex Traits." *Science (New York, N.Y.)* 265, no. 5181 : 2037–48.
Lango A, Estrada K, Lettre G, Berndt SI, Weedon MN, Rivadeneira F, Willer CJ, et al. (2010) "Hundreds of Variants Clustered in Genomic Loci and Biological Pathways Affect Human Height." *Nature* 467, no. 7317 : 832–38. doi:10.1038/nature09410.
Laurberg S., Sørensen K. E. (1981) "Associational and Commissural Collaterals of Neurons in the Hippocampal Formation (Hilus Fasciae Dentatae and Subfield CA3)." *Brain Research* 212, no. 2 : 287–300. doi:10.1016/0006-8993(81)90463-7.
LeDoux, J. E. (2000) "Emotion Circuits in the Brain." *Annual Review of Neuroscience* 23: 155–84. doi:10.1146/annurev.neuro.23.1.155.
Legare ME., Bartlett FS, Frankel WN. (2000) "A Major Effect QTL Determined by Multiple Genes in Epileptic EL Mice." *Genome Research* 10, no. 1: 42–48. doi:10.1101/gr.10.1.42.
Lein S., Hawrylycz MJ, Ao N, Ayres M, Bensinger A, Bernard A, Boe AF, et al. (2007) "Genome-wide Atlas of Gene Expression in the Adult Mouse Brain." *Nature* 445, no. 7124 : 168–76. doi:10.1038/nature05453.
Li F, Yang M, Wang L, Williamson I, Tian F, Qin M, Shah PK, Sharifi BG. "Autofluorescence Contributes to False-positive Intracellular Foxp3 Staining in Macrophages: A Lesson Learned from Flow Cytometry." *Journal of Immunological Methods* 386, no. 1–2 : 101–7. doi:10.1016/j.jim.2012.08.014.
Lindblad-Toh, K. (2004) "Genome Sequencing: Three's Company." *Nature* 428, no. 6982 :475–76. doi:10.1038/428475a.
Lloyd M. H., Wolfensohn S. E. (2003) "Handbook of Laboratory Animal Management and Welfare." *Ames, Iowa: Blackwell Science*, 2003.
Loepke AW, Istaphanous GK, McAuliffe JJ, Miles L, Hughes EA, McCann JC, Harlow KE, et al. (2009) "The Effects of Neonatal Isoflurane Exposure in Mice on Brain Cell Viability, Adult Behavior, Learning, and Memory:" *Anesthesia & Analgesia* 108, no. 1 : 90–104. doi:10.1213/ane.0b013e31818cdb29.

Loo D. T., Rillema J. R. (1998) “Measurement of Cell Death.” *Methods in Cell Biology* 57: 251–64.

Lopez-Aumatell R, Guitart-Masip M, Vicens-Costa E, Gimenez-Llort L, Valdar W, Johannesson M, Flint J, Tobeña A, Fernandez-Teruel A. (2008) “Fearfulness in a Large N/Nih Genetically Heterogeneous Rat Stock: Differential Profiles of Timidity and Defensive Flight in Males and Females.” *Behavioural Brain Research* 188, no. 1 : 41–55. doi:10.1016/j.bbr.2007.10.015.

López-Aumatell R, Martínez-Membrives E, Vicens-Costa E, Cañete T, Blázquez G, Mont-Cardona C, Johannesson M, Flint J, Tobeña A, Fernández-Teruel A. (2011) “Effects of Environmental and Physiological Covariates on Sex Differences in Unconditioned and Conditioned Anxiety and Fear in a Large Sample of Genetically Heterogeneous (N/Nih-HS) Rats.” *Behavioral and Brain Functions* 7, no. 1 : 1–15. doi:10.1186/1744-9081-7-48.

López-Aumatell R, Vicens-Costa E, Guitart-Masip M, Martínez-Membrives E, Valdar W, Johannesson M, Cañete T, et al. (2009) “Unlearned Anxiety Predicts Learned Fear: a Comparison Among Heterogeneous Rats and the Roman Rat Strains.” *Behavioural Brain Research* 202, no. 1 : 92–101. doi:10.1016/j.bbr.2009.03.024.

Lynch, M. (1998) *Genetics and Analysis of Quantitative Traits*. Sunderland, Mass: Sinauer Associates Inc.,U.S.

MacKenzie S, Ribas L, Pilarczyk M, Morera D, Kadri S, Huntingford FA. (2009) “Screening for Coping Style Increases the Power of Gene Expression Studies.” *PLoS ONE* 4, no. 4 : e5314. doi:10.1371/journal.pone.0005314.

Maguire EA, Gadian DG, Johnsrude IS, Good CD, Ashburner J, Frackowiak RS, Frith CD. (2000) “Navigation-related Structural Change in the Hippocampi of Taxi Drivers.” *Proceedings of the National Academy of Sciences of the United States of America* 97, no. 8 :4398–4403. doi:10.1073/pnas.070039597.

Maguire EA, Nannery R, Spiers HJ. (2006) “Navigation Around London by a Taxi Driver with Bilateral Hippocampal Lesions.” *Brain: a Journal of Neurology* 129, no. Pt 11 : 2894–2907. doi:10.1093/brain/awl286.

Maher, B. (2008) “Personal Genomes: The Case of the Missing Heritability.” *Nature News* 456, no. 7218 : 18–21. doi:10.1038/456018a.

Major Depressive Disorder Working Group of the Psychiatric GWAS Consortium, (2013) “A Mega-analysis of Genome-wide Association Studies for Major Depressive Disorder.” *Molecular Psychiatry* 18, no. 4 : 497–511. doi:10.1038/mp.2012.21.

Manolio TA., Collins FS, Cox NJ, Goldstein DB, Hindorff LA, Hunter DJ, McCarthy MI, et al. (2009) “Finding the Missing Heritability of Complex Diseases.” *Nature* 461, no. 7265 : 747–53. doi:10.1038/nature08494.

Mattheisen M., Samuels J. F., Wang Y., Greenberg B. D., Fyer A. J., McCracken J. T., Geller D. A., et al. (2014) “Genome-wide Association Study in Obsessive-compulsive Disorder: Results from the OCGAS.” *Molecular Psychiatry*. doi:10.1038/mp.2014.43.

Maunsbach, AB. (1966) “Isolation and Purification of Acid Phosphatase-containing Autofluorescent Granules from Homogenates of Rat Kidney Cortex.” *Journal of Ultrastructure Research* 16, no. 1–2 :13–34. doi:10.1016/S0022-5320(66)80020-5.

McClearn GE., Hofer SM. (1999) “Genes as Gerontological Variables: Genetically Heterogeneous Stocks and Complex Systems☆.” *Neurobiology of Aging* 20, no. 2 : 147–56. doi:10.1016/S0197-4580(99)00046-9.

McNaughton N, Gray JA. (2000) "Anxiolytic Action on the Behavioural Inhibition System Implies Multiple Types of Arousal Contribute to Anxiety." *Journal of Affective Disorders* 61, no. 3 :161–76. doi:10.1016/S0165-0327(00)00344-X.

McQueen MB., Devlin B., Faraone SV., Nimgaonkar VL., Sklar P, Smoller JW., Jamra RA, et al. (2005) "Combined Analysis from Eleven Linkage Studies of Bipolar Disorder Provides Strong Evidence of Susceptibility Loci on Chromosomes 6q and 8q." *The American Journal of Human Genetics* 77, no. 4 : 582–95. doi:10.1086/491603.

Miyata T, Maeda T, Lee JE. (1999) "NeuroD Is Required for Differentiation of the Granule Cells in the Cerebellum and Hippocampus." *Genes & Development* 13, no. 13 :1647–52.

Monici, M. (2005) "Cell and Tissue Autofluorescence Research and Diagnostic Applications." In *Biotechnology Annual Review*, edited by M.R. El-Gewely, Volume 11:227–56. Elsevier http://www.sciencedirect.com/science/article/pii/S1387265605110072.

Morris R. G. M., Garrud P., Rawlins J. N. P., O'Keefe J. (1982) "Place Navigation Impaired in Rats with Hippocampal Lesions." *Nature* 297, no. 5868 : 681–83. doi:10.1038/297681a0.

Morris, R. G. M., Schenk F., Tweedie F., Jarrard L. E. (1990) "Ibotenate Lesions of Hippocampus And/or Subiculum: Dissociating Components of Allocentric Spatial Learning." *European Journal of Neuroscience* 2, no. 12 : 1016–28. doi:10.1111/j.1460-9568.1990.tb00014.x.

Morris, R. (1984) "Developments of a Water-maze Procedure for Studying Spatial Learning in the Rat." *Journal of Neuroscience Methods* 11, no. 1 (May 1984): 47–60. doi:10.1016/0165-0270(84)90007-4.

Mott R, Talbot CJ, Turri MG, C. Collins AC, Flint J. (2000) "A Method for Fine Mapping Quantitative Trait Loci in Outbred Animal Stocks." *Proceedings of the National Academy of Sciences* 97, no. 23 (November 7, 2000): 12649–54. doi:10.1073/pnas.230304397.

Mott R, Yuan W, Kaisaki P, Gan X, Cleak J, Edwards A, Baud A, Flint J. (2014)"The Architecture of Parent-of-Origin Effects in Mice." *Cell* 156, no. 1–2 : 332–42. doi:10.1016/j.cell.2013.11.043.

Mühleisen TW., Leber M, Schulze TG, Strohmaier J, Degenhardt F, Treutlein J, Mattheisen M, et al. (2014) "Genome-wide Association Study Reveals Two New Risk Loci for Bipolar Disorder." *Nature Communications* 5 (March 11, 2014). doi:10.1038/ncomms4339.

Murphy, KL., Baxter MG. (2013) "Long-Term Effects of Neonatal Single or Multiple Isoflurane Exposures on Spatial Memory in Rats." *Frontiers in Neurology* 4. doi:10.3389/fneur.2013.00087.

Naglich, JG., Metherall JE, Russell DW, Eidels L. (1992) "Expression Cloning of a Diphtheria Toxin Receptor: Identity with a Heparin-binding EGF-like Growth Factor Precursor." *Cell* 69, no. 6 :1051–61. doi:10.1016/0092-8674(92)90623-K.

Nakazawa, Kazu, Thomas J. McHugh, Matthew A. Wilson, and Susumu Tonegawa. "NMDA Receptors, Place Cells and Hippocampal Spatial Memory." *Nature Reviews Neuroscience* 5, no. 5 (May 2004): 361–72. doi:10.1038/nrn1385.

Nakazawa, Kazu, Michael C. Quirk, Raymond A. Chitwood, Masahiko Watanabe, Mark F. Yeckel, Linus D. Sun, Akira Kato, et al. "Requirement for Hippocampal CA3 NMDA Receptors in Associative Memory Recall." *Science* 297, no. 5579 (July 12, 2002): 211–18. doi:10.1126/science.1071795.

Nakazawa, Kazu, Linus D Sun, Michael C Quirk, Laure Rondi-Reig, Matthew A Wilson, and Susumu Tonegawa. "Hippocampal CA3 NMDA Receptors Are Crucial for Memory Acquisition of One-Time Experience." *Neuron* 38, no. 2 (April 24, 2003): 305–15. doi:10.1016/S0896-6273(03)00165-X.

Negoescu, A., P. Lorimier, F. Labat-Moleur, C. Drouet, C. Robert, C. Guillermet, C. Brambilla, and E. Brambilla. "In Situ Apoptotic Cell Labeling by the TUNEL Method: Improvement and Evaluation on Cell Preparations." *The Journal of Histochemistry and Cytochemistry: Official Journal of the Histochemistry Society* 44, no. 9 (September 1996): 959–68.

Novembre, John, Toby Johnson, Katarzyna Bryc, Zoltán Kutalik, Adam R. Boyko, Adam Auton, Amit Indap, et al. "Genes Mirror Geography Within Europe." *Nature* 456, no. 7218 (November 6, 2008): 98–101. doi:10.1038/nature07331.

O'Keefe, J., and J. Dostrovsky. "The Hippocampus as a Spatial Map. Preliminary Evidence from Unit Activity in the Freely-moving Rat." *Brain Research* 34, no. 1 (November 12, 1971): 171–75. doi:10.1016/0006-8993(71)90358-1.

O'Keefe, J. "A Review of the Hippocampal Place Cells." *Progress in Neurobiology* 13, no. 4 (1979): 419–39. doi:10.1016/0301-0082(79)90005-4.

O'Keefe, J. "Place Units in the Hippocampus of the Freely Moving Rat." *Experimental Neurology* 51, no. 1 (1976): 78–109. doi:10.1016/0014-4886(76)90055-8.

O'keefe, J, and Lynn Nadel. *The Hippocampus as a Cognitive Map*. Vol. 3. Clarendon Press Oxford, 1978. http://www.getcited.org/pub/101782291.

O'Reilly, Randall C., and Jerry W. Rudy. "Conjunctive Representations in Learning and Memory: Principles of Cortical and Hippocampal Function." *Psychological Review* 108, no. 2 (2001): 311–45. doi:10.1037/0033-295X.108.2.311.

Oliver, Peter L., Mattéa J. Finelli, Benjamin Edwards, Emmanuelle Bitoun, Darcy L. Butts, Esther B. E. Becker, Michael T. Cheeseman, Ben Davies, and Kay E. Davies. "Oxr1 Is Essential for Protection Against Oxidative Stress-Induced Neurodegeneration." *PLoS Genet* 7, no. 10 (October 20, 2011): e1002338. doi:10.1371/journal.pgen.1002338.

Palència, Marta, Sira Díaz-Morán, Carme Mont-Cardona, Toni Cañete, Gloria Blázquez, Esther Martínez-Membrives, Regina López-Aumatell, Adolf Tobeña, and Alberto Fernández-Teruel. "Helplessness-like Escape Deficits of NIH-HS Rats Predict Passive Behavior in the Forced Swimming Test: Relevance for the Concurrent Validity of Rat Models of Depression." *World Journal of Neuroscience* 03, no. 02 (2013): 83–92. doi:10.4236/wjns.2013.32012.

Palmiter, Richard D., Richard R. Behringer, Carol J. Quaife, Françoise Maxwell, Ian H. Maxwell, and Ralph L. Brinster. "Cell Lineage Ablation in Transgenic Mice by Cell-specific Expression of a Toxin Gene." *Cell* 50, no. 3 (July 31, 1987): 435–43. doi:10.1016/0092-8674(87)90497-1.

Pappenheimer, A. M., Annabel A. Harper, Michael Moynihan, and Jeremy P. Brockes. "Diphtheria Toxin and Related Proteins: Effect of Route of Injection on Toxicity and the Determination of Cytotoxicity for Various Cultured Cells." *Journal of Infectious Diseases* 145, no. 1 (January 1, 1982): 94–102. doi:10.1093/infdis/145.1.94.

Pastrana, Erika. "Neuroscience: The Genetic Essence of Our Brains." *Nature Methods* 9, no. 11 (November 2012): 1044–45. doi:10.1038/nmeth.2236.

Pellow, Sharon, Philippe Chopin, Sandra E. File, and Mike Briley. "Validation of Open : Closed Arm Entries in an Elevated Plus-maze as a Measure of Anxiety in the Rat."

Journal of Neuroscience Methods 14, no. 3 (August 1985): 149–67. doi:10.1016/0165-0270(85)90031-7.

Perry, V. H. "Evidence for an Amacrine Cell System in the Ganglion Cell Layer of the Rat Retina." *Neuroscience* 6, no. 5 (May 1981): 931–44. doi:10.1016/0306-4522(81)90174-3.

Porsolt, R.D., M. Le Pichon, and M. Jalfre. "Depression: a New Animal Model Sensitive to Antidepressant Treatments." *Nature* 266, no. 5604 (1977): 730–32.

Pyapali, G.k., A. Sik, M. Penttonen, G. Buzsaki, and D.a. Turner. "Dendritic Properties of Hippocampal CA1 Pyramidal Neurons in the Rat: Intracellular Staining in Vivo and in Vitro." *The Journal of Comparative Neurology* 391, no. 3 (1998): 335–52. doi:10.1002/(SICI)1096-9861(19980216)391:3<335::AID-CNE4>3.0.CO;2-2.

Qian, Xun, Nicholas G. Moss, Robert C. Fellner, Bonnie Taylor-Blake, and Michael F. Goy. "The Rat Kidney Contains High Levels of Prouroguanylin (the Uroguanylin Precursor) but Does Not Express GC-C (the Enteric Uroguanylin Receptor)." *American Journal of Physiology - Renal Physiology* 300, no. 2 (February 1, 2011): F561–F573. doi:10.1152/ajprenal.00282.2010.

Resnik, Evgeny, James M. McFarland, Rolf Sprengel, Bert Sakmann, and Mayank R. Mehta. "The Effects of GluA1 Deletion on the Hippocampal Population Code for Position." *The Journal of Neuroscience* 32, no. 26 (June 27, 2012): 8952–68. doi:10.1523/JNEUROSCI.6460-11.2012.

Risch N, Merikangas K. "The Future of Genetic Studies of Complex Human Diseases." *SCIENCE* 273 (1996): 13.

Rudy, Jerry W., and Robert J. Sutherland. "The Hippocampal Formation Is Necessary for Rats to Learn and Remember Configural Discriminations." *Behavioural Brain Research* 34, no. 1–2 (August 1, 1989): 97–109. doi:10.1016/S0166-4328(89)80093-2.

Saito, Michiko, Takao Iwawaki, Choji Taya, Hiromichi Yonekawa, Munehiro Noda, Yoshiaki Inui, Eisuke Mekada, Yukio Kimata, Akio Tsuru, and Kenji Kohno. "Diphtheria Toxin Receptor–mediated Conditional and Targeted Cell Ablation in Transgenic Mice." *Nature Biotechnology* 19, no. 8 (August 2001): 746–50. doi:10.1038/90795.

Sanderson, DJ., Bannerman DM. (2012) "The Role of Habituation in Hippocampus-dependent Spatial Working Memory Tasks: Evidence from GluA1 AMPA Receptor Subunit Knockout Mice." *Hippocampus* 22, no. 5 (2012): 981–94. doi:10.1002/hipo.20896.

Sapoznikov A, Jung S. (2008) "Probing in Vivo Dendritic Cell Functions by Conditional Cell Ablation." *Immunology and Cell Biology* 86, no. 5 (April 15, 2008): 409–15. doi:10.1038/icb.2008.23.

Sarnat, Harvey B, David Nochlin, and Donald E Born. "Neuronal Nuclear Antigen (NeuN): a Marker of Neuronal Maturation in the Early Human Fetal Nervous System." *Brain and Development* 20, no. 2 (March 1998): 88–94. doi:10.1016/S0387-7604(97)00111-3.

Saucier D, Cain DP (1995). "Spatial Learning Without NMDA Receptor-dependent Long-term Potentiation." *Nature* 378, no. 6553 (November 9, 1995): 186–89. doi:10.1038/378186a0.

Schlake, Thomas, and Juergen Bode. "Use of Mutated FLP Recognition Target (FRT) Sites for the Exchange of Expression Cassettes at Defined Chromosomal Loci." *Biochemistry* 33, no. 43 (November 1, 1994): 12746–51. doi:10.1021/bi00209a003.

Schmuck, Gabriele, and Regine Kahl. “The Use of Fluoro-Jade in Primary Neuronal Cell Cultures.” *Archives of Toxicology* 83, no. 4 (April 2009): 397–403. doi:10.1007/s00204-008-0360-4.

Schönig, Kai, Tillmann Weber, Ariana Frömmig, Lena Wendler, Brigitte Pesold, Dominik Djandji, Hermann Bujard, and Dusan Bartsch. “Conditional Gene Expression Systems in the Transgenic Rat Brain.” *BMC Biology* 10, no. 1 (September 3, 2012): 77. doi:10.1186/1741-7007-10-77.

Schouten, W. G., and V. M. Wiegant. “Individual Responses to Acute and Chronic Stress in Pigs.” *Acta Physiologica Scandinavica. Supplementum* 640 (1997): 88–91.

Scoville, William Beecher, and Brenda Milner. “Loss of Recent Memory After Bilateral Hippocampal Lesions.” *Journal of Neurology, Neurosurgery & Psychiatry* 20, no. 1 (February 1, 1957): 11–21. doi:10.1136/jnnp.20.1.11.

Seehafer, Sabrina S, and David A Pearce. “You Say Lipofuscin, We Say Ceroid: Defining Autofluorescent Storage Material.” *Neurobiology of Aging*, This issue includes a special issue section:Protein misfolding in Alzheimer’s and other age-related neurodegenerative diseases, 27, no. 4 (April 2006): 576–88. doi:10.1016/j.neurobiolaging.2005.12.006.

Shaner, Nathan C., Robert E. Campbell, Paul A. Steinbach, Ben N. G. Giepmans, Amy E. Palmer, and Roger Y. Tsien. “Improved Monomeric Red, Orange and Yellow Fluorescent Proteins Derived from Discosoma Sp. Red Fluorescent Protein.” *Nature Biotechnology* 22, no. 12 (December 2004): 1567–72. doi:10.1038/nbt1037.

Shih, Regina A., Pamela L. Belmonte, and Peter P. Zandi. “A Review of the Evidence from Family, Twin and Adoption Studies for a Genetic Contribution to Adult Psychiatric Disorders.” *International Review of Psychiatry (Abingdon, England)* 16, no. 4 (November 2004): 260–83. doi:10.1080/09540260400014401.

Shors, Tracey J., George Miesegaes, Anna Beylin, Mingrui Zhao, Tracy Rydel, and Elizabeth Gould. “Neurogenesis in the Adult Is Involved in the Formation of Trace Memories.” *Nature* 410, no. 6826 (March 15, 2001): 372–76. doi:10.1038/35066584.

Silva, A. J., C. F. Stevens, S. Tonegawa, and Y. Wang. “Deficient Hippocampal Long-term Potentiation in Alpha-calcium-calmodulin Kinase II Mutant Mice.” *Science* 257, no. 5067 (July 10, 1992): 201–6. doi:10.1126/science.1378648.

Silventoinen, Karri, Sampo Sammalisto, Markus Perola, Dorret I. Boomsma, Belinda K. Cornes, Chayna Davis, Leo Dunkel, et al. “Heritability of Adult Body Height: a Comparative Study of Twin Cohorts in Eight Countries.” *Twin Research: The Official Journal of the International Society for Twin Studies* 6, no. 5 (October 2003): 399–408. doi:10.1375/136905203770326402.

So, Hon-Cheong, Allen H.S. Gui, Stacey S. Cherny, and Pak C. Sham. “Evaluating the Heritability Explained by Known Susceptibility Variants: a Survey of Ten Complex Diseases.” *Genetic Epidemiology* 35, no. 5 (July 1, 2011): 310–17. doi:10.1002/gepi.20579.

Solà, Carme, Josep M. Tusell, and Joan Serratosa. “Comparative Study of the Distribution of Calmodulin Kinase II and Calcineurin in the Mouse Brain.” *Journal of Neuroscience Research* 57, no. 5 (September 1, 1999): 651–62. doi:10.1002/(SICI)1097-4547(19990901)57:5<651::AID-JNR7>3.0.CO;2-G.

Solberg Woods, Leah C., Cary Stelloh, Kevin R. Regner, Tiffany Schwabe, Jessica Eisenhauer, and Michael R. Garrett. “Heterogeneous Stock Rats: a New Model to Study the Genetics of Renal Phenotypes.” *American Journal of Physiology. Renal*

Physiology 298, no. 6 (June 2010): F1484–1491. doi:10.1152/ajprenal.00002.2010.

Sonntag, S., K. Dedek, B. Dorgau, K. Schultz, K.-F. Schmidt, K. Cimiotti, R. Weiler, S. Lowel, K. Willecke, and U. Janssen-Bienhold. "Ablation of Retinal Horizontal Cells from Adult Mice Leads to Rod Degeneration and Remodeling in the Outer Retina." *Journal of Neuroscience* 32, no. 31 (August 1, 2012): 10713–24. doi:10.1523/JNEUROSCI.0442-12.2012.

Spencer, Hamish G. "Effects of Genomic Imprinting on Quantitative Traits." *Genetica* 136, no. 2 (June 2009): 285–93. doi:10.1007/s10709-008-9300-8.

Spruston, Nelson. "Pyramidal Neurons: Dendritic Structure and Synaptic Integration." *Nature Reviews Neuroscience* 9, no. 3 (March 2008): 206–21. doi:10.1038/nrn2286.

St George-Hyslop, P. H., J. L. Haines, L. A. Farrer, R. Polinsky, C. Van Broeckhoven, A. Goate, D. R. Crapper McLachlan, et al. "Genetic Linkage Studies Suggest That Alzheimer's Disease Is Not a Single Homogeneous Disorder." *Nature* 347, no. 6289 (September 13, 1990): 194–97. doi:10.1038/347194a0.

Steimer, Thierry, and Peter Driscoll. "Divergent Stress Responses and Coping Styles in Psychogenetically Selected Roman high-(RHA) and low-(RLA) Avoidance Rats: Behavioural, Neuroendocrine and Developmental Aspects." *Stress (Amsterdam, Netherlands)* 6, no. 2 (June 2003): 87–100. doi:10.1080/1025389031000111320.

Steimer, Thierry, Susanne la Fleur, and Pierre E. Schulz. "Neuroendocrine Correlates of Emotional Reactivity and Coping in Male Rats from the Roman High (RHA/Verh)-and Low (RLA/Verh)-Avoidance Lines." *Behavior Genetics* 27, no. 6 (November 1, 1997): 503–12. doi:10.1023/A:1021448713665.

Steinkamp, John A., and Carleton C. Stewart. "Dual-laser, Differential Fluorescence Correction Method for Reducing Cellular Background Autofluorescence." *Cytometry* 7, no. 6 (November 1, 1986): 566–74. doi:10.1002/cyto.990070611.

Stewart, S. E., D. Yu, J. M. Scharf, B. M. Neale, J. A. Fagerness, C. A. Mathews, P. D. Arnold, et al. "Genome-wide Association Study of Obsessive-compulsive Disorder." *Molecular Psychiatry* 18, no. 7 (July 2013): 788–98. doi:10.1038/mp.2012.85.

Steyvers, Mark, Joshua B. Tenenbaum, Eric-Jan Wagenmakers, and Ben Blum. "Inferring Causal Networks from Observations and Interventions." *Cognitive Science*, 2002 Rumelhart Prize Special Issue Honoring Richard Shiffrin, 27, no. 3 (May 2003): 453–89. doi:10.1016/S0364-0213(03)00010-7.

Sullivan PF, Kendler KS, and Neale MC. "Schizophrenia as a Complex Trait: Evidence from a Meta-analysis of Twin Studies." *Archives of General Psychiatry* 60, no. 12 (December 1, 2003): 1187–92. doi:10.1001/archpsyc.60.12.1187.

Sutherland, R. J., and J. W. Rudy. "Configural Association Theory: The Role of the Hippocampal Formation in Learning, Memory, and Amnesia." *Psychobiology* 17, no. 2 (June 1, 1989): 129–44. doi:10.3758/BF03337828.

Talbot, Christopher J., Alison Nicod, Stacey S. Cherny, David W. Fulker, Allan C. Collins, and Jonathan Flint. "High-resolution Mapping of Quantitative Trait Loci in Outbred Mice." *Nature Genetics* 21, no. 3 (March 1999): 305–8. doi:10.1038/6825.

Taube, J. S., R. U. Muller, and J. B. Ranck. "Head-direction Cells Recorded from the Postsubiculum in Freely Moving Rats. I. Description and Quantitative Analysis." *The Journal of Neuroscience* 10, no. 2 (February 1, 1990): 420–35.

Thompson, Carol L., Sayan D. Pathak, Andreas Jeromin, Lydia L. Ng, Cameron R. MacPherson, Marty T. Mortrud, Allison Cusick, et al. "Genomic Anatomy of the Hippocampus." *Neuron* 60, no. 6 (December 26, 2008): 1010–21. doi:10.1016/j.neuron.2008.12.008.

Tsien, Joe Z, Patricio T Huerta, and Susumu Tonegawa. "The Essential Role of Hippocampal CA1 NMDA Receptor–Dependent Synaptic Plasticity in Spatial Memory." *Cell* 87, no. 7 (December 27, 1996): 1327–38. doi:10.1016/S0092-8674(00)81827-9.

Uematsu, Masakazu, Yasuharu Hirai, Fuyuki Karube, Satoe Ebihara, Megumi Kato, Kuniya Abe, Kunihiko Obata, et al. "Quantitative Chemical Composition of Cortical GABAergic Neurons Revealed in Transgenic Venus-Expressing Rats." *Cerebral Cortex* 18, no. 2 (February 1, 2008): 315–30. doi:10.1093/cercor/bhm056.

Uittenbogaard, Martine, Kristin K. Baxter, and Anne Chiaramello. "NeuroD6 Genomic Signature Bridging Neuronal Differentiation to Survival via the Molecular Chaperone Network." *Journal of Neuroscience Research* 88, no. 1 (January 1, 2010): 33–54. doi:10.1002/jnr.22182.

Valdar, W, Leah C. Solberg, Dominique Gauguier, Stephanie Burnett, Paul Klenerman, William O. Cookson, Martin S. Taylor, J. Nicholas P. Rawlins, Richard Mott, and Jonathan Flint. "Genome-wide Genetic Association of Complex Traits in Heterogeneous Stock Mice." *Nature Genetics* 38, no. 8 (August 2006): 879–87. doi:10.1038/ng1840.

Valdar, William, Leah C. Solberg, Dominique Gauguier, William O. Cookson, J. Nicholas P. Rawlins, Richard Mott, and Jonathan Flint. "Genetic and Environmental Effects on Complex Traits in Mice." *Genetics* 174, no. 2 (October 1, 2006): 959–84. doi:10.1534/genetics.106.060004.

Van Keuren, Margaret L., Galina B. Gavrilina, Wanda E. Filipiak, Michael G. Zeidler, and Thomas L. Saunders. "Generating Transgenic Mice from Bacterial Artificial Chromosomes: Transgenesis Efficiency, Integration and Expression Outcomes." *Transgenic Research* 18, no. 5 (October 2009): 769–85. doi:10.1007/s11248-009-9271-2.

Van Oers, Kees, Piet J. Drent, Piet de Goede, and Arie J. van Noordwijk. "Realized Heritability and Repeatability of Risk-taking Behaviour in Relation to Avian Personalities." *Proceedings of the Royal Society B: Biological Sciences* 271, no. 1534 (January 7, 2004): 65–73.

Van Praag, Henriette, Gerd Kempermann, and Fred H. Gage. "Running Increases Cell Proliferation and Neurogenesis in the Adult Mouse Dentate Gyrus." *Nature Neuroscience* 2, no. 3 (March 1999): 266–70. doi:10.1038/6368.

Vicens-Costa, Elia, Esther Martínez-Membrives, Regina López-Aumatell, Marc Guitart-Masip, Toni Cañete, Gloria Blázquez, Adolf Tobeña, and Alberto Fernández-Teruel. "Two-way Avoidance Acquisition Is Negatively Related to Conditioned Freezing and Positively Associated with Startle Reactions: A Dissection of Anxiety and Fear in Genetically Heterogeneous Rats." *Physiology & Behavior* 103, no. 2 (May 3, 2011): 148–56. doi:10.1016/j.physbeh.2010.12.009.

Visscher, Peter M, Sarah E Medland, Manuel A. R Ferreira, Katherine I Morley, Gu Zhu, Belinda K Cornes, Grant W Montgomery, and Nicholas G Martin. "Assumption-Free Estimation of Heritability from Genome-Wide Identity-by-Descent Sharing Between Full Siblings." *PLoS Genet* 2, no. 3 (March 24, 2006): e41. doi:10.1371/journal.pgen.0020041.

Visscher, Peter M., Matthew A. Brown, Mark I. McCarthy, and Jian Yang. "Five Years of GWAS Discovery." *The American Journal of Human Genetics* 90, no. 1 (January 13, 2012): 7–24. doi:10.1016/j.ajhg.2011.11.029.

Visscher, Peter M., William G. Hill, and Naomi R. Wray. "Heritability in the Genomics Era — Concepts and Misconceptions." *Nature Reviews Genetics* 9, no. 4 (April 2008): 255–66. doi:10.1038/nrg2322.

Visscher, Peter M., Sarah E. Medland, Manuel A. R. Ferreira, Katherine I. Morley, Gu Zhu, Belinda K. Cornes, Grant W. Montgomery, and Nicholas G. Martin. "Assumption-free Estimation of Heritability from Genome-wide Identity-by-descent Sharing Between Full Siblings." *PLoS Genetics* 2, no. 3 (March 2006): e41. doi:10.1371/journal.pgen.0020041.

Von Holst, Dietrich. "The Concept of Stress and Its Relevance for Animal Behavior." *Advances in the Study of Behavior* 27 (1998): 1–131.

Wallace, Chris, Deborah J. Smyth, Meeta Maisuria-Armer, Neil M. Walker, John A. Todd, and David G. Clayton. "The Imprinted DLK1-MEG3 Gene Region on Chromosome 14q32.2 Alters Susceptibility to Type 1 Diabetes." *Nature Genetics* 42, no. 1 (January 2010): 68–71. doi:10.1038/ng.493.

Wang, Szu-Han, and Richard G.M. Morris. "Hippocampal-Neocortical Interactions in Memory Formation, Consolidation, and Reconsolidation." *Annual Review of Psychology* 61, no. 1 (2010): 49–79. doi:10.1146/annurev.psych.093008.100523.

Wechsler, Beat. "Coping and Coping Strategies: a Behavioural View." *Applied Animal Behaviour Science* 43, no. 2 (May 1995): 123–34. doi:10.1016/0168-1591(95)00557-9.

Wellcome Trust Case Control Consortium. "Genome-wide Association Study of 14,000 Cases of Seven Common Diseases and 3,000 Shared Controls." *Nature* 447, no. 7145 (June 7, 2007): 661–78. doi:10.1038/nature05911.

Wg, Schouten, and Wiegant Vm. "Individual Responses to Acute and Chronic Stress in Pigs." *Acta Physiologica Scandinavica. Supplementum* 640 (December 1996): 88–91.

Wharram, Bryan L., Meera Goyal, Jocelyn E. Wiggins, Silja K. Sanden, Sabiha Hussain, Wanda E. Filipiak, Thomas L. Saunders, et al. "Podocyte Depletion Causes Glomerulosclerosis: Diphtheria Toxin–Induced Podocyte Depletion in Rats Expressing Human Diphtheria Toxin Receptor Transgene." *Journal of the American Society of Nephrology* 16, no. 10 (October 1, 2005): 2941–52. doi:10.1681/ASN.2005010055.

Wildt, Sheryl J., Andrew I. Brooks, and Robert J. Russell. "Rodent Genetics, Models, and Genotyping Methods." In *Sourcebook of Models for Biomedical Research*, edited by P. Michael Conn, 179–86. Humana Press, 2008. http://link.springer.com/chapter/10.1007/978-1-59745-285-4_20.

Winocur, Gordon, Morris Moscovitch, and Melanie Sekeres. "Memory Consolidation or Transformation: Context Manipulation and Hippocampal Representations of Memory." *Nature Neuroscience* 10, no. 5 (May 2007): 555–57. doi:10.1038/nn1880.

Witter, Menno P., and David G. Amaral. "Chapter 21 - Hippocampal Formation." In *The Rat Nervous System (Third Edition)*, edited by George Paxinos, 635–704. Burlington: Academic Press, 2004. http://www.sciencedirect.com/science/article/pii/B9780125476386500225.

Wolf, H. K., R. Buslei, R. Schmidt-Kastner, P. K. Schmidt-Kastner, T. Pietsch, O. D. Wiestler, and I. Blümcke. "NeuN: a Useful Neuronal Marker for Diagnostic

Histopathology." *Journal of Histochemistry & Cytochemistry* 44, no. 10 (October 1, 1996): 1167–71. doi:10.1177/44.10.8813082.

Wolf, Jason B., James M. Cheverud, Charles Roseman, and Reinmar Hager. "Genome-Wide Analysis Reveals a Complex Pattern of Genomic Imprinting in Mice." *PLoS Genet* 4, no. 6 (June 6, 2008): e1000091. doi:10.1371/journal.pgen.1000091.

Wolfensohn, Sarah, and Maggie Lloyd. *Handbook of Laboratory Animal Management and Welfare*. Wiley, 2003.

Wood, Emma R., Paul A. Dudchenko, R. Jonathan Robitsek, and Howard Eichenbaum. "Hippocampal Neurons Encode Information About Different Types of Memory Episodes Occurring in the Same Location." *Neuron* 27, no. 3 (September 2000): 623–33. doi:10.1016/S0896-6273(00)00071-4.

Yalcin, Binnaz, and Jonathan Flint. "Association Studies in Outbred Mice in a New Era of Full-genome Sequencing." *Mammalian Genome* 23, no. 9–10 (October 1, 2012): 719–26. doi:10.1007/s00335-012-9409-z.

Yalcin, Binnaz, Saffron A. G. Willis-Owen, Jan Fullerton, Anjela Meesaq, Robert M. Deacon, J. Nicholas P. Rawlins, Richard R. Copley, Andrew P. Morris, Jonathan Flint, and Richard Mott. "Genetic Dissection of a Behavioral Quantitative Trait Locus Shows That Rgs2 Modulates Anxiety in Mice." *Nature Genetics* 36, no. 11 (November 2004): 1197–1202. doi:10.1038/ng1450.

Yamaizumi, Masaru, Eisuke Mekada, Tsuyoshi Uchida, and Yoshio Okada. "One Molecule of Diphtheria Toxin Fragment a Introduced into a Cell Can Kill the Cell." *Cell* 15, no. 1 (September 1978): 245–50. doi:10.1016/0092-8674(78)90099-5.

Yang, Jian, S. Hong Lee, Michael E. Goddard, and Peter M. Visscher. "GCTA: A Tool for Genome-wide Complex Trait Analysis." *The American Journal of Human Genetics* 88, no. 1 (January 7, 2011): 76–82. doi:10.1016/j.ajhg.2010.11.011.

Yartsev, Michael M., Menno P. Witter, and Nachum Ulanovsky. "Grid Cells Without Theta Oscillations in the Entorhinal Cortex of Bats." *Nature* 479, no. 7371 (November 3, 2011): 103–7. doi:10.1038/nature10583.

Zhang, Feng, Pavel Seeman, Pengfei Liu, Marian A. J. Weterman, Claudia Gonzaga-Jauregui, Charles F. Towne, Sat Dev Batish, et al. "Mechanisms for Nonrecurrent Genomic Rearrangements Associated with CMT1A or HNPP: Rare CNVs as a Cause for Missing Heritability." *The American Journal of Human Genetics* 86, no. 6 (June 11, 2010): 892–903. doi:10.1016/j.ajhg.2010.05.001.

Zheng, Sushuang, Kindiya Geghman, Sushila Shenoy, and Chenjian Li. "Retake the Center Stage – New Development of Rat Genetics." *Journal of Genetics and Genomics* 39, no. 6 (June 20, 2012): 261–68. doi:10.1016/j.jgg.2012.05.003.

10. LIST OF FIGURES AND TABLES

11. APENDIX

11.1. POE HERITABILITIES. The table contains the traits, their heritabilities for POE and the standard errors, as well as the number of individuals per trait (N).

Trait	H2.POE	H2.NOPOE	SE.POE	SE.NOPOE	N
AA_IL_nb_pos_qn	0.216601	0.616435	0.257878	0.301964	100
AA_IL_nb_qn	0.266273	0.609886	0.056031	0.045882	197
AA_IL_score_pos_qn	0.270508	0.565514	0.29494	0.342674	100
AA_IL_score_qn	0.269187	0.613329	0.053166	0.041973	197
AA_nb_pos_qn	0.338821	0.415936	0.334701	0.39331	77
AA_nb_qn	0.255494	0.596452	0.066275	0.059965	197
AA_score_pos_qn	0.229411	0.47443	0.296984	0.35269	77
AA_score_qn	0.254179	0.599818	0.064274	0.056788	197
AL	0.193984	0.15576	0.129749	0.185226	497
ALP_bc	0.46291	0.336304	0.080731	0.093403	604
ALT_bc	0.409214	0.033095	0.171613	0.237626	492
AST_bc	0.524962	0.047609	0.179223	0.23642	475
AUC_G_bc	0.431573	0.178926	0.154256	0.199922	418
AUC_bc	0.326413	0.025279	0.314436	0.440404	199
Abs_Bcells	0.715054	0.158161	0.170985	0.187632	374
Abs_CD25CD4	0.474801	0.247007	0.148585	0.18622	364
Abs_CD25CD8	0.351766	0.291997	0.130483	0.172051	366
Abs_gran	0.689909	0.014792	0.274319	0.341003	290
Abs_monocytes	0.854101	0.035929	0.255855	0.276433	286
AcquisitionPerformance_bc	0.091039	0.25129	0.09619	0.129696	572
Area_bc	0.398939	0.069573	0.172266	0.235661	459
Avoidances11_20_qn	0.125952	0.346422	0.077808	0.09661	602
Avoidances1_10_qn	0.150798	0.210716	0.1014	0.140799	602
Avoidances1_20_qn	0.129102	0.367275	0.074321	0.089649	602
Avoidances1_40_qn	0.146821	0.410371	0.066809	0.075091	602
Avoidances1_5_qn	0.015946	0.435644	0.062445	0.056933	602
Avoidances21_30_qn	0.137093	0.432523	0.062919	0.066559	602
Avoidances31_40_qn	0.079824	0.327823	0.079677	0.099989	602
Avoidances6_10_qn	0.034919	0.177599	0.098597	0.137075	602
BASO_bc	0.421487	0.074475	0.14572	0.201314	576
BD	0.021019	0.049022	0.112389	0.155066	612
BW_at_IPGTT_bc	0.846798	0.085947	0.125856	0.130983	614
BW_at_activity_test_bc	0.862478	0.02272	0.283193	0.305257	278
BW_at_day28_pi_bc	0.620561	0.241746	0.105714	0.11658	565

BW_at_day9_pi_bc	0.794094	0.135908	0.115619	0.120548	609
BW_at_day_immunization_bc	0.78827	0.157649	0.11527	0.118466	557
BW_at_zeromaze_test_bc	0.916041	0.015326	0.143752	0.149809	607
CD25expCD4	0.497651	0.057053	0.159299	0.214346	546
CD25expCD8	0.407724	0.036334	0.175587	0.245069	469
CD25highCD4	0.50593	0.408838	0.116724	0.122405	271
CD25highCD8	0.302205	0.075694	0.474456	0.808365	96
CD28expTcells	0.115942	0.081219	0.164038	0.233549	398
CD45RCexpCD4	0.569993	0.093396	0.297424	0.379044	227
CD45RCexpCD8	0.398049	0.309158	0.189701	0.240663	227
CD4Tcells_Abs	0.509747	0.321096	0.092122	0.103981	529
CD4_CD8_ratio	0.482127	0.34937	0.081459	0.09151	560
CD4_Pct	0.420633	0.374123	0.07643	0.087651	563
CD8Tcells_Abs	0.599687	0.255336	0.107575	0.119471	529
CD8_Pct	0.548665	0.294349	0.09412	0.105439	563
CHCM_bc	0.642995	0.150225	0.131964	0.154055	574
Calcium_bc	0.441967	0.041802	0.149724	0.207687	598
Chloride_bc	0.550438	0.071474	0.148382	0.193589	598
Creatinine_bc	0.451234	0.251758	0.10352	0.129303	593
Crossings_bc	0.343531	0.108536	0.129522	0.182257	603
DUR_bc	0.257972	0.034542	0.305286	0.431587	199
DeltaG_bc	0.554011	0.066672	0.190034	0.244632	417
Distance0_30_bc	0.275683	0.097287	0.129582	0.184278	595
Distance10_15_bc	0.32184	0.057496	0.139454	0.198542	597
Distance15_20_bc	0.207006	0.135032	0.1181	0.167491	599
Distance20_25_bc	0.222724	0.049212	0.134271	0.192048	598
Distance25_30_bc	0.035515	0.12395	0.106074	0.148406	602
Distance25_bc	0.251244	0.044627	0.136514	0.195553	601
Distance5_10_bc	0.159849	0.024949	0.132393	0.18788	602
Distance5_bc	0.354617	0.064778	0.139273	0.197075	601
EAE	0.468218	0.080225	0.140122	0.190318	615
EOS_bc	0.479841	0.263194	0.102484	0.124517	580
EntriesOpenSection_bc	0.345848	0.042464	0.142433	0.202947	604
G0_bc	0.354992	0.340869	0.107628	0.130554	417
G120_bc	0.395534	0.297615	0.119733	0.147514	417
G30_bc	0.293857	0.154692	0.157922	0.214422	415
G60_bc	0.529128	0.092741	0.181702	0.234079	417
Glucose_bc	0.44266	0.202707	0.11391	0.147695	601
HCT_bc	0.325078	0.425473	0.064437	0.07292	568
HDL_bc	0.550958	0.199528	0.116658	0.141058	595
HDW_bc	0.634121	0.266904	0.093994	0.100222	577
HW	0.487491	0.1816	0.139256	0.178784	497
Has1kidney	0.036412	0.126113	0.103509	0.145238	617
HeadDips_bc	0.370609	0.045629	0.143031	0.202782	606

IL_nb_pos_qn	0.359034	0.485628	0.277729	0.306284	74
IL_nb_qn	0.293301	0.57828	0.073973	0.073245	197
IL_score_pos_qn	0.628243	0.190444	0.539269	0.607959	74
IL_score_qn	0.332672	0.548059	0.088826	0.092788	197
INC	0.438688	0.102486	0.133927	0.182761	615
InterTrialCross11_20_bc	0.187575	0.111622	0.120543	0.171937	600
InterTrialCross1_10_bc	0.11783	0.152219	0.109239	0.154077	600
InterTrialCross1_20_bc	0.212283	0.214212	0.104139	0.144329	598
InterTrialCross1_40_bc	0.171242	0.334723	0.081237	0.10324	596
InterTrialCross21_30_bc	0.134284	0.239612	0.09597	0.131227	601
InterTrialCross31_40_bc	0.111428	0.220309	0.097802	0.134842	602
Iron_bc	0.311637	0.269927	0.096323	0.127092	599
LDL_bc	0.65404	0.033695	0.16075	0.200541	598
LFH	0.431845	0.473322	0.053141	0.053973	497
LT	0.523798	0.356473	0.08597	0.092949	497
LUC_bc	0.45044	0.034508	0.156456	0.216341	574
LW_bc	0.793469	0.06089	0.14624	0.161896	606
LYM_bc	0.715995	0.025463	0.167524	0.201295	575
Latency11_20_bc	0.336445	0.076354	0.136105	0.193079	599
Latency1_10_bc	0.500795	0.076105	0.144758	0.193883	600
Latency1_20_bc	0.45025	0.081548	0.141071	0.193011	600
Latency1_40_bc	0.3357	0.131282	0.12493	0.174866	601
Latency1_5_bc	0.512857	0.133935	0.132234	0.171198	598
Latency21_30_bc	0.242992	0.202932	0.107324	0.149047	599
Latency31_40_bc	0.136905	0.182619	0.105991	0.148429	598
Latency6_10_bc	0.274313	0.1294	0.122391	0.173405	600
LatencyOpenSection_bc	0.127111	0.032186	0.140948	0.198475	533
LineCrossings_bc	0.347881	0.08663	0.133653	0.18885	606
MCHC_bc	0.641609	0.128714	0.138673	0.164525	572
MCH_bc	0.490102	0.398343	0.064417	0.06824	574
MCV_bc	0.513409	0.388361	0.065249	0.068501	578
MONO_bc	0.706895	0.077055	0.15149	0.177232	579
MPC_bc	0.693712	0.020693	0.170021	0.207967	571
MPM_bc	0.704873	0.184315	0.117829	0.127212	561
MPV_bc	0.551812	0.031141	0.162903	0.215975	572
MPXI_bc	0.444731	0.298614	0.094186	0.113997	574
NEUT_bc	0.716518	0.066978	0.15427	0.18042	579
NW	0.486994	0.182481	0.139272	0.178763	496
ONSET_bc	0.457354	0.046833	0.315458	0.424042	199
PCDW_bc	0.539651	0.19369	0.121544	0.148654	573
PCT_bc	0.623187	0.127135	0.138831	0.167157	577
PDW_bc	0.644955	0.035509	0.164326	0.20588	576
PLT_bc	0.468455	0.294672	0.094792	0.113226	577

PltClumps_bc	0.694278	0.059136	0.161831	0.193341	554
PosturesClosedToOpen_bc	0.230008	0.157075	0.114484	0.161815	603
Potassium_bc	0.714747	0.029073	0.199446	0.238143	439
RBC_bc	0.360947	0.465365	0.052748	0.055534	568
RDW_bc	0.691312	0.209052	0.108764	0.116235	571
RT1AexpGran	0.541663	0.133117	0.151748	0.192608	494
RT1BexpBcell	0.634284	0.175741	0.163759	0.189276	398
Rearing0_30_bc	0.407889	0.082685	0.140042	0.194195	592
Rearing10_15_bc	0.256555	0.101996	0.127827	0.181809	593
Rearing15_20_bc	0.173233	0.177648	0.109742	0.153742	593
Rearing20_25_bc	0.262863	0.112792	0.125772	0.178563	595
Rearing25_bc	0.347777	0.084793	0.135585	0.191222	597
Rearing5_10_bc	0.244608	0.196243	0.109792	0.152406	592
Rearing5_bc	0.279273	0.252359	0.099695	0.133994	594
Sodium_bc	0.693556	0.020466	0.165075	0.202023	596
Tcell_Bcellratio	0.734695	0.156356	0.141773	0.152935	468
Tcells_Abs	0.507667	0.345527	0.083807	0.092551	536
Tcells_Pct	0.651199	0.245962	0.11676	0.125202	466
TimeOpenSection_bc	0.343595	0.032545	0.158372	0.224254	529
Tot.Chol_bc	0.478812	0.318309	0.095565	0.110806	511
Trig._bc	0.50365	0.146016	0.134961	0.173704	565
Urea_bc	0.35576	0.079289	0.163586	0.226127	473
WBCB_Abs	0.646169	0.233299	0.104503	0.113705	577
WBCB_bc	0.713117	0.163368	0.122091	0.133188	578
WL0_bc	0.415349	0.132663	0.13853	0.189489	545
WL9_ALT_bc	0.334817	0.125179	0.127207	0.177991	598
WL9_bc	0.286956	0.180603	0.122136	0.171428	543
abs_basos_bc	0.471526	0.0799	0.147548	0.19947	573
abs_eos_bc	0.497021	0.125189	0.136971	0.179286	580
abs_lucs_bc	0.602837	0.033644	0.164338	0.211486	573
abs_lymphs_bc	0.686665	0.223363	0.103063	0.109173	577
abs_monos_bc	0.755577	0.021231	0.167688	0.196375	577
abs_neuts_bc	0.697752	0.048111	0.161126	0.193398	575
bloodpressure	0.348068	0.017997	0.145782	0.208495	613
bloodpressure_bc	0.358758	0.021257	0.146251	0.208701	611
died	0.031589	0.015907	0.117448	0.160453	615
dist_femur_CRT_A	0.518572	0.041206	0.177358	0.239005	496
dist_femur_CRT_DEN	0.42726	0.113889	0.153539	0.210271	497
dist_femur_TOT_A	0.472444	0.037023	0.174994	0.241115	497
dist_femur_TOT_DEN	0.474449	0.330887	0.096958	0.112433	496
dist_femur_TRAB_A	0.406533	0.103043	0.154813	0.214615	497
dist_femur_TRAB_DEN	0.629947	0.045914	0.181762	0.229061	497
fem_biomech_EL	0.132583	0.038424	0.147586	0.210144	492
fem_biomech_Fu	0.488424	0.154847	0.146934	0.19132	494
fem_biomech_S	0.479206	0.122386	0.154939	0.206065	494

fem_biomech_W	0.242047	0.227746	0.118124	0.164172	494
fem_neck_CRT_A	0.598393	0.031742	0.184632	0.239024	496
fem_neck_CRT_DEN	0.559691	0.29865	0.103408	0.114644	496
fem_neck_IP_TOT_W	0.274341	0.207552	0.124908	0.173961	490
fem_neck_TOT_A	0.352908	0.223822	0.123494	0.16673	496
fem_neck_TOT_DEN	0.396399	0.509526	0.043429	0.042385	496
fem_neck_TRAB_A	0.328911	0.489526	0.054037	0.056487	496
fem_neck_TRAB_DEN	0.499557	0.310956	0.102342	0.118349	496
fem_neck_biomech_EL	0.233709	0.119125	0.151242	0.215577	447
fem_neck_biomech_Fu	0.332971	0.40526	0.084218	0.09988	447
fem_neck_biomech_S	0.217757	0.145184	0.144497	0.205247	447
fem_neck_biomech_W	0.200744	0.251488	0.120248	0.165307	447
femur_Area	0.575996	0.164979	0.145521	0.177344	498
femur_BMC	0.584467	0.29739	0.101487	0.110073	498
femur_BMD	0.520467	0.266129	0.115372	0.136263	498
femur_midshaft_CRT_A	0.52295	0.341331	0.091267	0.100343	497
femur_midshaft_CRT_DEN	0.499841	0.312023	0.101895	0.117685	497
femur_midshaft_IP_TOT_W	0.477104	0.415303	0.069445	0.07335	497
femur_midshaft_TOT_A	0.511926	0.396729	0.072642	0.075903	497
femur_midshaft_TOT_DEN	0.475416	0.420811	0.067668	0.071097	497
heart_weight	0.483378	0.295181	0.106542	0.126568	503
heart_weight_bc	0.551159	0.268645	0.113976	0.130839	496
is.DB	0.475307	0.385536	0.065676	0.071472	617
is.LB	0.549835	0.324537	0.078883	0.085794	617
is.albino	0.618646	0.342638	0.063171	0.063252	617
is.spotted	0.752797	0.168283	0.109056	0.114498	617
lob_Index_bc	0.589952	0.035065	0.162366	0.21043	579
lumbar_Area	0.480972	0.052439	0.171724	0.234597	498
lumbar_BMC	0.566696	0.276208	0.110437	0.124221	498
lumbar_BMD	0.582584	0.24764	0.119199	0.13559	498
lumbar_CRT_A	0.553274	0.081407	0.169019	0.219566	496
lumbar_CRT_DEN	0.563248	0.134131	0.154757	0.194118	496
lumbar_TOT_A	0.316202	0.210212	0.125131	0.17227	496
lumbar_TOT_DEN	0.488917	0.153328	0.147043	0.191564	496
lumbar_TRAB_A	0.267323	0.164577	0.132664	0.187749	496
lumbar_TRAB_DEN	0.483149	0.215083	0.130271	0.164308	496
max_bc	0.351313	0.061979	0.301987	0.41709	199
measHGB_bc	0.296459	0.413906	0.067541	0.078093	573
old_AA_IL_score_qn	0.247009	0.636424	0.040955	0.014629	196
pctBcells	0.712176	0.147573	0.130931	0.144751	557
pctCD25posCD4	0.506699	0.291573	0.099705	0.115893	539
pctCD25posCD8	0.365241	0.160803	0.133458	0.182091	522
pctCD45RChighCD4	0.598737	0.080784	0.30885	0.388433	224

pctCD45RChighCD8	0.496217	0.072954	0.296763	0.399149	227
pctCD45RClowCD4	0.562805	0.035624	0.322549	0.423909	226
pctCD45RClowCD8	0.526124	0.093293	0.29354	0.384529	226
pctCD45RCnegCD4	0.527156	0.029193	0.624393	0.878521	92
pctCD45RCnegCD8	0.529602	0.195588	0.506552	0.640792	92
pctCD45RCposCD4	0.493597	0.089656	0.288885	0.386564	228
pctCD45RCposCD8	0.549742	0.203242	0.245032	0.297238	227
pctDN	0.528151	0.188568	0.523103	0.665204	90
pctDP	0.522042	0.266185	0.137036	0.162909	384
pctRT1BposTcell	0.346591	0.302218	0.19523	0.264433	205
time_freezing_bc	0.253781	0.176919	0.154936	0.207884	407

11.2. PARENTAL HERITABILITIES. The table contains the traits, their heritabilities for parental effects, and the standard errors, as well as the number of individuals per trait (N).

Trait	H2.PATERNAL	H2.MATERNAL	SE.PATERNAL	SE.MATERNAL	N
AA_IL_nb_pos_qn	0.374545	0.042962	0.451111	0.434019	100
AA_IL_nb_qn	0.099118	0.794526	0.25531	0.302151	197
AA_IL_score_pos_qn	0.475303	0.039388	0.469796	0.441061	100
AA_IL_score_qn	0.021519	0.295532	0.178148	0.212792	197
AA_nb_pos_qn	0.042334	0.560629	0.553592	0.621632	77
AA_nb_qn	0.139207	0.728287	0.284269	0.326002	197
AA_score_pos_qn	0.047892	0.413159	0.623054	0.678192	77
AA_score_qn	0.129468	0.737618	0.283192	0.326185	197
AL	0.212157	0.126586	0.237642	0.235825	497
ALP_bc	0.340884	0.293003	0.108744	0.106855	604
ALT_bc	0.090893	0.460048	0.21127	0.224695	492
AST_bc	0.336535	0.35127	0.196499	0.195838	475
AUC_G_bc	0.112825	0.53203	0.184652	0.201232	418
AUC_bc	0.231799	0.259858	0.463285	0.456947	199
Abs_Bcells	0.453487	0.382924	0.146128	0.142294	374
Abs_CD25CD4	0.580253	0.063779	0.194638	0.168816	364
Abs_CD25CD8	0.21232	0.309871	0.212383	0.213963	366
Abs_gran	0.392813	0.424495	0.24878	0.246074	290
Abs_monocytes	0.650618	0.267872	0.18572	0.166983	286
AcquisitionPerformance_bc	0.152592	0.046558	0.201363	0.196249	572
Area_bc	0.281338	0.289886	0.223079	0.223175	459
Avoidances11_20_qn	0.061029	0.174014	0.157962	0.163431	602
Avoidances1_10_qn	0.174184	0.09632	0.193984	0.190838	602
Avoidances1_20_qn	0.107351	0.12659	0.15472	0.155924	602
Avoidances1_40_qn	0.177009	0.081437	0.140701	0.137109	602
Avoidances1_5_qn	0.016775	0.026289	0.140589	0.142519	602
Avoidances21_30_qn	0.253269	0.022266	0.133527	0.124926	602
Avoidances31_40	0.079086	0.080299	0.17292	0.173923	602

_qn					
Avoidances6_10_qn	0.040914	0.042885	0.212458	0.215061	602
BASO_bc	0.264119	0.326695	0.183215	0.185302	576
BD	0.023323	0.036981	0.226457	0.23131	612
BW_at_IPGTT_bc	0.466787	0.449943	0.085425	0.084815	614
BW_at_activity_test_bc	0.535425	0.392499	0.188494	0.184686	278
BW_at_day28_pi_bc	0.343497	0.426591	0.103105	0.1054	565
BW_at_day9_pi_bc	0.508977	0.370417	0.086025	0.082132	609
BW_at_day_immunization_bc	0.379997	0.513104	0.08403	0.087371	557
BW_at_zeromaze_test_bc	0.520605	0.435959	0.089133	0.086871	607
CD25expCD4	0.493813	0.160771	0.184865	0.172137	546
CD25expCD8	0.268518	0.306391	0.226389	0.226949	469
CD25highCD4	0.510247	0.180602	0.159248	0.143887	271
CD25highCD8	0.099391	0.394756	0.917582	0.877282	96
CD28expTcells	0.348199	0.017606	0.306547	0.293003	398
CD45RCexpCD4	0.578235	0.151799	0.337836	0.315257	227
CD45RCexpCD8	0.379679	0.181318	0.298797	0.287787	227
CD4Tcells_Abs	0.108659	0.549055	0.098962	0.11404	529
CD4_CD8_ratio	0.340062	0.309735	0.106711	0.105236	560
CD4_Pct	0.334436	0.255339	0.113605	0.110364	563
CD8Tcells_Abs	0.295923	0.454662	0.107324	0.112397	529
CD8_Pct	0.361336	0.347826	0.106908	0.106127	563
CHCM_bc	0.513446	0.279959	0.127006	0.118859	574
Calcium_bc	0.468355	0.129798	0.187502	0.174936	598
Chloride_bc	0.594498	0.120848	0.160431	0.14359	598
Creatinine_bc	0.194025	0.428004	0.128471	0.136937	593
Crossings_bc	0.174406	0.349993	0.178256	0.184702	603
DUR_bc	0.034023	0.416335	0.458138	0.470405	199
DeltaG_bc	0.312808	0.404571	0.199838	0.20337	417
Distance0_30_bc	0.162824	0.267536	0.197413	0.202032	595
Distance10_15_bc	0.291457	0.196582	0.199558	0.196042	597
Distance15_20_bc	0.11013	0.241485	0.199555	0.206078	599
Distance20_25_bc	0.039513	0.346816	0.203269	0.217218	598
Distance25_30_bc	0.033471	0.053259	0.221301	0.22557	602
Distance25_bc	0.086531	0.314224	0.205132	0.215688	601
Distance5_10_bc	0.163862	0.114024	0.226559	0.225379	602
Distance5_bc	0.389446	0.14125	0.193856	0.184108	601
EAE	0.447747	0.182218	0.169236	0.159194	615
EOS_bc	0.390787	0.261336	0.129907	0.12489	580
EntriesOpenSectio	0.05686	0.462573	0.182578	0.198168	604

n_bc					
G0_bc	0.425901	0.08123	0.16045	0.147203	417
G120_bc	0.082154	0.520246	0.159276	0.177176	417
G30_bc	0.078306	0.418527	0.230558	0.244877	415
G60_bc	0.214635	0.481009	0.194905	0.205149	417
Glucose_bc	0.430734	0.185673	0.148477	0.13921	601
HCT_bc	0.378604	0.105867	0.121505	0.111255	568
HDL_bc	0.448988	0.273357	0.129641	0.123356	595
HDW_bc	0.48068	0.2978	0.093376	0.087573	577
HW	0.550595	0.107017	0.167355	0.149988	497
Has1kidney	0.150964	0.014619	0.220918	0.214633	617
HeadDips_bc	0.05733	0.47979	0.178909	0.194864	606
IL_nb_pos_qn	0.454368	0.064088	0.495588	0.467081	74
IL_nb_qn	0.033656	0.84575	0.256566	0.312314	197
IL_score_pos_qn	0.675234	0.103555	0.599337	0.557238	74
INC	0.426809	0.179181	0.169727	0.160215	615
InterTrialCross11_20_bc	0.193345	0.13153	0.209909	0.207619	600
InterTrialCross1_10_bc	0.096435	0.126343	0.210094	0.213052	600
InterTrialCross1_20_bc	0.242347	0.119614	0.186207	0.18099	598
InterTrialCross1_40_bc	0.253064	0.06042	0.16166	0.153643	596
InterTrialCross21_30_bc	0.289287	0.023706	0.1931	0.181289	601
InterTrialCross31_40_bc	0.143051	0.06556	0.197591	0.194587	602
Iron_bc	0.134597	0.338406	0.147032	0.155196	599
LDL_bc	0.454847	0.335726	0.146162	0.141964	598
LFH	0.446643	0.169805	0.090355	0.080889	497
LT	0.500095	0.197576	0.108217	0.097526	497
LUC_bc	0.279747	0.343531	0.186032	0.188144	574
LW_bc	0.414773	0.470737	0.106168	0.107598	606
LYM_bc	0.455988	0.377799	0.139173	0.136417	575
Latency11_20_bc	0.495673	0.036799	0.194097	0.176376	599
Latency1_10_bc	0.606927	0.072303	0.165468	0.146049	600
Latency1_20_bc	0.56777	0.061687	0.173761	0.154956	600
Latency1_40_bc	0.516443	0.033699	0.183071	0.164383	601
Latency1_5_bc	0.544351	0.144015	0.153478	0.138568	598
Latency21_30_bc	0.407023	0.033006	0.186052	0.170609	599
Latency31_40_bc	0.278387	0.029882	0.207319	0.196245	598
Latency6_10_bc	0.428647	0.054013	0.194442	0.179354	600
LatencyOpenSection_bc	0.015252	0.304428	0.232291	0.247983	533
LineCrossings_bc	0.12812	0.39114	0.179752	0.189824	606

MCHC_bc	0.523966	0.264926	0.133412	0.124327	572
MCH_bc	0.33855	0.318167	0.086101	0.085168	574
MCV_bc	0.30646	0.376965	0.0821	0.084085	578
MONO_bc	0.334774	0.493303	0.123993	0.129032	579
MPC_bc	0.21711	0.606141	0.132564	0.145329	571
MPM_bc	0.389753	0.435945	0.099495	0.100751	561
MPV_bc	0.3994	0.311135	0.171725	0.168309	572
MPXI_bc	0.272625	0.34311	0.125855	0.128159	574
NEUT_bc	0.386062	0.450638	0.125808	0.127744	579
NW	0.486313	0.139038	0.169544	0.155913	496
ONSET_bc	0.650465	0.0311	0.384479	0.345957	199
PCDW_bc	0.264264	0.427081	0.128833	0.134356	573
PCT_bc	0.483046	0.28553	0.135142	0.128101	577
PDW_bc	0.353199	0.431675	0.148702	0.151137	576
PLT_bc	0.328232	0.31109	0.122902	0.121973	577
PltClumps_bc	0.144839	0.638139	0.121923	0.138725	554
PosturesClosedTo Open_bc	0.098935	0.306819	0.187096	0.196247	603
Potassium_bc	0.336797	0.492553	0.164517	0.169976	439
RBC_bc	0.184421	0.343053	0.087052	0.092154	568
RDW_bc	0.655636	0.171149	0.098746	0.083901	571
RT1AexpGran	0.295372	0.403774	0.164282	0.167788	494
RT1BexpBcell	0.467137	0.308544	0.160581	0.153007	398
Rearing0_30_bc	0.092233	0.493021	0.168873	0.18367	592
Rearing10_15_bc	0.188781	0.221194	0.20132	0.202804	593
Rearing15_20_bc	0.033086	0.310672	0.19295	0.206361	593
Rearing20_25_bc	0.031286	0.4405	0.183347	0.200054	595
Rearing25_bc	0.131088	0.383075	0.183855	0.193703	597
Rearing5_10_bc	0.02191	0.442091	0.15864	0.175871	592
Rearing5_bc	0.131379	0.314663	0.157977	0.165307	594
Sodium_bc	0.316156	0.502471	0.136178	0.142186	596
Tcell_Bcellratio	0.174993	0.67273	0.104235	0.120518	468
Tcells_Abs	0.178757	0.486528	0.096684	0.106863	536
Tcells_Pct	0.394282	0.395721	0.110083	0.109742	466
TimeOpenSection _bc	0.070923	0.465163	0.200633	0.215901	529
Tot.Chol_bc	0.479139	0.177192	0.123965	0.11258	511
Trig._bc	0.335627	0.336463	0.156011	0.155399	565
Urea_bc	0.532255	0.026015	0.22842	0.208261	473
WBCB_Abs	0.307371	0.474544	0.095463	0.100606	577
WBCB_bc	0.419551	0.416802	0.102644	0.102415	578
WL0_bc	0.055112	0.560446	0.164995	0.183815	545
WL9_ALT_bc	0.165656	0.35665	0.177501	0.18495	598
WL9_bc	0.108312	0.37492	0.187583	0.198135	543
abs_basos_bc	0.232231	0.406432	0.171696	0.177736	573
abs_eos_bc	0.330367	0.334614	0.158871	0.1587	580

abs_lucs_bc	0.359489	0.392539	0.158926	0.159891	573
abs_lymphs_bc	0.418093	0.398623	0.091151	0.090433	577
abs_monos_bc	0.337382	0.522388	0.126876	0.132667	577
abs_neuts_bc	0.23308	0.602505	0.125216	0.137273	575
bloodpressure	0.450115	0.051139	0.203127	0.187649	613
bloodpressure_bc	0.463042	0.051079	0.201241	0.185426	611
died	0.030195	0.059244	0.226632	0.232368	615
dist_femur_CRT_A	0.176994	0.50701	0.187039	0.200311	496
dist_femur_CRT_DEN	0.240913	0.361321	0.195971	0.201552	497
dist_femur_TOT_A	0.359707	0.283865	0.20775	0.205475	497
dist_femur_TOT_DEN	0.103666	0.577016	0.117686	0.136134	496
dist_femur_TRAB_A	0.26405	0.31555	0.205103	0.208021	497
dist_femur_TRAB_DEN	0.365372	0.406976	0.170699	0.172504	497
fem_biomech_EL	0.017224	0.282964	0.252385	0.269673	492
fem_biomech_Fu	0.511246	0.14709	0.182146	0.168135	494
fem_biomech_S	0.084731	0.582539	0.166061	0.186511	494
fem_biomech_W	0.223633	0.165634	0.207727	0.206775	494
fem_neck_CRT_A	0.044675	0.709713	0.156081	0.181467	496
fem_neck_CRT_DEN	0.479461	0.245101	0.117123	0.108663	496
fem_neck_IP_TOT_W	0.049922	0.423701	0.192389	0.20972	490
fem_neck_TOT_A	0.150191	0.381097	0.177663	0.188126	496
fem_neck_TOT_DEN	0.248813	0.312795	0.077566	0.079829	496
fem_neck_TRAB_A	0.136007	0.347155	0.096884	0.105238	496
fem_neck_TRAB_DEN	0.4027	0.268888	0.127283	0.1222	496
fem_neck_biomech_EL	0.27133	0.122606	0.259878	0.256507	447
fem_neck_biomech_Fu	0.429473	0.098272	0.15027	0.137618	447
fem_neck_biomech_S	0.290623	0.089982	0.258859	0.252999	447
fem_neck_biomech_W	0.157753	0.177943	0.224032	0.228262	447
femur_Area	0.41227	0.328769	0.155123	0.152049	498
femur_BMC	0.457249	0.288522	0.10957	0.103665	498
femur_BMD	0.368377	0.323238	0.136997	0.135319	498
femur_midshaft_	0.356133	0.331475	0.110301	0.109381	497

CRT_A					
femur_midshaft_ CRT_DEN	0.152341	0.518671	0.119088	0.133304	497
femur_midshaft_I P_TOT_W	0.348545	0.298082	0.09598	0.094162	497
femur_midshaft_ TOT_A	0.324051	0.352456	0.091528	0.092412	497
femur_midshaft_ TOT_DEN	0.339332	0.306228	0.093878	0.092671	497
heart_weight	0.222042	0.417938	0.129199	0.136954	503
heart_weight_bc	0.256781	0.445089	0.122171	0.129294	496
is.DB	0.15458	0.474215	0.081667	0.091984	617
is.LB	0.263407	0.455427	0.08746	0.093314	617
is.albino	0.329365	0.435489	0.064136	0.066773	617
is.spotted	0.442071	0.41812	0.086065	0.085214	617
lob_Index_bc	0.238219	0.507729	0.152825	0.161901	579
lumbar_Area	0.311534	0.339089	0.200823	0.202481	498
lumbar_BMC	0.364561	0.36028	0.120305	0.120127	498
lumbar_BMD	0.383709	0.354924	0.125506	0.124446	498
lumbar_CRT_A	0.234146	0.468731	0.177593	0.187181	496
lumbar_CRT_DEN	0.334561	0.392593	0.163316	0.165846	496
lumbar_TOT_A	0.111228	0.398459	0.191767	0.205214	496
lumbar_TOT_DEN	0.140298	0.523926	0.164867	0.180739	496
lumbar_TRAB_A	0.162273	0.277844	0.21954	0.226328	496
lumbar_TRAB_DE N	0.162434	0.471063	0.148489	0.161371	496
max_bc	0.403594	0.137755	0.440434	0.419357	199
measHGB_bc	0.350214	0.095054	0.124289	0.114774	573
old_AA_IL_score_ qn	0.044952	0.319215	0.201804	0.2374	196
pctBcells	0.200094	0.636218	0.101077	0.1147	557
pctCD25posCD4	0.249387	0.428086	0.116683	0.122511	539
pctCD25posCD8	0.194398	0.345084	0.188812	0.194238	522
pctCD45RChighCD 4	0.356783	0.39325	0.325569	0.326836	224
pctCD45RChighCD 8	0.479346	0.192986	0.37221	0.357401	227
pctCD45RClowCD 4	0.189438	0.529482	0.34726	0.363919	226
pctCD45RClowCD 8	0.365037	0.325526	0.348958	0.346236	226
pctCD45RCnegCD 4	0.056459	0.644532	0.841914	0.881406	92
pctCD45RCnegCD 8	0.153176	0.534618	0.669527	0.694489	92
pctCD45RCposCD 4	0.081916	0.590275	0.344427	0.370642	228

pctCD45RCposCD8	0.440213	0.267402	0.284298	0.274713	227
pctDN	0.698235	0.040998	0.712349	0.6444	90
pctDP	0.269158	0.418785	0.160778	0.165338	384
pctRT1BposTcell	0.47792	0.094664	0.372638	0.340587	205
time_freezing_bc	0.170521	0.243931	0.250968	0.254692	407